Theme I: The influence of strength and deformations of the following nonlinear phenomena

Objekttyp: **Group**

Zeitschrift: **IABSE congress report = Rapport du congrès AIPC = IVBH Kongressbericht**

Band (Jahr): **9 (1972)**

PDF erstellt am: **21.07.2024**

Nutzungsbedingungen

Die ETH-Bibliothek ist Anbieterin der digitalisierten Zeitschriften. Sie besitzt keine Urheberrechte an den Inhalten der Zeitschriften. Die Rechte liegen in der Regel bei den Herausgebern.
Die auf der Plattform e-periodica veröffentlichten Dokumente stehen für nicht-kommerzielle Zwecke in Lehre und Forschung sowie für die private Nutzung frei zur Verfügung. Einzelne Dateien oder Ausdrucke aus diesem Angebot können zusammen mit diesen Nutzungsbedingungen und den korrekten Herkunftsbezeichnungen weitergegeben werden.
Das Veröffentlichen von Bildern in Print- und Online-Publikationen ist nur mit vorheriger Genehmigung der Rechteinhaber erlaubt. Die systematische Speicherung von Teilen des elektronischen Angebots auf anderen Servern bedarf ebenfalls des schriftlichen Einverständnisses der Rechteinhaber.

Haftungsausschluss

Alle Angaben erfolgen ohne Gewähr für Vollständigkeit oder Richtigkeit. Es wird keine Haftung übernommen für Schäden durch die Verwendung von Informationen aus diesem Online-Angebot oder durch das Fehlen von Informationen. Dies gilt auch für Inhalte Dritter, die über dieses Angebot zugänglich sind.

Ein Dienst der *ETH-Bibliothek*
ETH Zürich, Rämistrasse 101, 8092 Zürich, Schweiz, www.library.ethz.ch

http://www.e-periodica.ch

I

L'influence sur la résistance et les déformations des phénomènes non-linéaires suivants

Der Einfluss auf die Traglast und die Verformung der folgenden nichtlinearen Vorgänge

The Influence on Strength and Deformations of the following Nonlinear Phenomena

I a

Plasticité et viscosité

Plastizität und Viskosität

Plasticity and Viscosity

Leere Seite
Blank page
Page vide

DISCUSSION PRÉPARÉE • VORBEREITETE DISKUSSION • PREPARED DISCUSSION

Prediction of Thermal Residual Stresses in Hot-Rolled Plates and Shapes of Structural Steel

Evaluation des tensions résiduelles thermiques dans les tôles et les profiles d'acier

Berechnung der thermischen Eigenspannungen in warmgewalzten Stahlplatten und Stahlprofilen

GÖRAN A. ALPSTEN
Dr. Techn., Docent
Sweden

INTRODUCTION

Residual stresses can play an important role in determining the strength of structural steel members, in particular with respect to the stability of compressed members, see review papers on this subject [1,2]. Much effort has been devoted to experimental studies of residual stresses in structural steel members. However, since such experiments are tedious and very expensive, it has been possible to test only very few out of a vast number of existing shapes with different geometry, manufactured under various conditions, of several steel grades with different thermo-physical and mechanical properties etc. For the same reason, it is natural that most experimental work in this area has been deterministic rather than statistical in nature [3].

This paper presents a theoretical computerized method for determining thermal residual stresses ("cooling stresses") in structural steel plates and shapes produced by hot-rolling. Plates are included here because they are components of welded shapes. Investigations have shown that the initial residual stresses existing in the plates prior to welding may be more important than the welding stresses [4,5]. The paper summarizes some particular aspects of the results of a more general study previously discussed in a research report in Swedish [6]. Reference is made to that report for fuller details of the theoretical method, and to [7] for an extensive discussion of the technical results with respect to residual stresses in structural steel members.

The method presented may be useful for illustrating the mechanism of formation of residual stresses, for identifying the important variables, and for studying the influence of these variables on the resulting residual stresses. An experimental study of this kind would not be feasible since it is practically impossible to separate the different variables. Another important application of the theoretical method is predictions of residual stresses, for instance, for revised manufacturing conditions or for a new steel grade -- apart from the experimental measurement being of the order of 100 times more expensive than a theoretical determination, the manufacturing of the test specimen may be excessively expensive at that investigative stage. Finally, the computer method is well suited for simulations of the statistical scatter of thermal residual stresses as influenced by scatter in the relevant variables.

The study is based upon an evaluation of the non-stationary thermal history and the

thermal stress-strain state during the manufacturing process. A finite-difference solution was developed and the numerical computations wereperformed on a digital computer. Plastic and viscous deformations were considered, including the effect of variable properties with temperature.

The method of analysis is applicable also to studies of several other thermal stress problems, such as determining the temperature-time field and thermal stresses for a structural steel member exposed to fire [8], or calculating the temperature, cooling rates, and thermal strains and stresses in a quenching process, in a post-heat treatment, or in any other thermal process involved in the manufacture and fabrication of steel plates and shapes.

METHOD OF TEMPERATURE ANALYSIS

An analytical analysis of the non-stationary heat flow in cooling - with complicated boundary conditions and variable thermo-physical coefficients of the steel - is practically impossible. For this reason, a finite-difference solution of the Fourier heat conduction equation was applied. The solution is based upon the implicit alternating direction (IAD) method. The cross section is divided into a mesh with variable spacing, see Fig. 1. The governing finite-difference equation for interior mesh points may be written on the form

$$\frac{T_{ijk+1}-T_{ijk}}{\Delta t}=\frac{1}{\rho_{ijk+1/2}\,c_{pijk+1/2}}\left[\frac{\lambda_{i+1/2\,j\,k+1/2}\dfrac{T_{i+1jk+1}-T_{ijk+1}}{\Delta x_i}-\lambda_{i-1/2\,j\,k+1/2}\dfrac{T_{ijk+1}-T_{i-1jk+1}}{\Delta x_{i-1}}}{\dfrac{\Delta x_i+\Delta x_{i-1}}{2}}\right.$$

$$\left.+\frac{\lambda_{ij+1/2\,k+1/2}\dfrac{T_{ij+1k}-T_{ijk}}{\Delta y_j}-\lambda_{ij-1/2\,k+1/2}\dfrac{T_{ijk}-T_{ij-1k}}{\Delta y_{j-1}}}{\dfrac{\Delta y_j+\Delta y_{j-1}}{2}}\right]$$

where T is temperature, t is time, ρ is density, c_p is specific heat, λ is thermal conductivity, and x and y are coordinates. The subscripts i and j refer to location in the cross section and k is the order of the time interval. For every second time step, the direction of integration is altered so that subscripts k and (k+1) of the temperatures T are exchanged in the right member of the equation. Similarly, a finite-difference equation may be formulated for the surface mesh points, based upon the equation

$$-\lambda\frac{\partial T}{\partial n}=h\,(T-T_{amb.})$$

where n is a coordinate normal to the surface and h is the surface coefficient of heat transfer. The detailed derivation of the finite-difference equations employed is given in [6].

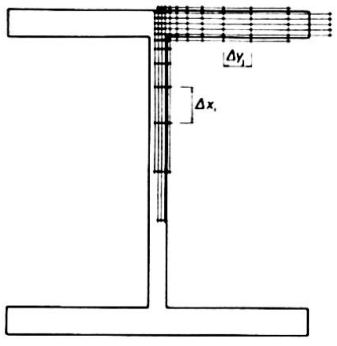

Fig. 1 Subdivision of an H-shape for finite-difference solution

The variable thermo-physical coefficients of structural steels as summarized from measurements in the literature were applied in the solution. A further complication results from the development of latent heat in the phase transformation of the steel around 727 °C. This effect was treated formally as a fictitious addition to the latent heat [6].

Results of calculations performed on a digital computer are shown in Fig. 2 as cooling

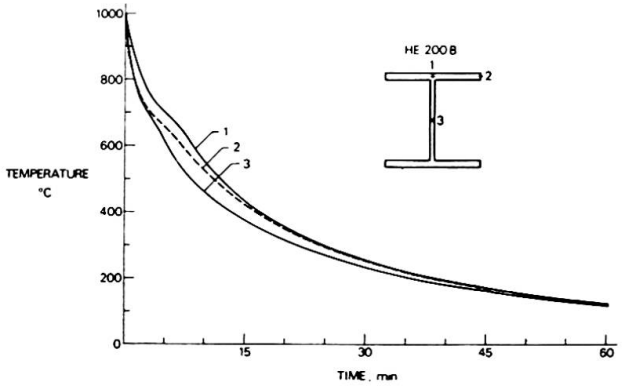

Fig. 2 Predicted cooling curves for an H-shape HE 200 B

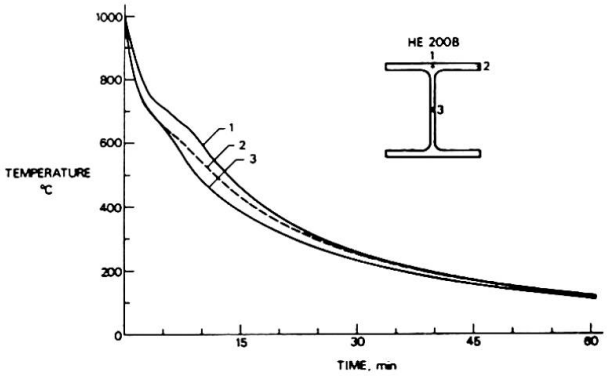

Fig. 3 Measured cooling curves for an H-shape HE 200 B

curves for three points on the cross section of an H-shape HE 200 B. This diagram may be compared with experimental cooling curves as given in Fig. 3. There is a good agreement between theory and experiment as evidenced by this comparison. Several such experimental temperature measurements were carried out and compared with calculations. For reasons which will be explained further below, a diagram of temperature differences over the cross section as a function of temperature will give a relevant representation of the cooling behavior. Figure 4 is such a diagram based upon the theoretical prediction of Fig. 2 and three repeated measurements on an HE 200 B shape. Considering the experimental scatter, and the fact that the prediction was based upon nominal average material coefficients, the agreement between prediction and measurements is most satisfactory.

METHOD OF THERMAL STRESS ANALYSIS

The thermal stress field at any instant during the cooling process may be calculated from the temperature field, considering the compatibility and equilibrium conditions. The longitudinal strain in a particular fiber (i, j) of the cross section can be written

$$\varepsilon_{ijk+1} = \Delta\varepsilon^{C}_{ijk+1/2} - \left(-\varepsilon^{E}_{ijk} + \Delta\varepsilon^{T}_{ijk+1/2}\right)$$

where ϵ^C is the strain increment due to compatibility conditions, ϵ^E is the elastic strain, and ϵ^T is the free thermal strain. The expression within parenthesis is the strain of a free fiber.

The formal addition of strains is represented graphically in Fig. 5, where $\Delta\epsilon$ equals $(\Delta\epsilon^C - \Delta\epsilon^T)$. Generally, the strain ϵ is composed of three parts

$$\varepsilon_{ijk+1} = \varepsilon^{E}_{ijk+1} + \varepsilon^{P}_{ijk+1} + \varepsilon^{V}_{ijk+1}$$

that is, an elastic, a plastic, and a viscous strain component. The elastic strain is the cause of stresses equal to

$$\sigma_{ijk+1} = E_{ijk+1}\,\varepsilon_{ijk+1}$$

where E is the modulus of elasticity. The plastic and viscous components are accumulated as remaining deformations in the fiber considered.

The method discussed here is formally somewhat different from similar computational procedures used previously for theoretical investigations of welding residual stresses [9]. The difference is exemplified in Fig. 6 (method B for adding strains is the method discussed above). Although the method of adding stresses will lead to physically impossible results for large increments of strains [6], the differences between

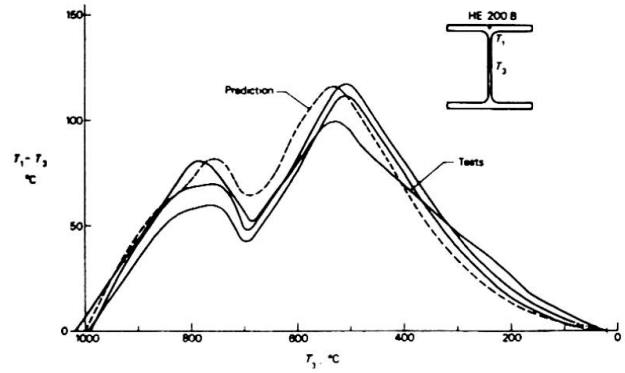

Fig. 4 Comparison betwen predicted and experimental cooling behavior

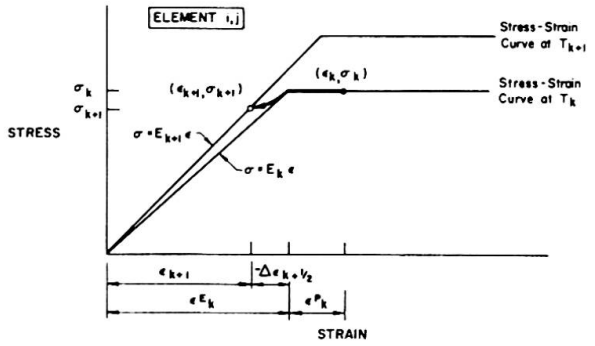

Fig. 5 Model for calculating thermal stresses at varying temperatures

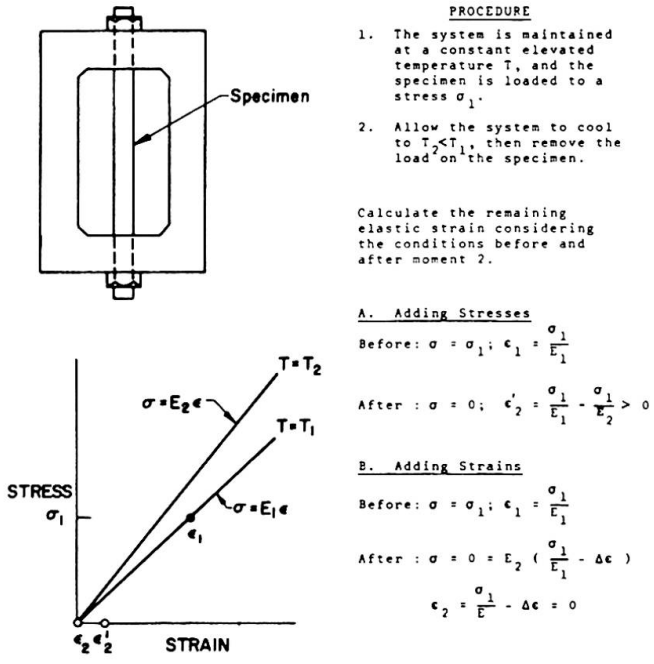

Fig. 6 Simplified model for comparison between calculation procedures

results obtained with the two methods are reasonably small for smaller strain increments.

In Fig. 5 the stress-strain curves were drawn as for elastic perfectly-plastic behavior. While this is a reasonable assumption for structural carbon steels at room temperature, real stress-strain curves at elevated temperatures are somewhat different as exemplified in Fig. 7. The dashed lines are elastic perfectly-plastic approximations fitted through the stress corresponding to 0.2 percent offset. Such approximations were applied in the present investigation. However, if sufficient mechanical data is available for a particular steel, the computational method discussed above is equally suited for a Ramberg-Osgood or some other parametric type representation of the stress-strain curve.

Figures 8 and 9 summarize limits of literature data for yield strength σ_F ($\sigma_{0.2}$ at elevated temperatures) and modulus of elasticity E of structural carbon steels. Also shown are the curves used for calculations. Results of both short-time tensile tests and creep tests are included in Fig. 8. In the present investigation, the viscous deformations were included in the plastic deformations. When curves for σ_F and E are adjusted appropriately, this leads to a reasonable approximation. Figure 10 shows the implications of this assumption. Comparative calculations for cooling processes of normal-size members, including a more detailed estimation of the viscous strains, indicated that the error of the above approximate method is negligible compared to the errors resulting from an inaccurate knowledge of the short time stress-strain curve at high temperatures. This conclusion may not be correct for a heating process, where high temperatures normally are maintained at longer duration of time, for instance, when applying the method for predictions of temperatures and thermal stresses in a member exposed to fire. For such cases a detailed

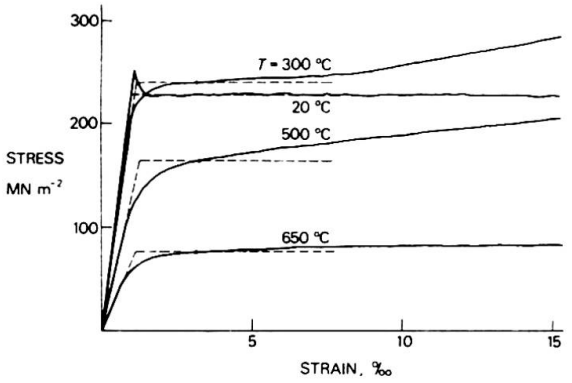

Fig. 7 Examples of stress-strain curves at different temperatures for a structural carbon steel

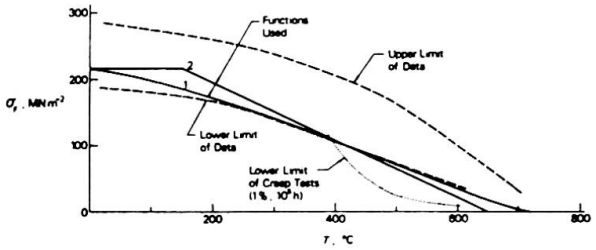

Fig. 8 Yield strength σ_F of structural carbon steels versus temperature

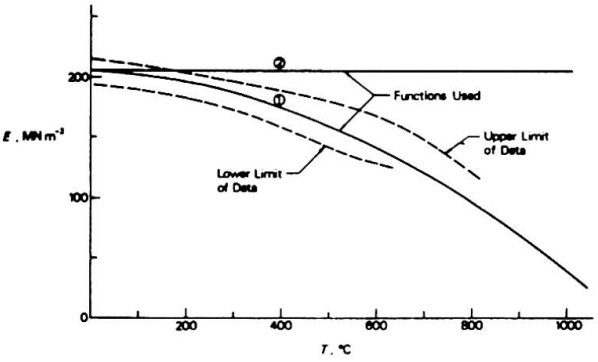

Fig. 9 Modulus of elasticity E of structural carbon steel versus temperature

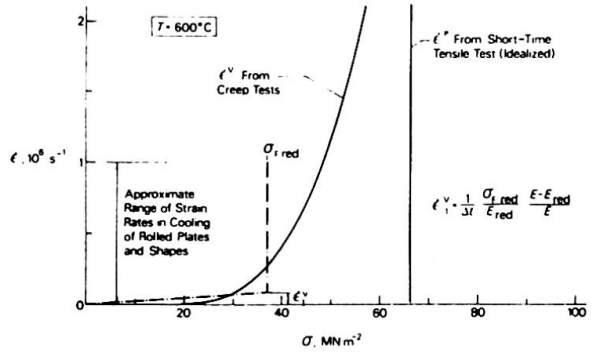

Fig. 10 Approximate method for calculating viscous strains (schematic)

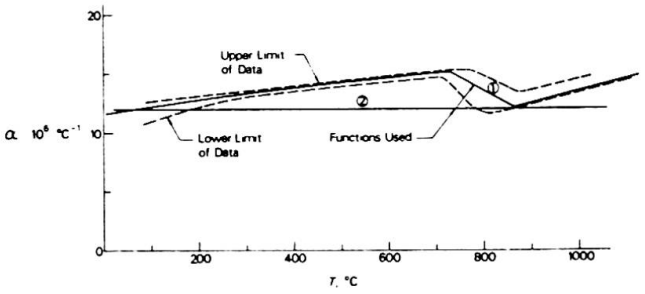

Fig. 11 Coefficient of linear expansion α of structural carbon steels versus temperature

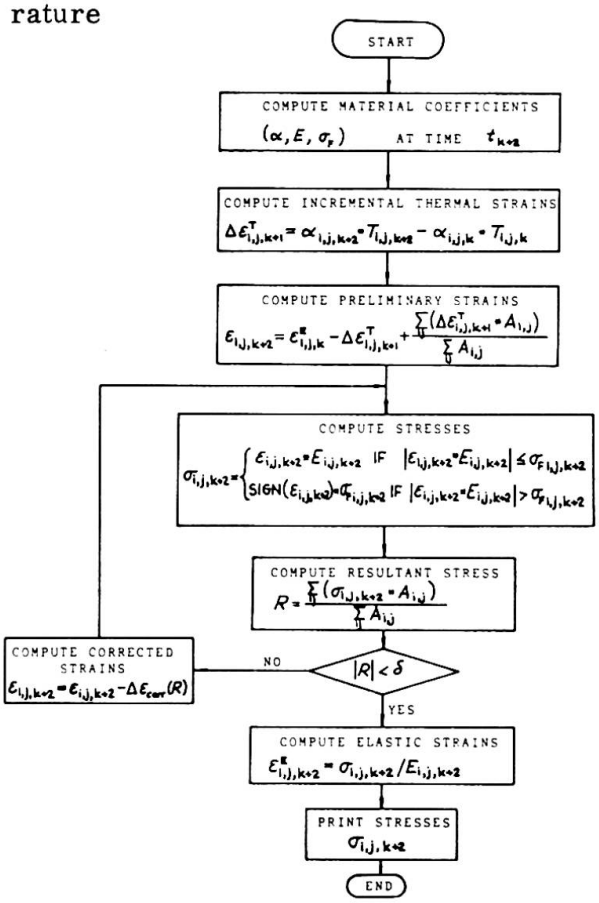

Fig. 12 Short flow diagram of subroutine for thermal stress analysis

account of the viscous deformations may become necessary. The computer procedure as discussed here (see also Fig. 12 above) has been revised to include a separate account of viscous strains. In the residual stress calculations, however, it was assumed that E_{red} in Fig. 10 is equal to E, which leads to negligible errors for normal-size shapes. For very heavy members, this assumption overestimates slightly the elastic strains and the resulting residual stresses.

A further mechanical property entering the stress-strain calculation is the coefficient of linear expansion α. Figure 11 shows the limits of literature data and the assumed functions. The relationship is influenced by the gradual phase transformation $\gamma \rightarrow \alpha$ which is accompanied by a volume expansion.

The various other conditions and assumptions involved in the calculation were discussed in detail in the original report [6]. The computer subroutine used for calculating thermal stresses is given in Fig. 12 (in this flow chart, viscous deformations are considered in σ_F but not in E).

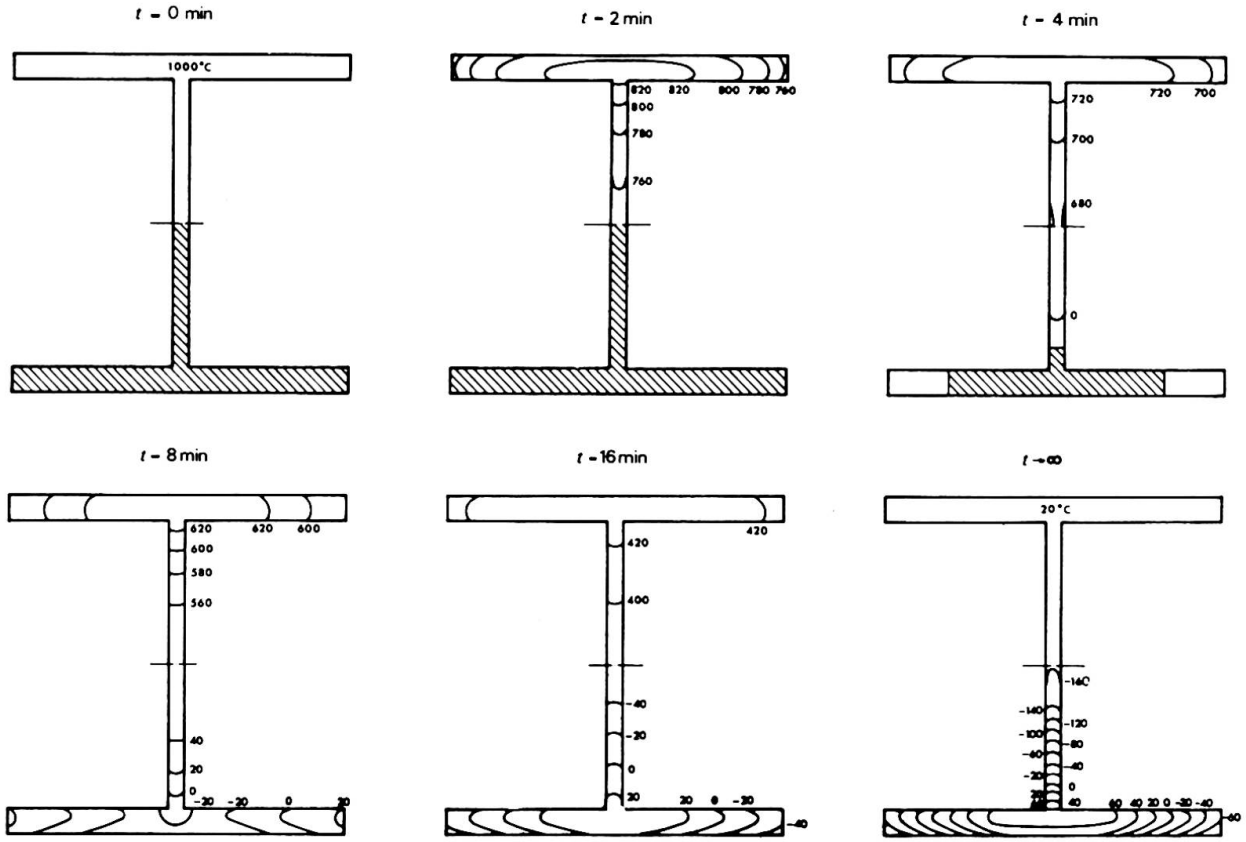

Fig. 13 Predicted cooling behavior and transient thermal stresses in an HE 200 B shape

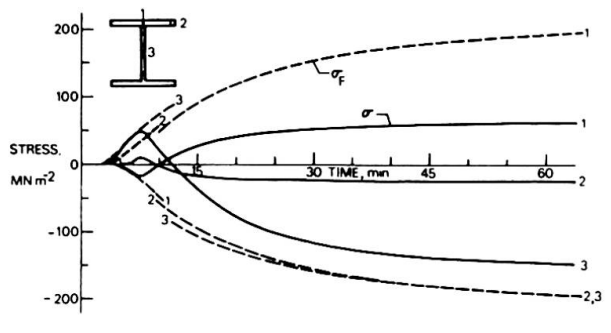

Fig. 14 Predicted thermal stress and associated yield strength as a function of cooling time, HE 200 B

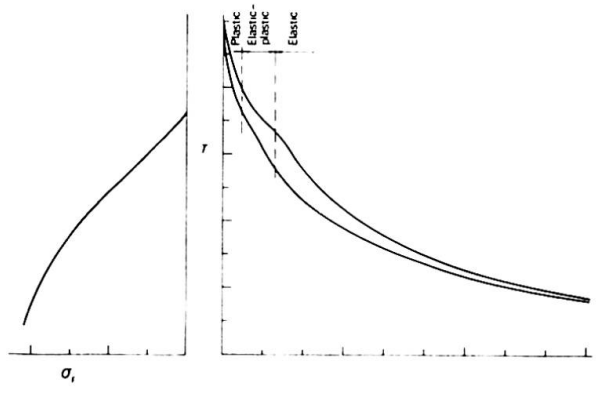

Fig. 15 Different regions of mechanical behavior during the cooling of an H-shape, HE 200 B

RESULTS

Figure 13 shows the computed temperature and thermal stress fields at different stages during cooling of an H-shape HE 200 B. A constant temperature of 1 000 °C was assumed for the initial state. The thermal stresses obtained when the member approaches the ambient temperature are the resulting residual stresses. As a rule-of-thumb, the regions cooling first will develop compressive residual stresses, balanced by tensile stresses in the remainder of the cross section.

The relative stress level at various stages of the cooling process may be studied in Fig. 14. It is interesting to note that the stresses are completely plastic and completely elastic, except for a short intermediate time interval. The three regions are indicated in Fig. 15. The intermediate elastic-plastic region is closely related to the temperature range where the yield strength approaches zero. The important implication is that temperature differences existing in this intermediate temperature range are the major cause of residual stresses to form after cooling to ambient temperature.

The influence of various assumptions on the residual stresses may be studied in Fig. 16. In summary, the initial temperature state is not an important variable; constant thermophysical coefficients will lead to large deviations in the results, but reasonably small variations in the various coefficients will cause only small differences in the computed results; cooling conditions are most important in the formation of residual stresses.

In Fig. 17 is a comparison between predicted and measured residual stresses in two shapes, a light I-shape IPE 200 and a heavy H-shape W 14x426, weighing 22.4 and 632 kg per linear meter, respectively. The diagrams give an idea of the agreement between predictions and tests for two shapes towards the ends of the span of different existing rolled shapes. A comparison between Figs. 17 a and 17 b also gives an indication of the effect of geometry on the magnitude of residual stresses.

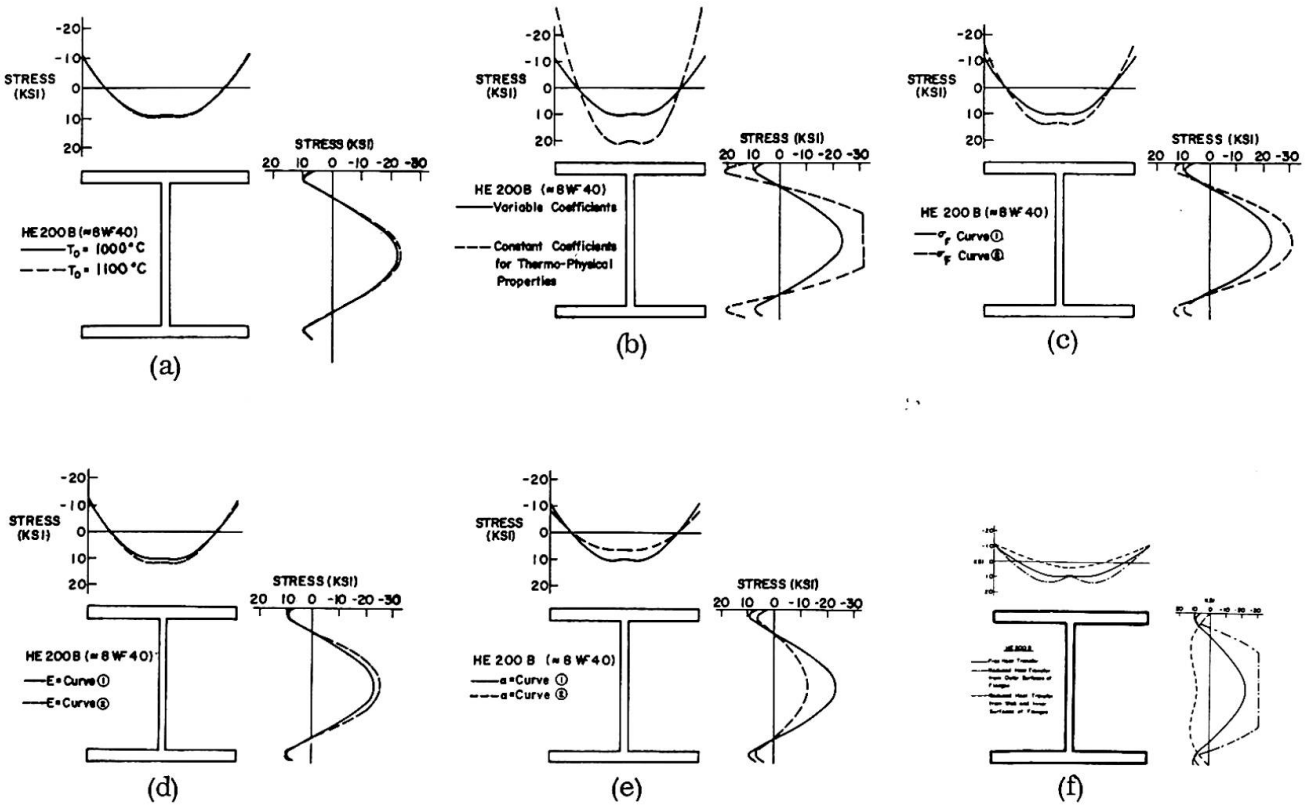

Fig. 16 Influence of different assumptions on the predicted residual stresses, HE 200 B (Scales graded in ksi. 1 ksi=6.9 MN/m^2)

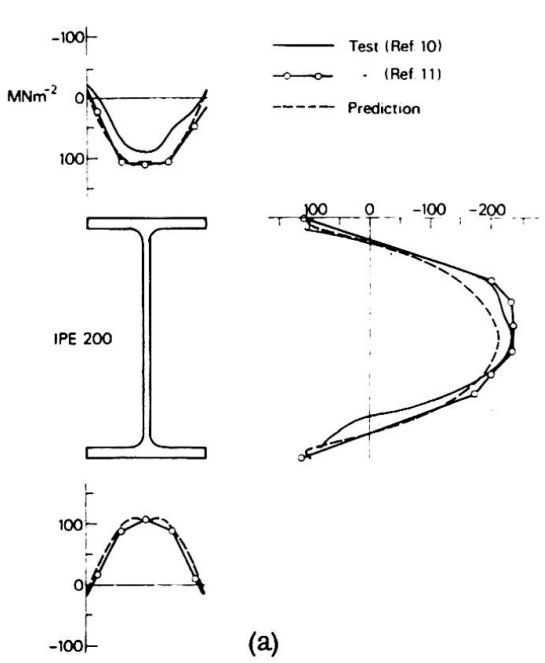

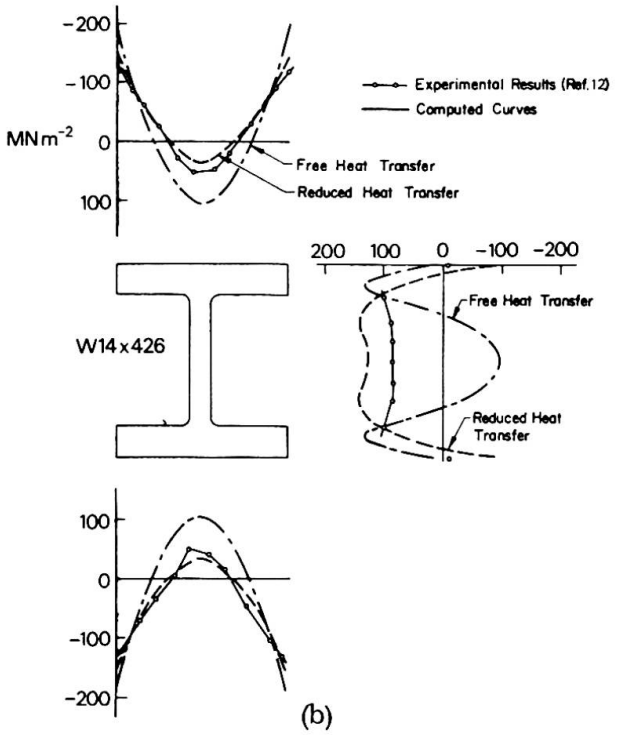

Fig. 17 Predicted and measured residual stresses in (a) a light I-beam IPE 200 and (b) a heavy H-shape W 14x426

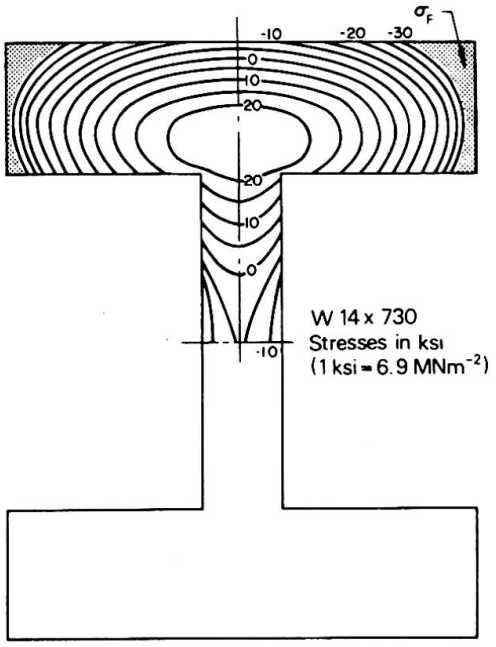

Fig. 18 Predicted two-dimensional variation of residual stresses in a "jumbo" shape W 14x730

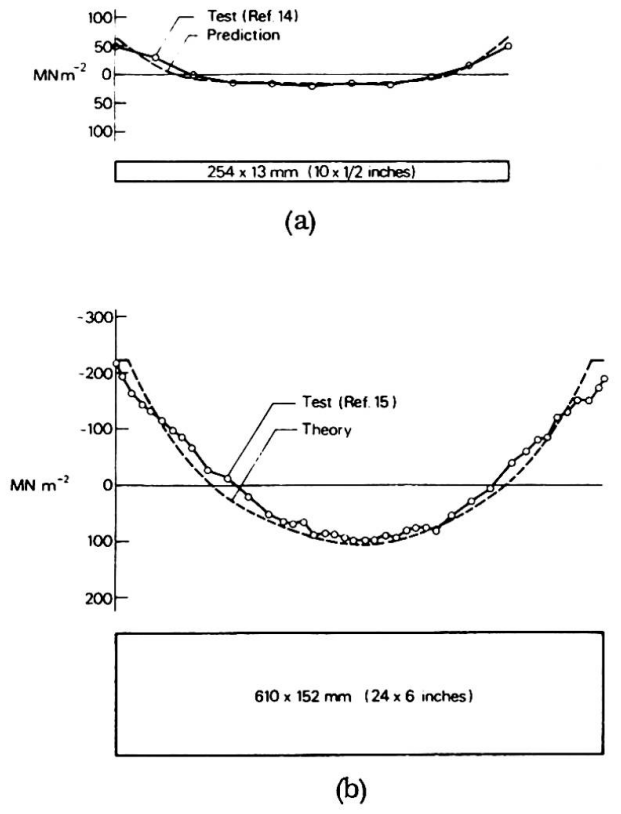

Fig. 19 Predicted and measured residual stresses in two universal-mill plates with as-rolled edges

Figure 18 shows the predicted two-dimensional variation of residual stresses in a still heavier H-shape W 14x730, that is the heaviest "jumbo" shape being rolled in the U.S. today. The calculated temperature differences in this extremely heavy shape (1 087 kg/m) are sufficient to cause residual stresses approaching the yield at the flange tips. Another important feature is the great through-thickness variation of residual stresses. Experimental measurements of residual stress have been carried out also for this "jumbo" shape [13]. The measured residual stresses were, however, much lower than predicted in Fig. 18, probably because the test member had been cold-straightened after cooling in the mill.

The effect of geometry on cooling residual stresses, as predicted by the theory [6,7], and as exemplified in Fig. 17, has been verified also by experiments on universal-mill plates with as-rolled edges [15]. Two examples are shown in Fig. 19. The compressive residual stress in the heavy plate is about three times greater than in the smaller plate. Thus, member size and geometry is one of the major variables affecting thermal residual stresses in hot-rolled plates and shapes.

Residual stresses affect the strength of centrically loaded columns. The variation of residual stresses as caused by different shape size may reduce the maximum strength by as much as 30 percent [2,7]. Thus, it appears necessary that the detrimental effect of high residual stresses be considered in the design of steel columns. Alternatively, measures should be taken to limit such stresses below acceptable values. A controlled roller-straightening procedure could be used for this purpose [16]. Experimental studies of roller-straightened columns have shown that the column strength may be increased by 10 to 15 percent from the roller-straightening process, even for a shape HE 200 A with relatively small thermal residual stresses [17].

REFERENCES

1. L. S. BEEDLE and L. TALL: Basic Column Strength. Journal of the Structural Division, ASCE, Vol. 86, No. ST7, July 1960, pp. 139 - 173.

2. L. TALL and G. A. ALPSTEN: Prediction of Behavior of Steel Columns Under Load. IABSE Symposium on Concepts of Safety of Structures and Methods of Design, London, September 1969, pp. 179 - 190.

3. L. TALL and G. A. ALPSTEN: On the Scatter in Yield Strength and Residual Stresses in Steel Members. IABSE Symposium on Concepts of Safety of Structures and Methods of Design, London, September 1969, pp. 151-163.

4. G. A. ALPSTEN and L. TALL: Residual Stresses in Heavy Welded Shapes. Welding Journal, Vol. 49, No. 3, March 1970, pp. 93-s - 115-s.

5. G. A. ALPSTEN: Theoretical Study of Residual Stresses in Medium-Size to Heavy Welded Shapes. Paper to be presented at the 9th IABSE Congress, Amsterdam, Holland, May 1972.

6. G. A. ALPSTEN: Egenspänningar i varmvalsade stålprofiler (Residual Stresses in Hot-Rolled Steel Profiles). Institution of Structural Engineering and Bridge Building, Royal Institute of Technology, Stockholm, June 1967.

7. G. A. ALPSTEN: Thermal Residual Stresses in Hot-Rolled Steel Members. Fritz Engineering Laboratory Report No. 337.3, Lehigh University, December 1968 (to be published in the Welding Journal).

8. G. A. ALPSTEN: Om numerisk simulering av bärförmågan hos oisolerade stålpelare utsatta för brandpåverkan (On Numerical Simulation of the Strength of Non-Protected Steel Columns Exposed to Fire). Scandinavian Research Conference on Steel Construction 1970. Final Report No. R 39:1971, National Swedish Institute for Building Research, Stockholm.

9. L. TALL: Residual Stresses in Welded Plates -- A Theoretical Study. Welding Journal, Vol. 43, No. 1, January 1964, pp. 10-s - 23-s.

10. E. MAS and C. MASSONNET: Belgium's Part in the Experimental Research on the Buckling of Axially Loaded Mild-Steel Members Conducted by the European Convention of Constructional Steelworks. Acier-Stahl-Steel, No. 9, September 1966, pp. 385 - 392.

11. M. COMO and F. M. MAZZOLANI: Ricerca teorico-sperimentale sullo svergolamento nel piano e fuori del piano dei profilati in presenza di tensioni residue (Theoretical and Experimental Research on the Buckling of H-shapes Considering Residual Stresses). Costruzioni Metalliche, Vol. 21, No. 3, May-June 1969, pp. 212 - 243

12. Y. FUJITA: The Magnitude and Distribution of Residual Stresses. Fritz Engineering Laboratory Report No. 220 A. 20, Lehigh University, May 1955.

13. J. BROZZETTI, G. A. ALPSTEN, and L. TALL: Residual Stresses in a Heavy Rolled Shape 14WF730. Fritz Engineering Laboratory Report No. 337.10, Lehigh University, February 1970.

14. N. R. NAGARAJA RAO and L. TALL: Residual Stresses in Welded Plates. Welding Journal, Vol. 40, No. 10, October 1961, pp. 468-s - 480-s.

15. R. BJØRHOVDE, J. BROZZETTI, G. A. ALPSTEN, and L. TALL: Residual Stresses in Thick Welded Plates. Fritz Engineering Laboratory Report No. 337.13, Lehigh University, June 1971.

16. G. A. ALPSTEN: Egenspänningar och materialhållfasthet i kallriktade bredflänsprofiler (Residual Stresses and Mechanical Properties of Cold-Straightened H-Shapes). Jernkontorets Annaler, Vol. 154, No. 6, 1970, pp. 255 - 283.

17. O. ERSVIK and G. A. ALPSTEN: Experimentell undersökning av knäckhållfastheten hos bredflänsprofiler HE 200 A riktade på olika sätt (Experimental Investigation of the Column Strength of Wide-Flange Shapes HE 200 A Roller-Straightened in Different Manners). Swedish Institute of Steel Construction, Stockholm, Report 19:3, December 1970.

SUMMARY

A computerized method for predicting thermal residual stresses in hot-rolled steel plates and shapes is presented. The procedure is based upon a finite-difference solution using an implicit alternating direction method for calculating the non-stationary heat flow. From the temperature field the transient thermal stress-strain conditions are evaluated, considering elastic, plastic, and (approximately) viscous strain components, and taking into account the variable mechanical coefficients of structural carbon steel. Predicted temperature-time curves and residual stress distributions agree well with experimental results. The method is applicable also to several other types of thermal problems.

RESUME

On présente ici une méthode, utilisant l'ordinateur, pour prédire les tensions thermiques résiduelles dans les plaques et les coques en acier laminé à chaud. Ce procédé est basé sur une solution aux différences finies utilisant pour calculer le flux thermique non-stationnaire une méthode implicite aux directions alternantes. On évalue les conditions transitoires d'allongement et de tensions thermiques à partir du champ des températures, considérant les composantes d'allongement élastiques, plastiques et (approximativement) visqueuses et tenant compte des coefficients mécaniques variables de l'acier de construction au carbone. Les courbes température-temps et les distributions des tensions résiduelles obtenues, concordent bien avec les résultats expérimentaux. La méthode est aussi applicable à d'autres types de problèmes thermiques.

ZUSAMMENFASSUNG

Es wird eine mittels Computer durchgeführte Methode zur Vorausbestimmung von Eigenspannungen in warmgewalzten Stahlblechen und Stahlprofilen vorgelegt. Der Vorgang stützt sich auf eine endliche Differenzenlösung unter Verwendung einer impliziten Methode zur Berechnung des nichtstationären Wärmeflusses. Aus dem Temperaturfeld werden die transienten thermischen Eigenspannungsbedingungen ausgewertet unter Berücksichtigung der elastischen plastischen und (annähernd) viskosen Spannungskomponenten und unter Berücksichtigung der variablen mechanischen Koeffizienten von Kohlenstoffstahl. Die vorausgesagten Temperatur/Zeit-Kurven und die Verteilung der Eigenspannungen stimmen mit den experimentellen Ergebnissen gut überein. Die Methode ist auch auf verschiedene andere Typen thermischer Probleme anwendbar.

Leere Seite
Blank page
Page vide

Prediction of Residual Stresses in Medium-Size to Heavy Welded Steel Shapes

Evaluation des tensions résiduelles dans les tôles d'acier soudées de dimensions moyennes et grandes

Berechnung der Eigenspannungen in geschweissten Stahlblechen mittleren und grossen Ausmasses

GÖRAN A. ALPSTEN
Dr. Techn., Docent
Sweden

Heavy welded steel shapes, that is, members built up of components ranging from 25 mm and up in thickness, are today commonly used in multistory buildings and other major structures. Figure 1 shows a few examples of medium-size to heavy welded steel columns as used in buildings in North America and Europe. While such members are commonplace in modern construction, their basic structural behavior had not been studied up to recently. The design rules for compression members of heavy steel shapes were merely extrapolated from the well-documented behavior of lighter members. This may not be a completely rational procedure, particularly when it is realized that such factors as mechanical properties and residual stresses are greatly influenced by the member geometry.

Thus, in order to develop rational design criteria for heavy welded steel columns there is a need for information on the magnitude and distribution of residual stresses in heavy fabricated members. Means for determining these stresses are experimental measurements and theoretical predictions. While experimental procedures are the only way to find the actual distribution of residual stresses in a single given member, such methods are often expensive and time-consuming. This is particularly true for heavy members. In addition, all methods for the measurement of residual stresses, except X-ray and ultrasonics measurement of surface residual stresses, require the destruction of the specimen, at least locally. Theoretical methods, on the other hand may be used for predictions which are sufficiently accurate for many purposes. Such methods appear particularly useful to study the effect of geometry, or the effect of various manufacturing and fabrication conditions on residual stresses . An experimental study of this kind would require several specimens and, if at all economically feasible, it would be complicated or even impossible to control all relevant variables.

This report presents briefly a theoretical study for predicting longitudinal residual stresses in medium-size to heavy welded plates and shapes. A full account of the investigation will be presented elsewhere [1] . The method of analysis differs from previous investigations of welding residual stresses in several respects. Some of these are:

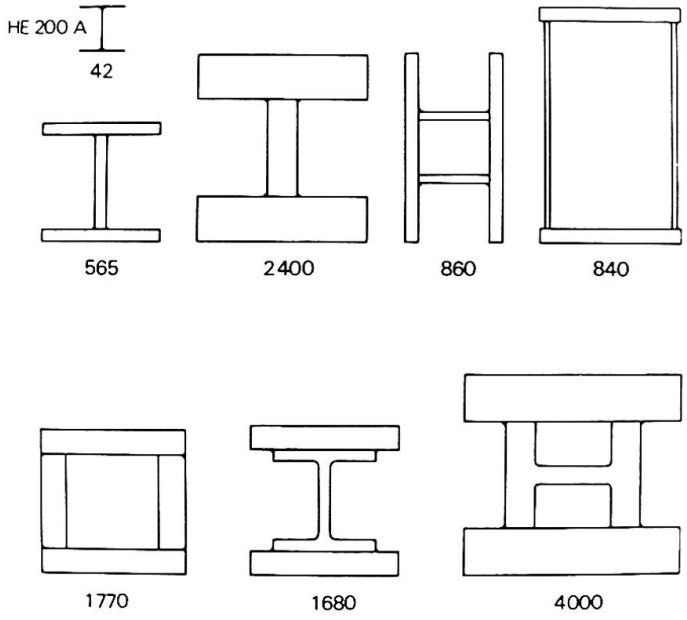

Fig. 1 Examples of heavy welded shapes used as columns in recent buildings (Numbers indicate weight in kg per linear meter; a rolled European standard shape HE 200 A is included for comparison)

1. The action of the complete member being welded is considered, not merely a separate plate with a weld bead.

2. The three-dimensional variation of temperature, and the resulting through-thickness variation of longitudinal stresses, are taken into account -- in thick plates, the through-thickness variation may be quite significant.

3. Most importantly, it is recognized that the initial residual stresses, that is, the residual stresses existing in the component plates prior to welding, may be of major importance in the formation of residual stresses in a welded shape [2] .

The welding residual stresses are generated by local plastic deformations occuring during the welding. These stresses are computed from an analysis of the temperature and the elastoplastic stress-strain history during welding. The analysis of heat flow is based upon the well-known theory for moving point heat sources as developed by Rosenthal [3, 4] and others. A review of some of the important earlier investigations concerned with welding residual stresses is given in [5] .

The study of heavy welded shapes discussed in this report supplements the previous investigations of residual stresses as related to the strength of structural steel columns. Extensive studies of residual stresses were previously carried out for hot-rolled members [6, 7, 8, 9] , small welded plates [5, 10] , and shapes built up from universal-mill plates [11] . Recent or current experimental studies include also welded shapes of flame-cut plates [12] and heavy welded plates and shapes [2, 13, 14] .

The method of analysis discussed here is not only applicable to the welding residual stresses in medium-size to heavy welded columns. Other important applications include thermal stress effects in heavy steel installations exposed to local heat; residual stresses in heavy welded plates, for instance, as used in submarine hulls; or temperature and stress conditions in plates welded by modern methods producing a very localized heated zone, such as electron beam welding.

INITIAL STRESSES

Although the possible effect of initial stresses existing in the parent plates before fabrication of a welded member was pointed out as early as 1936 [15] , it is surprising to note that this effect has not been investigated in previous studies. In fact, many experimental investigations of residual stresses purposely excluded this factor by stress-relieving the parent plates of the test specimens prior to welding. The results thereby obtained would barely have any practical value for medium-size to heavy welded members, since the initial stresses may be of greater importance that the stresses created by the welding process [2] .

Component plates in medium-size to heavy welded members are either universal-mill plates with as-rolled edges ("UM plates") or oxygen-cut plates ("OC plates") taken from larger rolled parent plates. Initial residual stresses in UM plates my be predicted from the cooling procedure, using a theoretical method discussed elsewhere [7, 8, 9]. Such stresses alternatively may be estimated from recent measurements [14] . Similarly, residual stresses in OC plates may be predicted, for instance, by using the method reported below, or may be estimated from measurements [14] . When calculating residual stresses in OC plates, the thermal stresses produced by the oxygen-cutting have to be superimposed upon the cooling stresses existing in the rolled parent plates.

Figure 2 shows predicted residual stresses in two heavy UM plates with dimensions 356 x 64 mm and 254 x 38 mm, respectively (14 x 2 1/2 and 10 x 1 1/2 inch, respectively). These plates were chosen here because experimental results are available for comparisons [2] . In the prediction, the viscous deformations during the cooling process were considered specifically [9, 16] using viscous coefficients for structural steel as determined in the literature [17] .

The compressive stresses at the plate edges of the larger plate (Fig 2 a) are up to 75 percent of the assumed yield strength, and balanced by tensile stresses in the center of the plate. The maximum compressive stress predicted for the smaller plate, Fig 2 b, is about half the yield strength.

The heat input introduced into a plate during oxygen-cutting may be treated as a moving linear heat source acting along the plate edge [3] . Mathematical expressions for this and several other heating cases have been conveniently summarized in Ref. 18.

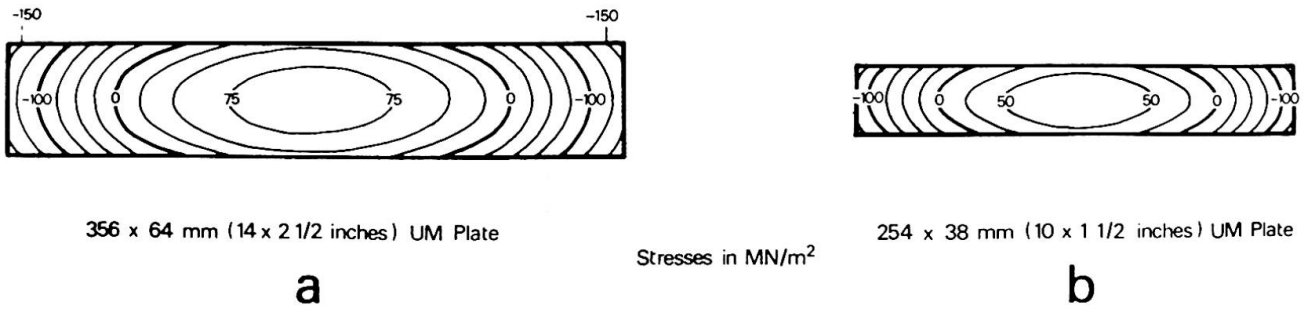

Fig. 2 Predicted residual-stress distributions in two thick universal-mill plates

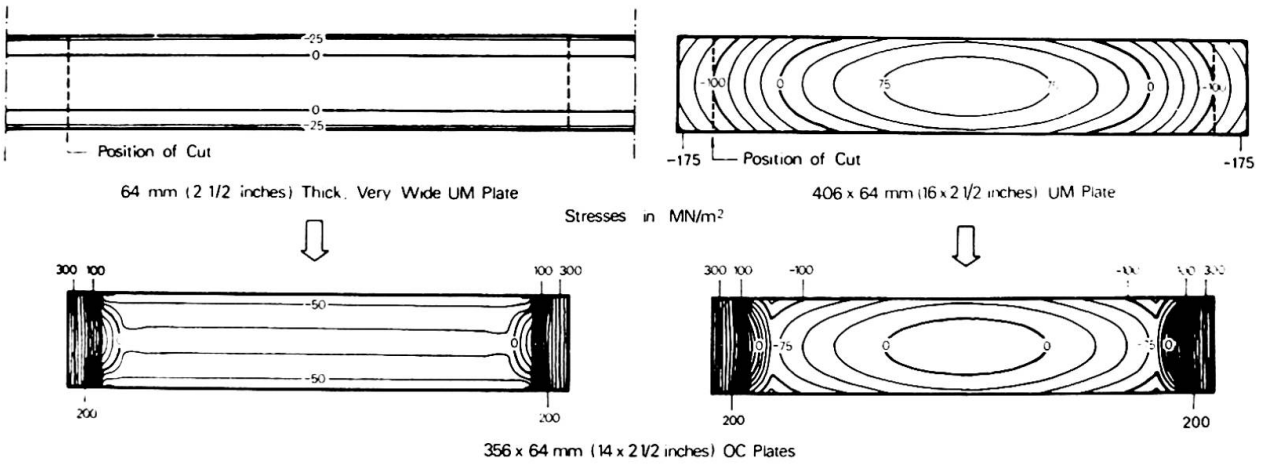

Fig. 3 Predicted residual-stress distributions in thick oxygen-cut plates taken from a very wide universal-mill plate and a narrower universal-mill plate

However, because the heat input may vary throughout the thickness, the heat source can also be treated numerically as a line of several moving point heat sources. The relative intensity of these point sources may be chosen to simulate the different heating conditions on the near and far side of the plate. The formal computations can be made using the same method as discussed below for the welding.

Residual-stress distributions predicted for an OC plate of the same size as in Fig. 2 a are seen in Fig. 3. Two distributions are given, one corresponding to a very wide parent plate, with initial stresses varying only across the thickness, and one corresponding to a narrower parent plate, the plate presumably being oxygen-cut only to obtain straight edges. The width of the parent plate in the second case was chosen arbitrarily to be 407 mm (16 inches). In this prediction, all point heat sources along the oxygen-cut edges were simply assumed equal, the total heat input given away to heat each plate edge being 16 kJ.

TEMPERATURE ANALYSIS IN WELDING

For the case of interest here, the heated zone around a weld is small compared to the thickness of the material. Under such conditions the actual geometry of the member being welded can be considered as a segment of a three-dimensional continuum. Different practical boundary conditions for heavy shapes may be approximated as shown in Fig. 4.

The heat input in welding normally is treated in the literature as the result of a moving point heat source [3, 4, 5, 13, 18] . However, because of the finite size of the molten pool, the high-temperature region around a real weld is much wider than obtained for a point heat source . To simulate the actual conditions, the weld may conveniently be approximated as an aggregate of heat sources, all located within the molten weld pool, the total heat input of the point sources being equal to the weld heat input.

Further details of the computational method and a derivation of the equations used may be found in the full report [1] . For calculating the temperatures during welding, the cross section is divided into a mesh of sectional points, these same points being used also for expressing the thermal stress-strain conditions.

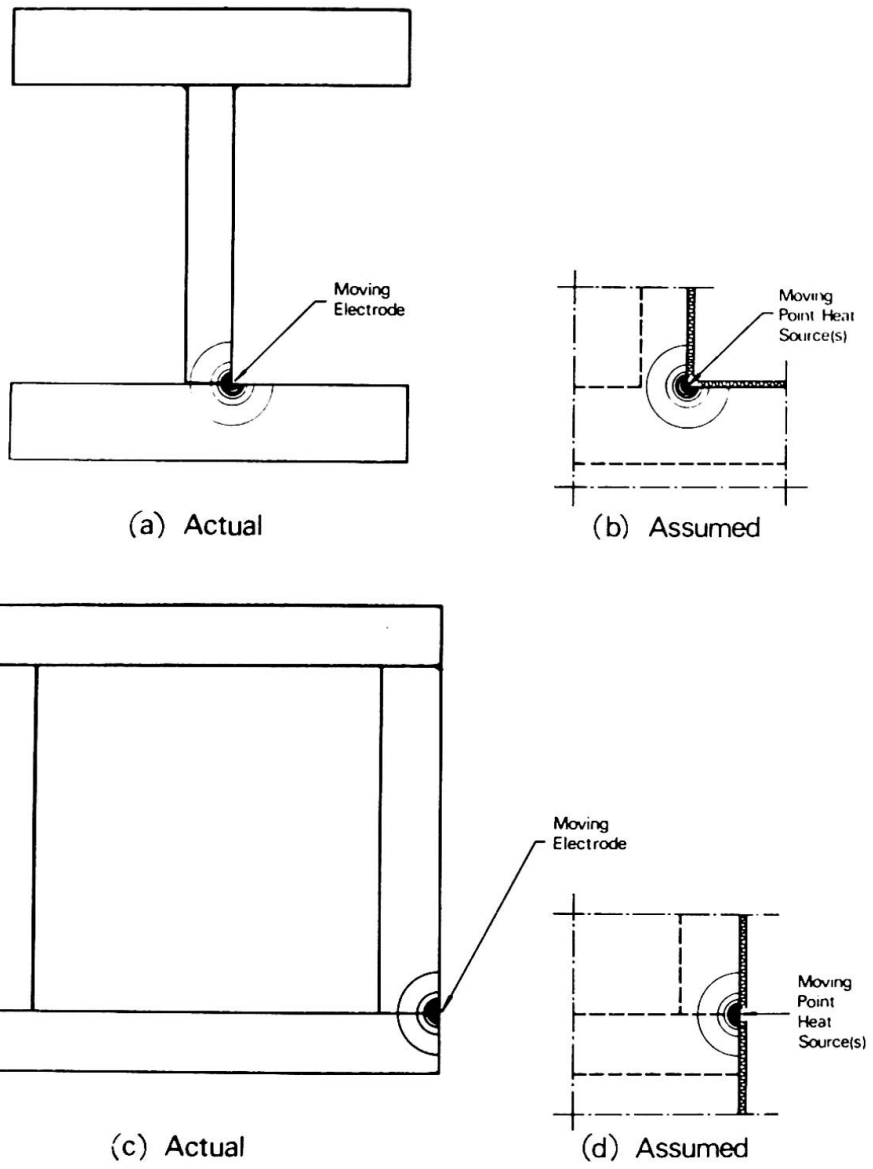

Fig. 4 Theoretical boundary conditions simulating the actual conditions in heated heavy members

The temperature conditions may be studied in incremental time steps, see Fig. 5. However, since the welding stresses normally constitute only a small fraction of the final residual stresses in a fabricated member, it is reasonable to adopt a simple approximate method. Following suggestions advanced in the literature [13], only three instances will be considered here: the initial state corresponding to the preheat temperature (or ambient temperature if no preheat is applied), an intermediate state corresponding to the conditions at the maximum temperature envelope (see Fig. 5) and the final state after the completed weld run. The resulting "three-step method" may be considered a generalization of the previously developed "two-step method" [13]. In Fig. 6 is shown in a non-dimensional diagram the relationship between maximum temperature and distance from weld line for a moving heat source. The maximum temperature envelope may be obtained conveniently with the aid of the diagram.

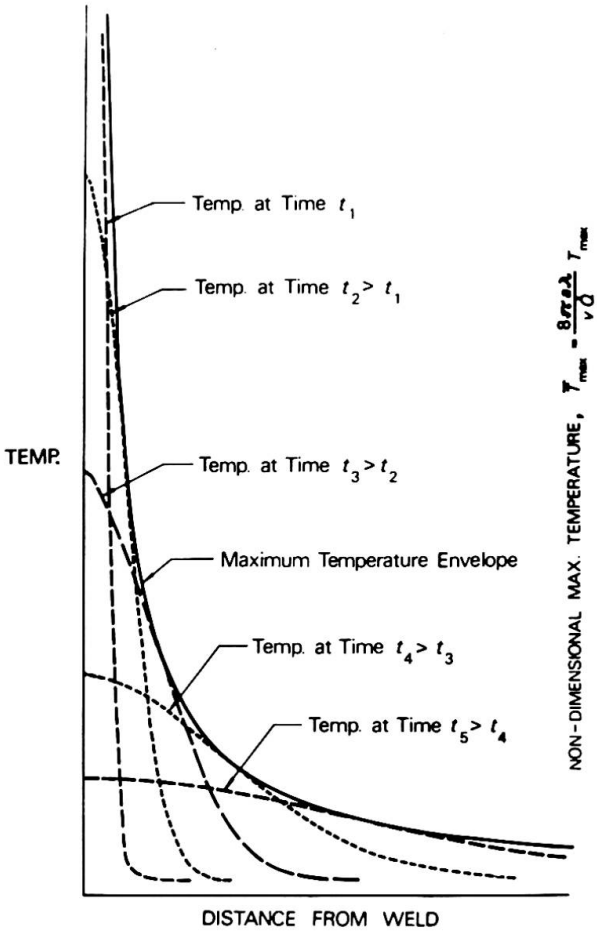

Fig. 5 Examples of temperature distributions at different times after onset of welding (schematic)

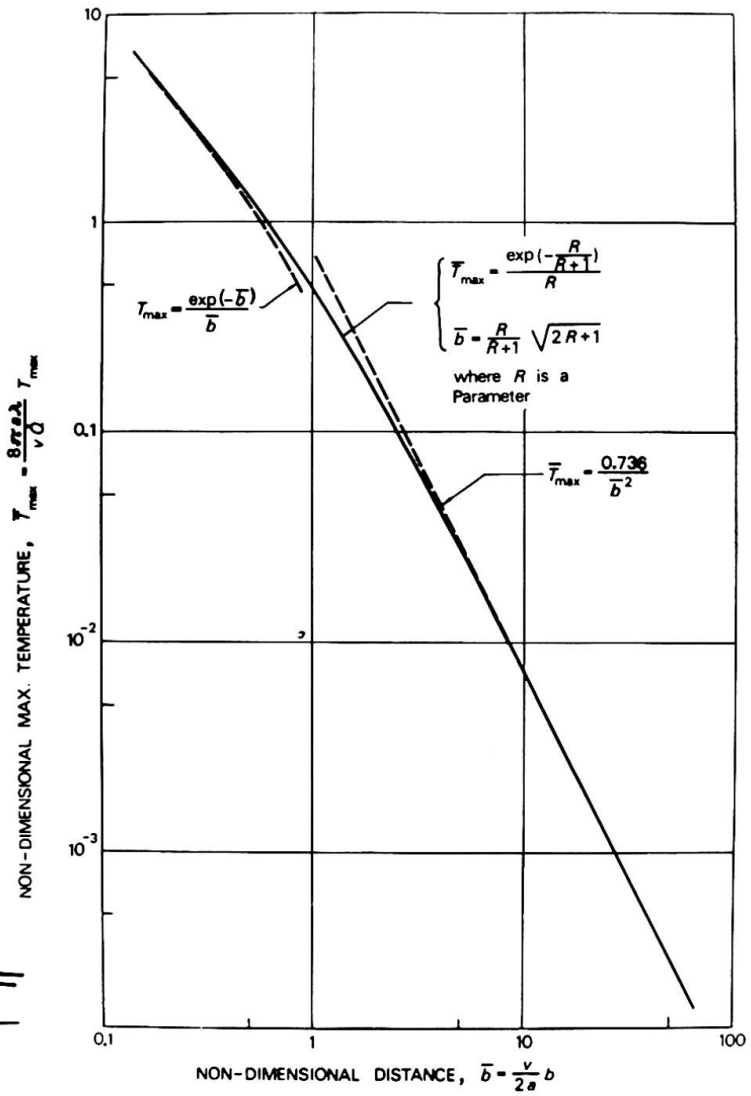

Fig. 6 Non-dimensional curves for the maximum temperature envelope around a point heat source moving in an infinite solid along a line with constant speed (solid line is theoretical curve, dashed lines are approximations, a = thermal diffusivity, λ = thermal conductivity, b = radial distance from weld, and $\dot{Q}$ = rate of heat input)

THERMAL STRESS ANALYSIS

A numerical method for the analysis of thermal stresses of an elastic-plastic material with temperature dependent coefficients, that is, modulus of elasticity, coefficient of linear expansion, and yield strength, was described previously [7, 8, 9] . In the three-step method discussed here, however, this comparatively complicated procedure is not justifiable, because of the more approximate nature of the temperature analysis. Thus, a less laborious method may be used here. First, the viscous strain components may be included in the plastic strain [4] . Further, the factor $E\alpha$ entering the thermal stress equations may be considered a constant. This appears to be a reasonable approximation because E tends to decrease and α to increase with increasing temperature.

For any fiber of the cross section the stress corresponding to the maximum temperature T_{max} may now be calculated from

$$\sigma_t = \sigma_{init} - E\alpha(T_{max} - T_{init}) + \sigma_{eq}$$

$$|\sigma_t| \leq \sigma_F\ (T_{max})$$

where σ_{init} is the initial residual stress, T_{init} is the initial temperature, σ_{eq} is the "equilibrium stress", and $\sigma_F\ (T_{max})$ is the yield strength corresponding to the maximum temperature. The equilibrium stress, being distributed along a plane for compatibility, is determined from the equilibrium equations.

The final residual stresses σ_r after completed welding and cooling to ambient temperature T_{amb} are computed from a similar equation as above, or

$$\sigma_r = \sigma_t - E\alpha(T_{amb} - T_{max}) + \sigma'_{eq}$$

$$|\sigma_r| \leq \sigma_F\ (T_{amb})$$

The resulting equation systems may be solved by a straight-forward trial-and-error procedure. However, for the case studied here, with a highly localized temperature rise, the calculations can be simplified when applying an iterative computional scheme as described further in Ref. 1. In fact, the convergence is so fast that hand calculations may be used for a specific problem. The various calculations discussed here, including the plotting of results, were programmed for an electronic computer. The computer program can handle any type of shape built up of rectangular component plates.

The relationship between yield strength and temperature used in the predictions was an average curve of literature data for structural steels. A further factor to be considered is the increase in yield strength of the weld area, due to high cooling rates and the effect of higher strength electrode material. For welded structural steel members it was found experimentally [2, 11] that the yield strength of the weld region is of the order of 50 percent above the yield strength of the base material. Thus, in the computations the material that had become liquefied in the heating cycle was assumed to gain a 50 percent increase in yield strength at ambient temperature. For maximum temperatures between the melting temperature and the transformation temperature at approx.727^{o}C for carbon steel, the yield strength after cooling was assumed here to be linear with temperature.

SOME RESULTS

Results of calculations will be exemplified here only for one shape -- an H-shape composed of 356 x 64 mm (14 x 2 1/2 inches) flanges and 254 x 38 mm (10 x 1 1/2 inches) web. Iso-stress diagrams from predictions are given in Fig. 7 for a shape being built up of universal-mill plates and in Fig. 8 for the same shape but of oxygen-cut plates. The initial residual stresses in the parent plates were predicted as shown in Figs. 2 and 3.

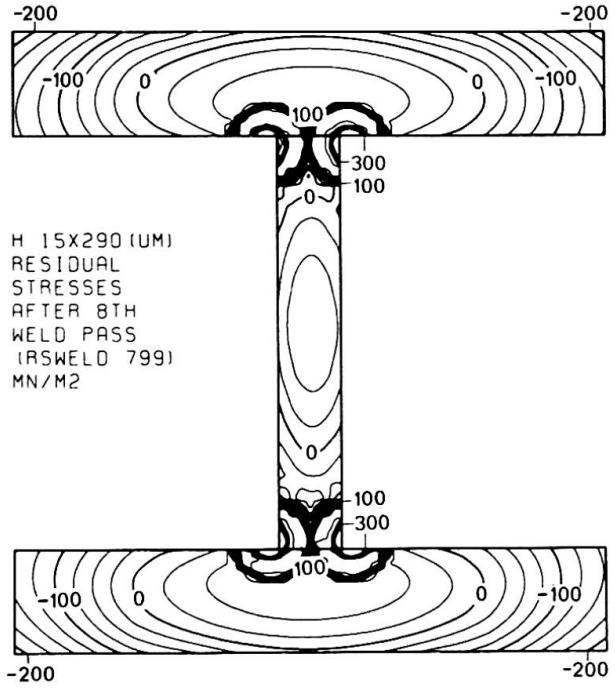

Fig. 7 Iso-stress diagram for predicted residual stresses in a heavy welded H-shape built up of universal-mill plates with as-rolled edges

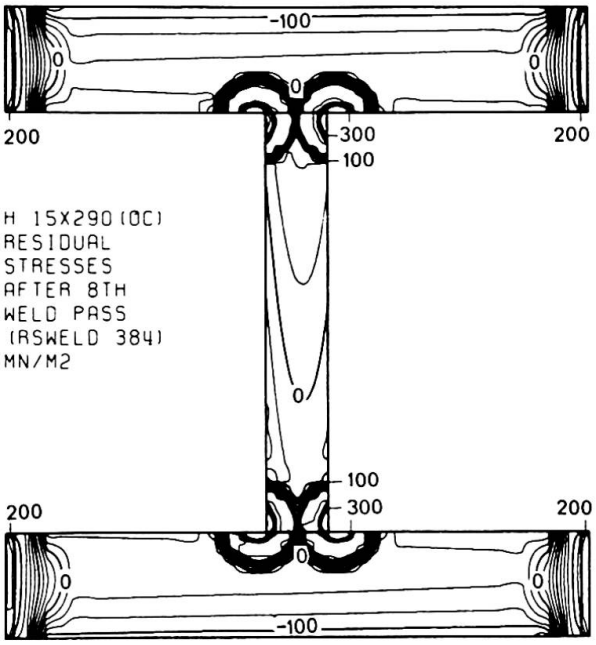

Fig. 8 Iso-stress diagram for predicted residual stresses in a heavy welded H-shape built up of oxygen-cut flange plates

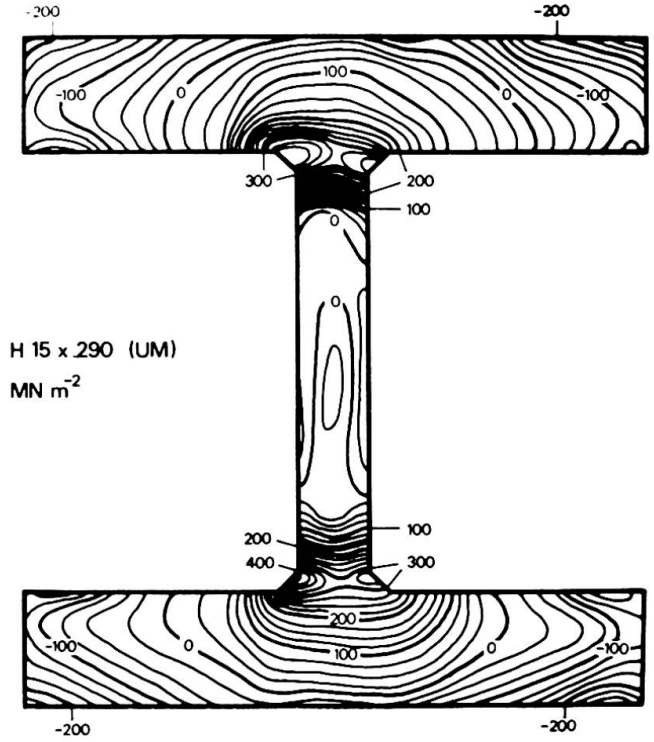

Fig. 9 Iso-stress diagram for measured residual stresses in a heavy welded H-shape built up of universal mill plates with as-rolled edges [2]

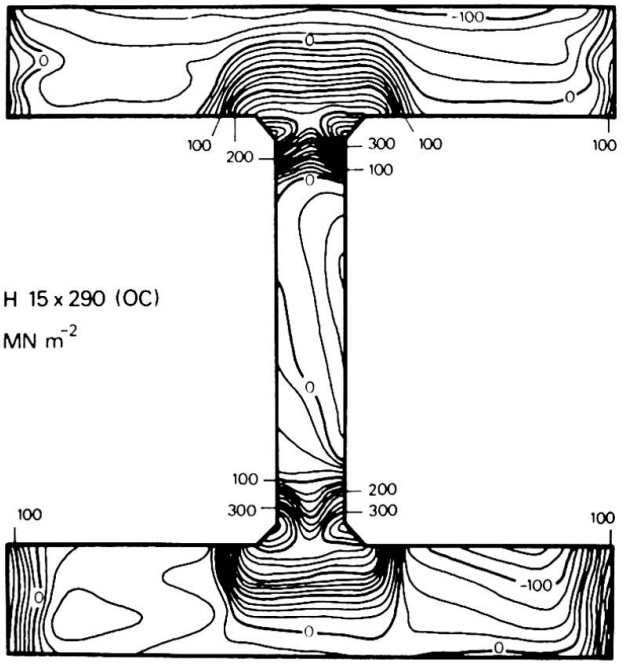

Fig. 10 Iso-stress diagram for measured residual stresses in a heavy welded H-shape built up of oxygen-cut plates [2]

The theoretical results in Figs. 7 and 8 may compared with experimentally obtained results [2] , see Figs. 9 and 10, respectively. There is a satisfying agreement between the predicted and the measured results.

It may be noted by comparing the predicted initial-stress diagrams (Figs. 2 and 3) and the predicted residual-stress diagrams (Figs. 7 and 8) that the effect of the welding is indeed rather small except for in the weld area. It may also be seen that there is a radical difference between the predicted residual-stress distributions in the two members shown in Fig. 7 and Fig. 8, differing only in the manufacturing procedure assumed to have been used for the component plates. These observations, substantiated by further predictions for other shapes [1], verify the same indications drawn from the experimental study [2].

The effect of the high compressive residual stresses in the flanges of Fig. 7 is to reduce column strength, while the tensile stresses at the flange edges of Fig. 8 are beneficial for the column strength of such a member. It appears reasonable that design criteria for heavy columns should recognize this basic difference in properties due to the manufacturing process of welded shapes. The method discussed here for predicting residual stress in such members should be useful for determining the effects of geometry as well as manufacture and fabrication procedures.

ACKNOWLEDGMENTS

The theoretical results in the paper were calculated on an IBM 360/75 at the Stockholm Computer Center with computer time provided by the Office of the Chancellor of the Swedish Universities. Experimental results quoted in the paper for comparison purposes were obtained at Fritz Engineering Laboratory, Lehigh University in an investigation of residual stresses in thick welded plates -- references to the original reports are given in the paper.

REFERENCES

1. G.A. ALPSTEN: Residual Stresses in Heavy Welded Plates and Shapes - A Theoretical Study. In preparation.

2. G.A. ALPSTEN, and L. TALL: Residual Stresses in Heavy Welded Shapes. Welding Journal, Vol. 49, No. 3, March 1970, pp. 93-s - 115-s.

3. D. ROSENTHAL: Mathematical Theory of Heat Distribution During Welding and Cutting. Welding Journal, Vol. 20, No. 5, May 1941, pp. 220-s - 234-s.

4. D. ROSENTHAL: The Theory of Moving Sources of Heat and Its Application to Metal Treatments. Transactions, ASME, Vol. 68, No. 11, November 1946, pp. 849 - 866.

5. L. TALL: Residual Stresses in Welded Plates - A Theoretical Study. Welding Journal, Vol. 43, No. 1, January 1964, pp. 10-s - 23-s.

6. L.S. BEEDLE, and L. TALL: Basic Column Strength. Proceedings of the Structural Division, ASCE, Vol. 86, No. ST7, July 1960, pp. 139 - 173.

7. G.A. ALPSTEN: Egenspänningar i varmvalsade stålprofiler (Residual Stresses in Hot-Rolled Steel Profiles). Institution of Structural Engineering and Bridge Building, Royal Institute of Technology, Stockholm, June 1967.

8. G.A. ALPSTEN: Thermal Residual Stresses in Hot-Rolled Steel Members. Fritz Engineering Laboratory Report No. 337.3, Lehigh University, December 1968 (to be published in the Welding Journal).

9. G.A. ALPSTEN: Prediction of Thermal Residual Stresses in Hot-Rolled Plates and Shapes of Structural Steel. Final Report, 9th IABSE Congress in Amsterdam, May 1972.

10. N.R. NAGARAJA RAO, and L. TALL: Residual Stresses in Welded Plates. Welding Journal, Vol. 40, No. 10, October 1961, pp. 468-s - 480-s.

11. N.R. NAGARAJA RAO, F.R. ESTUAR, and L. TALL: Residual Stresses in Welded Shapes. Welding Journal, Vol. 43, No. 7, July 1964, pp. 295-s - 306-s.

12. Y. KISHIMA, G. A. ALPSTEN, and L. TALL: Residual Stresses in Welded Shapes of Flame-Cut Plates in ASTM A 572 (50) Steel, Fritz Engineering Laboratory Report No. 321.2, Lehigh University, June 1969.

13. F.R. ESTUAR: Welding Residual Stresses and the Strength of Heavy Column Shapes. Ph. D. Dissertation, Lehigh University, August 1965 (University Microfilm, Inc., Ann Harbor).

14. R. BJØRHOVDE, J. BROZZETTI, G.A. ALPSTEN, and L. TALL: Residual Stresses in Thick Welded Plates. Fritz Engineering Laboratory Report No. 337.13, Lehigh University, June 1971.

15. H.W. TOWNSHEND: Discussion to N. S. Boulton, and H.E. Lance Martin: Residual Stresses in Arc-Welded Plates. Proceedings, The Institution of Mechanical Engineers, Vol. 133, 1936, p. 345.

16. G.A. ALPSTEN: Behavior and Strength of Non-Protected Steel Columns Exposed to Fire. In preparation.

17. T.Z. HARMATHY, and W.W. STANZAK: Elevated - Temperature Tensile and Creep Properties of Some Structural and Prestressing Steels. Division of Building Research, National Research Council, Canada, Research Paper No. 424, 1970.

18. P.S. MYERS, O.A. UYEHARA, and G.L. BORMAN: Fundamentals of Heat Flow in Welding. Welding Research Council Bulletin No. 123, July 1967.

SUMMARY

A method for predicting residual stresses in medium-size to heavy welded steel shapes is discussed, and some results are given. The prediction is based upon a three-step analysis of the temperature rise and thermal stresses. The welding stresses are caused by plastic deformations occuring during the welding cycle. The initial residual stresses existing in the parent plates prior to welding are considered in the predictions. These initial stresses are shown to be the major source of residual stresses in a heavy welded member. Predicted results show good agreement with experimental measurements.

RESUME

On discute une méthode pour prédire les tensions résiduelles dans les tôles d'acier soudées de moyennes et grandes dimensions et quelques résultats sont communiqués. La prédiction est basée sur une analyse à trois échelons de l'augmentation de la température et des tensions thermiques. Les tensions dues au soudage sont causées par des déformations plastiques pendant la marche de la soudure. Dans les prédictions on a tenu compte des tensions résiduelles initiales dans les tôles primitives avant le soudage. Ces tensions initiales forment, comme il est démontré, la source principale des tensions résiduelles dans une grande tôle soudée. Les résultats prédits montrent une bonne concordance avec les mesures expérimentales.

ZUSAMMENFASSUNG

Es wird eine Methode zur Vorausbestimmung der Eigenspannungen in geschweissten mittelgrossen und grossen Stahlblechen diskutiert und einige Ergebnisse werden mitgeteilt. Die Vorausbestimmung stützt sich auf eine Dreistufenanalyse der Temperaturerhöhung und thermischen Spannungen. Die Schweissspannungen werden durch plastische Deformationen während des Schweissvorganges verursacht. Die anfänglichen Eigenspannungen in den ursprünglichen Blechen vor dem Schweissen sind in den Vorausbestimmungen berücksichtigt. Diese Anfangsspannungen bilden nachweislich die Hauptquelle der Restspannungen in einem grossen geschweissten Blech. Die vorausgesagten Ergebnisse zeigen eine gute Uebereinstimmung mit den experimentellen Messungen.

Leere Seite
Blank page
Page vide

DISCUSSION LIBRE • FREIE DISKUSSION • FREE DISCUSSION

An Approximate Procedure for Probabilistic Limit Analysis

Une méthode approchée pour l'analyse limite probabiliste

Eine Näherungsmethode für wahrscheinliche Grenzwerte

GIULIANO AUGUSTI
Università di Firenze
Florence, Italy

In the final paragraph of their Introductory Report (Ref.1), Massonnet and Save underline the necessity of "making a considerable effort towards a better knowledge of the laws of material behaviour and of the ways of load application, in order not to lose in the uncertainty of the data all the advances achieved in the methods of calculation".

However, the data of any structural problem (loads, material characteristics, etc.) are, and indeed always will be by their very nature, uncertain: as a matter of fact, they are essentially random, like most physical quantities.

Therefore, it is my strong opinion that further "advances in the methods of calculation" are in danger of remaining pure academic exercises, unless this concept of unavoidable randomness is accepted and rationally taken into account. In other words, the engineering profession will have to be persuaded that certain answers to many problems can be given only by appropriate descriptions (in probabilistic terms) of the uncertainty.

Following this approach, as noted by Massonnet and Save themselves (Ref.1, p.3), the solution of a structural problem could be formulated as a problem of stochastic programming. Unfortunately, this technique appears to be too complicated to be at present acceptable as the basis for practical design procedures, notwithstanding some very recent promising results (Ref.2).

Because of these considerations, in collaboration with Dr. Baratta of the University of Naples, I have been engaged in the development of simpler techniques, based on a fully rigorous and exact theory, but at the same time able to give, by appropriate simplification of the numerical procedures, acceptable approximations of the complete (exact) probabilistic solution with a reasonable computational effort.

So far (Refs.3-8) our attention has been confined to structures that satisfy the basic hypotheses of limit analysis, as summarized in Ref.1, the only difference being that the limit moment Mp (or in general, the local yield strength) is, in each point of the structure, a random quantity with a

given probability distribution law. Consequently, if the load magnitude depends on one scalar parameter $P^{(*)}$, the overall strength of the structure is described by the probability distribution function of the limit (collapse) value of the load parameter, P_L; i.e., by the function

$$F(P) = \text{Prob}\ (P_L \leq P)\ ;\quad 0 \leq P < \infty \tag{1}$$

The procedure that we have proposed consists in the determination of functions that bound F(P) from above and below, thus allowing an evaluation of the degree of approximation achieved. To this aim, in Refs.3 and 4 two theorems have been demonstrated, which are the probabilistic analogues of the two bounding theorems of limit analysis (static theorem and kinematic theorem: cf. Ref.1, ineqs. 2 and 5 respectively).

The bounding theorems, whose practical relevance in classical limit analysis had been rather obscured in the last few years by the development of optimization techniques, regain thus their usefulness in probabilistic limit analysis, where the computational problems are still overwhelming.

In the formulation of the probabilistic theorems, auxiliary distribution functions are defined as follows:

a) let $F_\psi(P)$ be the probability that, investigating a number of stress fields in equilibrium with the loads measured by P, none of these fields is statically admissible (i.e. satisfies the yield condition throughout the structure);

b) let $F_\gamma(P)$ be the probability that, investigating a number of possible collapse mechanisms, at least in one case the loads measured by P are found kinematically sufficient (i.e., such that the power of the loads exceeds the dissipated plastic power).

It has then been proved that

$$F_\psi(P) \geq F(P) \geq F_\gamma(P) \tag{2}$$

for any function $F_\psi(P)$ and any function $F_\gamma(P)$.

It has also been shown that the average and the variance (dispersion) associated with the function F(P) can be conveniently bounded when a function $F_\psi(P)$ and a function $F_\gamma(P)$ are known.

The ease of calculation of the bounding functions $F_\psi(P)$ and $F_\gamma(P)$ depends on the number and complexity of the investigated mechanisms and stress fields. Numerical examples have shown that even the crudest assumptions may yield technically relevant results (Refs.3-4); however, if the initial choices did not lead to acceptably close bounds, the process could be repeated with different assumptions. Some appropriate artifices to increase convergence have been proposed (Ref.5); in general it is worth underlining that an increase in the closeness of the bounding functions requires a great increase in the amount of computational work, often unwarranted by the present scarce knowledge of the input statistical properties.

Further current studies deal with the extension of our procedures to multi-parameter loading (Ref.6), in particular to variable repeated loads that may cause incremental collapse (Ref.7), and with the formulation of the static approach in very general terms (Ref.8).

(*) The same symbols as in Ref.1 (rather than those of Refs.3-8) are used, as far as possible, in this contribution.

For a comparison with works by other authors, it is interesting to remark that the presentation of ineqs.(2) as the basis of our treatment shows that the results obtained via the kinematic approach are inherently unsafe: in fact, unless all possible collapse mechanisms are taken into account, for any value of the load parameter P a probability of collapse $F_\gamma(P)$, smaller than the actual one F(P), is calculated. However, all other works with similar aims that are known to the writer, have made exclusive use of the kinematic approach (cf. e.g. Refs.9-11): these works, explicitly or implicitly, rely on the fact that, in most if not all of the few examples of probabilistic limit analysis so far published, $F_\gamma(P)$ is a very close evaluation of the true distribution, even if not many mechanisms are investigated. Therefore, when by an appropriate truncation in the calculation of $F_\gamma(P)$, an upper bound to this distribution

$$F_+(P) > F_\gamma(P) \tag{3}$$

is obtained (Ref.9), it is quite likely that the true distribution has been bounded on both sides, i.e.

$$F_+(P) \gtrsim F(P) \gtrsim F_\gamma(P) \tag{4}$$

The present writer, however, thinks that the validity of ineq.(4), which is based on the closeness of $F_\gamma(P)$ and F(P), should still be tested in many more examples before being taken for granted in general: it is worth underlining that the number of mechanisms which may contribute to the probability of collapse, is very large even for the simplest structure. For example, the portal frame investigated in Refs.3-4, where the possibility of plastic deformations is concentrated in 11 sections, has more than 200 significant mechanisms (Ref.8).

The only rigorously safe (upper) bound $F_\psi(P)$ to the true probability of collapse F(P) is obtained via the static (equilibrium) approach, which has been proposed for the first time in Refs.3 and 4. It must, however, be admitted that in simple (perhaps unrealistic) examples the latter approach yields, with comparable amount of computations, a much worse approximation (albeit on the safe side) than the kinematic approach: on the other hand, the static approach appears to yield better to generalizations and extensions (Ref.8).

As a matter of fact, the determination of an $F_\psi(P)$ is immediate if the joint probability distribution of the local strengths is known. Therefore, if for instance the individual distributions of the local strengths are not the normal ones usually assumed in the demonstrative examples (but are statistically independent), each point of $F_\psi(P)$ is still given by a product of n terms (n being the number of elements into which the structure has been divided for the computations); on the contrary, each point of $F_\gamma(P)$ involves the calculation of an n-fold integral.

Lifting of the unrealistic assumption of statistical independence of the local strengths is a very complicated (and as yet, little investigated) problem, whose solution the writer thinks essential to increase the practical relevance of probabilistic structural analysis. However, once this problem is solved, the static approach guarantees that no new computational problems will be raised.

Finally, note that, differently from other authors (e.g. Refs.2, 12), we have separated the variables concerning strength (among which geometrical and other parameters could be included) from the variables concerning loads: each group of variables can be deterministic or stochastic. For example, if the strength variables are deterministic, all procedures reduce to the classical limit analysis, with all its properties, as explicitly pointed out in Ref.6.

REFERENCES

1) Ch. Massonnet, M. Save: "L'influence de la plasticité et de la viscosité sur la résistance et la déformation des constructions". A.I.P.C./ I.A.B.S.E. 9th Congress; Introductory Report, 1971.

2) C. Gavarini, D. Veneziano: "Minimum weight limit design under uncertainty". Meccanica, AIMETA (in the press).

3) G. Augusti, A. Baratta: "Analisi limite di strutture con variazioni aleatorie di resistenza". 1st Italian Natl.Congr.Theor. & Applied Mechs. (AIMETA), Udine, 1971.

4) G. Augusti, A. Baratta: "Limit analysis of structures with stochastic strength variations". Journ.Structural Mechs., Vol.1, No.1, 1972.

5) A. Baratta: "An improvement in the static method for limit analysis of structures with stochastic strength variations". Journ.Structural Mechs. (in the press).

6) G. Augusti, A. Baratta: "Theory of probability and limit analysis of structures under multi-parameter loading". International Symposium on Foundations of Plasticity (A. Sawczuk, Editor); Wolters-Noordhoff, Groningen 1972.

7) A. Baratta, G. Augusti: "Shakedown of plastic structures with stochastic strengths (in preparation).

8) A. Baratta: "The static approach in probabilistic limit analysis" (in preparation).

9) C.A. Cornell: "Bounds on the reliability of structural systems". J.Struct.Div., ASCE, Vol.93, No. ST 1, 1967.

10) F. Moses, J.D. Stevenson: "Reliability-based structural design". J.Struct.Div., ASCE, Vol.96, No. ST 2, 1970.

11) J.D. Stevenson, F. Moses: "Reliability analysis of frame structures". J.Struct.Div., ASCE, Vol.96, No. ST 11, 1970.

12) C. Gavarini, D. Veneziano: "Sulla teoria probabilistica degli stati limite delle strutture". Giorn.Genio Civ., Vol.108, Nos.11-12, 1970.

Fliessgelenklinien-Analyse der senkrechten und schiefen Platten-Balken-Brückenkonstruktionen

Yield-Line Analysis of Reinforced Concrete Right and Skew Beam-Slab Bridge Structures

Analyse des lignes de rupture des poutres en té rectangulaires et obliques de ponts en béton armé

TIBOR JÁVOR
Doc. Ing. CSc.
Bratislava, CSSR

Anknüpfend an die Abhandlungen von Prof. Freudenthal, die im Vorbericht zu dem I. Thema des Kongresses der IVBH veröffentlicht wurden, können wir feststellen, dass die Grenztragfähigkeit der Platten üblich hilfs der Kraft- oder kinematischen Methode gelöst wird. Indem die Kraftmethode bei der Grenztragfähigkeit von Platten in der Gleichheit der Innenkräftenmomente gegründet ist, bedingt die kinematische Methode eine Gleichheit zwischen der Virtualarbeit der Aussen- und Innenkräfte.

An der Tragfähigkeitsgrenze wandelt sich eine Platte in einen beweglichen Mechanismus um. Unter der Wirkung einer Aussenkraft biegt sich dieselbe um einen Betrag z.B. δ und die Kraft P_m leistet dabei eine Arbeit $P_m \cdot \delta$. Die einzellnen Plattenteile drehen sich gegeneinander in plastischen Zylindergelenken um die Winkel φ. Dieses Nachdrehen hindern die Grenzmomente $m_T \cdot r_i$, die in den Zylindergelenken wirken und dabei wird die Arbeit $m_T \cdot r_i \cdot \varphi$ geleistet.

Bekannt ist der Lösungsvorgang der senkrechten und schieffen isotropen oder ortotropen Platten in den Beiträgen von Johansen, Wood, Jones, Sobotka, Nagaraja, Sawczuk und Jaeger u.A. Gelöst sind sowohl senkrechte durch einen Trägerrost gestützte Durchlaufplatten, wobei üblich der Fall gelöst wird, wo die

Grenztragfähigkeit der Platte etwas früher als die der stützenden Rippen ausgeschöpft wird. Weniger vollkommen sind die Beiträge zur Lösung der Platten-Rost-, der sogenannten Platten-Balken-Brückenkonstruktionen, schieffen, oder gekrümmten im Grundriss.

Bei allen Lösungen der Platten-Balkensysteme hilfs der Fliessgelenklinien-Analyse /Bruchlinien-/ erhebt sich die Frage des Beitrags der Zusammenwirkung der Platte mit den Balken, Abgrenzung einer Lösung des Falles als T-Querschnitt, oder einer Durchlaufplatte auf einem Trägerrost, als weichen /nachgiebigen/ Lagerung. Nur in wenigen Fällen wird die Torsionsteifigkeit der Träger als auch die Beiwirkung der Querträger ansichts ihrer Torsionsteifigkeit bedacht. Dieses Problem erwies sich besonders bei schieffen Konstruktionen mit einer grösseren Anzahl von Trägern aktuell, da die Torsionsteifigkeitsfrage der Balken nicht mehr ausser Beachtung bleiben kann.

Wir beschäftigen uns mit senkrechten, schieffen und im Grundriss gekrümmten Platten-Balken-Strassenbrücken, die wir mittels verschiedener Lastsysteme bis zur Zerstörung geprüft hatten. Die Brücken wurden unter Kombination der Bruchlinientheorie und der Bruchgelenktheorie entworfen und die Ergebnisse hilfs der in der linearen Elastizität üblichen Theorie verglichen. Die im Massstab 1 : 4 hergestellten Modelle wurden auf entgegenstehenden Ränden frei gelagert unter Trägern und völlig frei unter den bleibenden zwei Ränden. Die Belastungsverteilung in den schieffen Ecken und in den Stützen wurde mittels Messdosen und Dehnungsmessstreifen nachgeprüft. Die untersuchten Modelle besassen je 4 Hauptträger, die durch die obenliegende Stahlbetonplatte und Querträger über der Auflagerung verbunden waren. Die Messungen erfolgten sowohl in den Labors der University of Manitoba in Canada als auch der VÚIS in Bratislava, ČSSR.

Die Fliessgelenklinien-Verläufe an der Oberfläche der Modelle sind charakteristisch und allgemein erwartet. Bemerkenswert ist der Verlauf der Spiralrisse an den durch eine einsame Last exzentrisch belasteten Trägern. Ihr Verlauf ist von der Torsionfestigkeit sowohl der Hauptträger, als auch

der Querträger auf beiden Enden abhängig. Der Fliesslinienverlauf bei vorgespannten Modellen ist von den nicht vorgespannten kaum unterschiedlich. Die Träger der vorgespannten Modelle verhielten sich jedoch als Querschnitte typisch vorgespannte mit einer geringen Anzahl von Biegungsrissen, wobei die Zerstörung durch eine Schubbelastung erfolgte.

Die in Bratislava erfolgten Dehnungsmessungen wurden vollautomatisiert u.zw. mittels der Messzentrale MBM 5000 an das Lochstanzengerät ADDO geschaltet, das direkt mit dem Rechenautomaten PDP 8 verbunden war. Die Messergebnisse wurden auf dem Rechenautomat sofort ausgewertet und in Tabellenform verarbeitet. So gewonnen wir bereits die Beträge der Hauptspannungen, der Höchst. Schubspannungen, die Richtungen der Hauptspannungsachsen usw. Die Ergebnisse der Versuche wurden mit der theoretischen Analyse verglichen. Die Abschlüsse zeigen, dass die Kombinationsmethode der Bruchlinien und der Bruchgelenke für Platten mit zwei Hauptträger gültig ist. Für den Entwurf von Platten-Balken-Konstruktionen mit drei oder mehreren Trägern empfehlen wir eine neue Verwendung der Fliessgelenklinientheorie, u.zw. in zwei Schritten: Der erste liegt in der Bestimmung der Querverteilung der Belastung mittels der klassischen Theorie, die bei Trägerrösten oder Waagerechten Rahmen verwendet wird, wobei die berücksichtigung der verschiedene Torsionsteifigkeiten bei einzellnen Trägern des Rostes von grosser Wichtigkeit ist. Der zweite Schritt liegt in der Untersuchung der einzellnen Platten zwischen der Balken mittels der Fliessgelenklinientheorie und zwar unter Belastung mittels zwei Lastengruppen. Die Erste Gruppe bilden Läste die die Platte direkt belasten, die zweite Gruppe wird durch Trägerwirkungen gebildet, d.h. durch den Einfluss verschiedener geradliniger Belastungen oder Momente die aus der Berechnung der Querverteilung der Belastung längs einzellner Träger erworben wurden. Die Träger werden dann auf der Tragfähigkeitsgrenze zugleich mit der Platte beurteilt u zw. durch Einführung der Momenten- Durchbiegungs- und Torsionskapazität in Bruchgelenken der Träger und Torsionskapazität in Gelenken der End-Querträger.

Die derart erworbenen Momente an der Trägfähigkeitsgrenze berücksichtigen wir bei dem Bewehrungsentwurf der Träger, die durch kombinierte Belastung mittels einer Schieffen Durchbiegung und Torsion beansprucht sind. Die Lagerung der vorgespannten und nicht vorgespannten Hauptbewehrung als auch der Schubkraftbewehrung in Beziehung zu verschiedenen Arten besonders von Kastenträgern untersuchten wir im Rahmen einer umfangreichen Forschung an Gips- und Betonmodellen, als auch durch Messungen an Baustellen. Diese Fragen beeinflussen demnächst sowohl die richtige Beurteilung der Lastkraftverteilung am Trägerrost oder Platten-Balkensystem, beeinflussen also den gesammten Lösungsvorgang ganz vom Anfang.

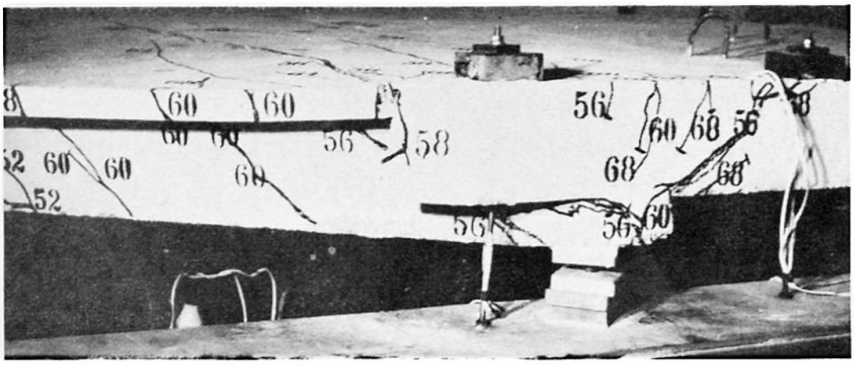

Abb.1. Der Verlauf der Risse im stumpfen Ecke des Stahlbetonmodells der Platten-Balkenbrücke.

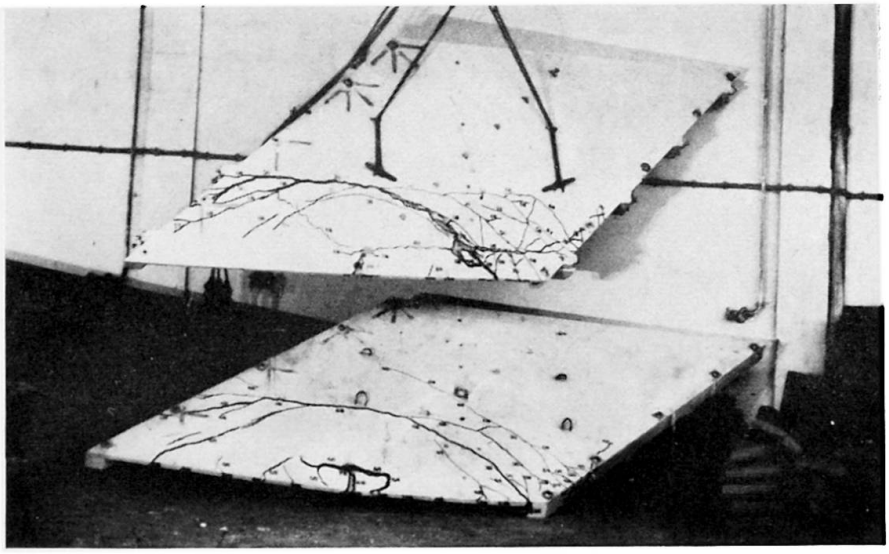

Abb.2. Die Fliessgelenklinien an der Oberfläche der stahlbeton /unten/ und der vorgespannten /oben/ Platten-Balken-Brückenmodelle.

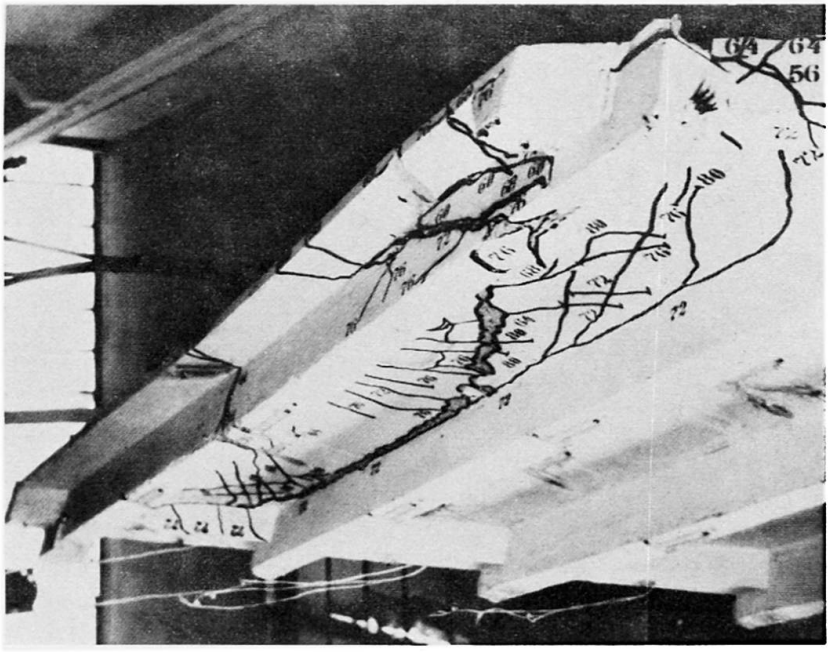

Abb.4. Ein vorgespanntes Modell der Platten-Balkenbrücke beim Versuch mit der Messzentrale MBM 5000.

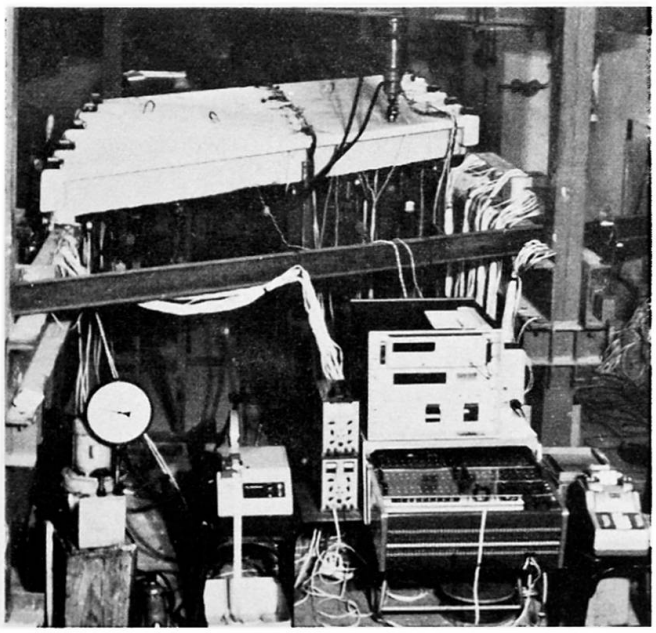

Abb.3. Die Träger des vorgespannten Modelles mit einer geringen Anzahl von Biegungsrissen, wobei die Zerstörung durch eine Schubbelastung erfolgte.

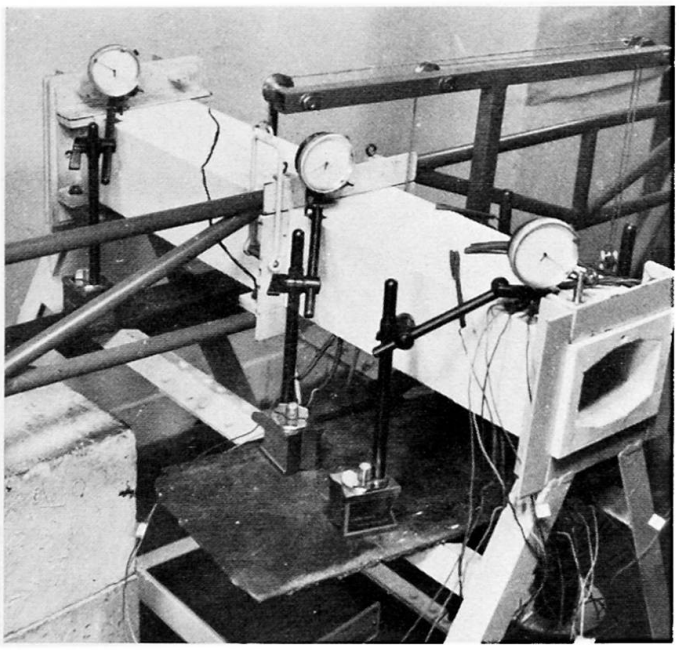

Abb.5. Die Schubkraftbevehrung- und die Torsionsteifigkeituntersuchungen mittels Gips-modellen.

ZUSAMMENFASSUNG

Plattenbalkenfahrbahnen von geraden, schiefen und gekrümmten Strassenbrücken mit I-Trägern wurden unter Belastung mit schweren Fahrzeugen bis zur Zerstörung geprüft. Für den Entwurf von Plattenbalken mit drei oder mehreren Trägern empfiehlt sich eine neue Anwendung der Fliessgelenklinientheorie. Aus den Versuchsergebnissen ist zu schliessen, dass die plastische Bruchmethode der Berechnung von Bauwerken mit Plattenbalken aus Stahlbeton ein einfaches Mittel zur Bestimmung der Festigkeit eines solchen Bauwerkes unter mehrfacher statischer Belastung bildet; vorausgesetzt, dass die Lastverteilung unter Berücksichtigung der Torsionssteifigkeit der Träger richtig berechnet wird.

SUMMARY

Right, skew and curved beam-slab highway bridge decks were tested to destruction under a system of heavy wheel loads. For design of beam-slabs with three or more beams a new application of yield-line theory is recommended. From the results of tests presented, it would appear that the plastic collapse method of analysing reinforced concrete beam-slab structures is a reasonably simple mean of establishing the strength of such a structure under several static loading, if the load distribution is correctly calculated, taken into account the torsion rigidity of the beams.

RESUME

Des tabliers de ponts-routes à poutres en té droits, obliques et courbes ont été examinés jusqu'à la rupture sous des charges de véhicules lourds. Pour le projet de poutres en té avec trois ou plusieurs poutres, une nouvelle méthode par l'analyse des lignes de fluage est recommandée. Les résultats d'essais montrent que la méthode d'analyse limite plastique de structures à poutres en té en acier-béton constitue un moyen simple pour la détermination de la résistance d'une telle structure sous charges statiques multiples, si la distribution de la charge, compte tenu de la rigidité torsionnelle des poutres, est correctement calculée.

Leere Seite
Blank page
Page vide

Prestressed Concrete Box Girders

Poutres en béton précontraint à section en forme de caisson

Vorgespannte Betonkastenträger

A. D. EDWARDS
Senior Lecturer
Department of Civil Engineering
Imperial College
London, England

D. N. TRIKHA
Reader in Civil Engineering
University of Roorkee
India

Introduction

The behaviour, in the post-cracking phase, of reinforced or prestressed concrete box girders subjected to eccentric loads is complex due to the anisotropy and non-linearity of the concrete, the non-linearity of the steel, and, not least, to the change of structural topology due to the initiation and propagation of cracks.

Experimental investigations of reinforced or prestressed concrete beams have been mostly restricted to the determination of crack widths and crack spacing, and to the establishment of empirical relations for the assessment of the ultimate load carrying capacity. Recently Ngo and Scordelis (1) have reported an elastic finite element analysis of reinforced concrete members in which the cracks must be prelocated on the basis of prior knowledge. A linear spring linkage was introduced to represent the bond between steel and concrete. Nilson (2) extended this approach by taking into account the non-linearity of the materials and by simulating the deterioration of bond by using non-linear springs. This approach, however, only allows development of cracks along predefined element boundaries and requires the preparation of new input data after each crack initiation. It does not consider directly the redistribution of stresses due to the energy released by cracking, nor does it consider box girders.

An automatic incremental iterative finite element procedure for the complete analysis of post-tensioned box girders (3) has been developed which takes account of many of the above problems. The three dimensional character of the girders is synthesised and structural actions such as shear lag, load diffusion, and distortion of the box are automatically included in the analysis. The effect of diaphragms of given shear and warping stiffness placed anywhere in the structure can be investigated. To prove the program, a series of twelve post-tensioned simply supported, but torsionally restrained, single cell box girders were tested to destruction under various midspan bending moment/torsion moment ratios (4). The strain distribution, first cracking load, crack pattern, deflection characteristics, and collapse load were compared with those predicted by the analysis.

Analytical Procedure

The flanges and webs of the box are represented, in the usual way, by finite elements lying in the appropriate planes and interconnected at their nodes. Rectangular and triangular membrane elements are used to idealise the concrete, and bar elements are used for the longitudinal, transverse, and shear reinforcement. The steel elements are connected to the adjacent concrete elements at the common nodes. Although the flexural stiffness of the elements forming the structure is neglected, the distortional stiffness of the box is simulated in the assembly of the structural stiffness, as explained later.

The structure is first analysed as an ordinary reinforced concrete one, the prestress being applied as external forces. The contribution of the prestressing steel to the overall stiffness is neglected since, at this stage, the steel is unbonded. For the subsequent application of external loads, the prestressing steel is assumed to be bonded to the concrete and the prestressing steel element stiffnesses are included in the overall structural stiffness matrix.

The external loads are applied in small steps, the element stiffnesses for each load increment being deduced from the state of strain at the end of the previous load step, and from the predicted strain increment for the current load step. The superposition of strains to obtain the total strain is carried out along fixed although arbitary axes.

Material Properties

At the engineering level, concrete in its hardened state can be considered as having no directional dependence as regard its mechanical and physical properties. However, different strain levels are attained in the principal directions of an element after each increment of load. As a consequence, the instantaneous "elastic" constants in the two principal directions differ. The concrete is, therefore, treated as an isotropic material with the principal directions of elasticity coinciding with the principal directions of stress. In the absence of any quantitative evidence, it is assumed that the stress-strain relationship for concrete in a biaxial state of stress is the same in the two principal directions, and is identical to the one for uni-axial state of stress (5).

The stress-strain relationship for prestressing steel was obtained experimentally, and a third degree polynomial fitted to the results by linear regression analysis. For all other reinforcement, a single bi-linear law based on experimental results was adopted.

Diaphragms and Distortional Rigidity

The shear stiffness of a diaphragm is simulated by considering it to be an ordinary plane stress rectangular element connected at its nodes to the four corners of the box. Since the flexural stiffness of the elements is not included in the analysis, the warping restraint provided by the diaphragm is calculated on the basis of a square plate subjected to four self equilibriating corner loads. For the case of rectangular diaphragms, an equivalent square plate is adopted.

The distortional rigidity of the box is simulated by introducing imaginary diaphragms of appropriate shear stiffness at each mesh line.

Structural Stiffness

The stiffness of the structure is redefined at the beginning of each load increment to take into account the non-linearity of the materials and the

partial loss of stiffness of newly cracked elements.

Once the principal tensile stress in a concrete element exceeds the allowable tensile stress, a crack is assumed normal to its direction and passing through the centroid. The inclination of the crack remains fixed thereafter. The element after cracking cannot sustain stresses normal to the direction of the crack. For an element with two nodes common with a prestressing steel element, the loss of stiffness due to cracking is made gradual to correspond to the increasing deterioration of bond with load.

The forces released by cracking are redistributed using the stiffness of the elements corresponding to the tangent moduli of elasticity at the time of cracking. Normally, after the first redistribution of the release forces, a search is made for further cracking and the new release forces are applied with the next load increment. However, an option is retained in the program such that it is possible to carry on redistributing release forces until no further cracking takes place, or until less than a given number of elements crack.

The box girder is assumed to fail due to the deterioration of the structural stiffness matrix caused either by high compression in the concrete or by excessive cracking, or by "local" yielding of the steel. If the analysis fails by one of these causes, the load increment is reduced and a reanalysis carried out.

Comparison of Analytical and Test Results

The analytical results obtained for the girders of the previously mentioned test program were compared with the experimental results (6). The girders had spans of 4.57 m and 2.74 m and had various span/depth ratios. The mid-span bending moment/torsion moment ratios investigated were 0, 1.0, 1.5, 2.0 and ∞. For the data reported here, the dimensions and reinforcement of the girders were as in fig. 1, the mid-span bending moment/torsion moment ratio for girder B6 was 1.0 and that for girder B7 was 2.0.

The analytical history of loading for girder B7 is given in table 1. The second load increment was made three times the size of the first load increment. The analysis failed at a downward web load of 60.0 kN plus the release forces due to 41 elements cracking. The failure was due to excessive steel strain. The downward web load was then reduced to 50.0 kN, and the release forces due to 41 elements that had previously cracked, but which had been carried forward to load stage V, were applied. This caused a further 30 elements to crack, and when the release forces corresponding to these were applied, the analysis again failed due to excessive steel strain. The downward web load was reduced to 45.0 kN and further iterations carried out with release forces due to cracking. The girder was subsequently analysed at smaller load increments in order to establish the first cracking load, and the deflection characteristics, more accurately.

Fig. 2 shows the analytical and experimental results obtained for the deflection at the point of application of the downward web load at mid-span for girders B6 and B7. It can be seen that reasonable agreement was obtained throughout the whole of the load history.

The first visual cracks in the test on girder B6 were recorded at a downward web load of 27.9 kN. In the analysis 2 elements cracked at 25.0 kN and a further 7 elements cracked at 30 kN.

The first visual cracks in the test on girder B7 were recorded at a downward web load of 21.9 kN. In the analysis 4 elements cracked at 20.0 kN and a further 26 cracked at 25.0 kN.

The 'safe' theoretical values for the downward web collapse load were 50.0 kN for girder B6 and 45.0 kN for girder B7. The corresponding collapse loads were 50.8 kN and 46.8 kN.

The predicted crack pattern for girder B7 is shown in the left hand half and the experimental crack pattern is shown in the right hand half of fig. 3. In the analytical crack pattern, the longitudinal cracks due to transverse bending are shown to extend for the full length of the beam. These cracks were not computed by the program and are only intended to show the expected position of the transverse bending cracks. It should be pointed out that the analytical crack pattern is only a reasonable representation of the cracks occurring in individual elements.

Conclusions

Comparison of analytical and experimental results shows that the method is capable of predicting deflections, crack patterns, first cracking loads and collapse loads with reasonable accuracy.

References

1) NGO, D., and SCORDELIS, A. C., Finite element analysis of reinforced concrete beams. Journal of American Concrete Institute, 1967, 64 (March) 152 - 163.

2) NILSON, A. H., Finite element analysis of reinforced concrete. Ph.D. thesis, University of California, Berkeley, May 1967.

3) TRIKHA, D. N., An analytical and experimental investigation of post-tensioned single cell box girders. Ph.D. thesis, University of London, October, 1971.

4) TRIKHA, D. N., and EDWARDS, A. D., An experimental study of post-tensioned single cell box girders. Paper submitted to Journal of American Concrete Institute.

5) DESAYI, P., and KRISHNAN, S., Equation for the stress-strain curve of concrete. Journal of American Concrete Institute, 1964, 61 (March) 345 - 350.

6) TRIKHA, D. N., and EDWARDS, A. D., Analysis of concrete box girders before and after cracking. Paper submitted to Institution of Civil Engineers.

Load Stage	Increase in downward web load kN	Total downward web load P(kN) + (no. of cracked elements loading structure)	Distributed cracked elements. 1st iteration	Carried over cracked elements	Remarks
I	-	-	-	-	Prestress only
II	10.0	10.0	0	0	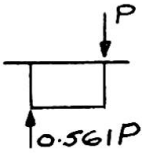
III	30.0	40.0	104	67	
IV	10.0	50.0 + (67)	65	41	
V	10.0	60.0 + (41)			Steel strain > 0.015
IV(a)					
(i)	0.0	50.0 + (41)	-	30	
(ii)	0.0	50.0 + (30)	-	-	Steel strain > 0.015
IV(b)					
(i)	5.0	45.0 + (67)	-	56	
(ii)	0.0	45.0 + (56)	-	42	
(iii)	0.0	45.0 + (42)	-	31	
(iv)	0.0	45.0 + (31)	-	10	Time lapse

Table 1

History of loading (analysis) for Beam 7

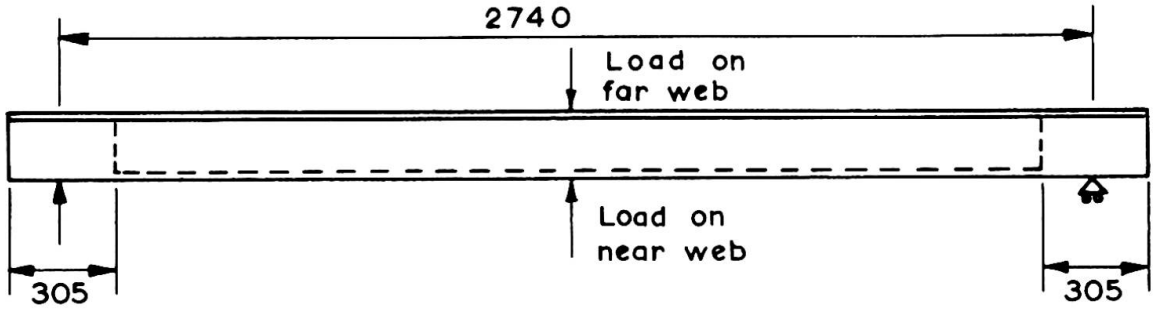

ELEVATION

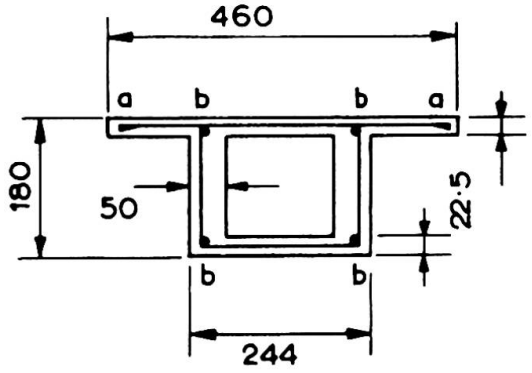

Prestressing steel not shown
Bar 'a' 3·2 ϕ at 150 ℄
Bar 'b' 6·35 ϕ
Stirrups 5·5 ϕ at 150 ℄

CROSS - SECTION

Fig. 1 Girder dimensions and reinforcement

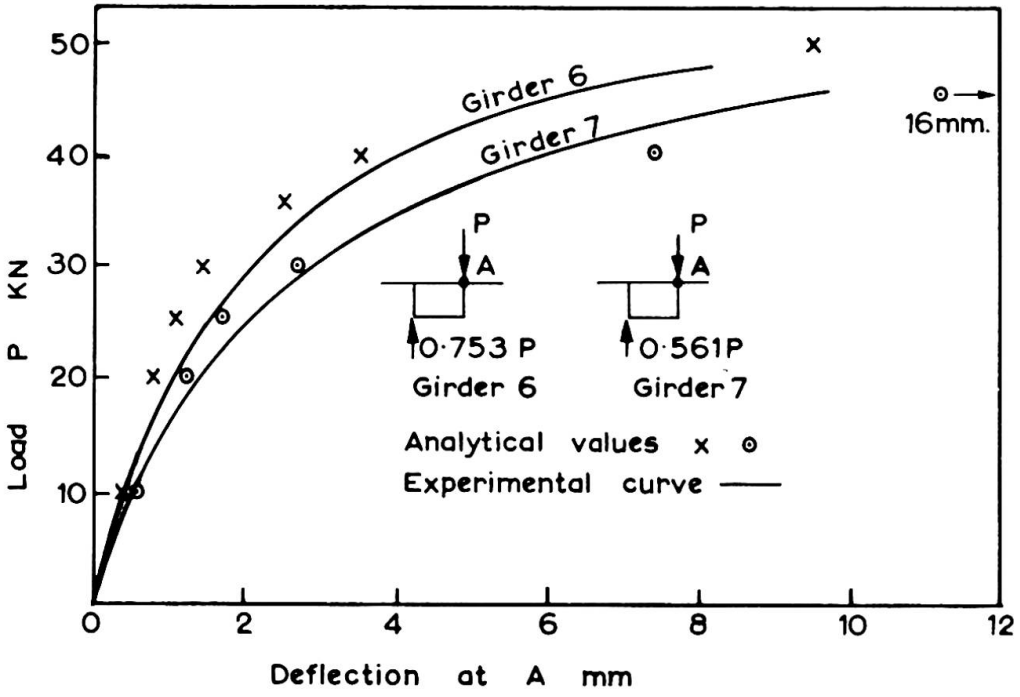

Fig. 2 Vertical deflection

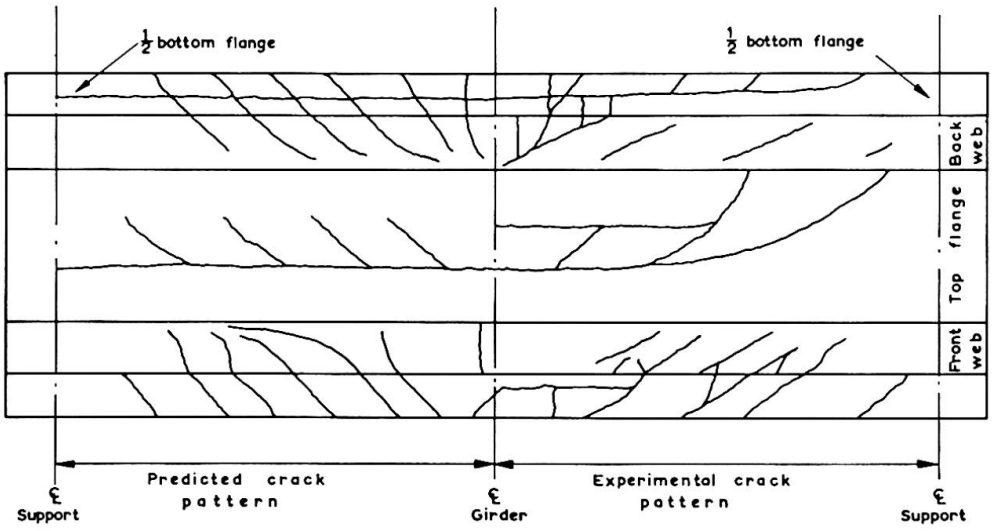

Fig. 3 Predicted and experimental crack patterns Girder B6

SUMMARY

An automatic incremental iterative finite element procedure for the analysis of post-tensioned box girders subject to combined bending and torsion in the uncracked and post-cracking range is reported. The results of the analysis of two post-tensioned single cell box girders, each subjected to a different midspan bending moment/torsion moment ratio, are given, and compared with the experimental results obtained from the corresponding concrete model tests.

RESUME

Ce travail présente une méthode progressive d'analyse itérative automatique, basée sur les éléments finis, pour l'étude de poutres en caisson précontraintes soumises à la flexion et à la torsion dans le domaine non-fissuré et le domaine fissuré. On nous donne ici les résultats de l'analyse de deux poutres en caisson "post-tendues", soumises toutes deux, au milieu de la portée, à différents rapports moment de flexion/moment de torsion. Ces résultats théoriques sont comparés ensuite avec les résultats obtenus lors de tests sur des modèles correspondants en béton précontraint.

ZUSAMMENFASSUNG

In diesem Beitrag wird ein Verfahren zur Berechnung von nachgespannten Kastenträgern unter kombinierter Biegung und Torsion im ungerissenen und gerissenen Zustand vorgestellt. Das iterative und automatisch wachsende Verfahren beruht auf endlichen Elementen. Die Rechenergebnisse von zwei nachgespannten, einzelligen Kastenträgern, von denen jeder in der Mitte durch ein anderes Verhältnis Biegemoment zu Torsionsmoment belastet ist, werden aufgezeigt und mit verschiedenen experimentellen Ergebnissen verglichen, die aus den entsprechenden Modellversuchen gewonnen werden.

Leere Seite
Blank page
Page vide

Einfluss der Viskosität und Plastizität auf Verformung und Traglast

The Influence of Viscosity and Plasticity on the Deformation and the Ultimate Strength

Influence de la viscosité et de la plasticité sur la déformation et la charge ultime

J. J. RIEVE
Dr.-Ing.
Düsseldorf, BRD

Der Einfluß der Viskosität und Plastizität auf die Verformung biegesteifer Stahlbetonstäbe läßt sich einfach und übersichtlich an der Figur 1 erörtern, bei der die Randzerrungen ε_b des Betons und ε_e des Stahles über die bezogene Bewehrung μ/μ_G aufgetragen sind (μ_G = Grenzbewehrung). Die Verformungen des biegesteifen Stahlbetonstabes ergeben sich aus der Summe der Zerrungen der Einzelbaustoffe, wobei der Einfluß der Einzelbaustoffe auf die Gesamtverdrehung $\varepsilon_e + \varepsilon_b = h\,d\varphi$ abhängt von der bezogenen Bewehrung μ/μ_G . Vereinfachend bleibe die Plastizität des Betons außen vor und es gilt dann: Viskosität gehört zum Beton und Plastizität zum Stahl. Die Waageachse der Fig. 1 trägt sowohl nach links wie auch nach rechts die bezogene Bewehrung μ/μ_G auf, nach oben die Betonstauchung ε_b des Druckrandes, nach unten die Stahlzerrung ε_e der Stahleinlagen. Links stellt den ν-fach Gebrauchs-, rechts den Bruchzustand dar. Links gilt: $\varepsilon_e = \varepsilon_{ep}$, für $\mu/\mu_G \leqq 1$. Es gibt im Stahlbeton kein Mindestwertprinzip des Baustoffaufwandes, wie im Einführungsbericht [1] beschrieben; denn die Stahleinlagen sind stets ausgenutzt. Traglastverfahren bringen keine kleinere Stahlmenge als die Elastizitätstheorie, sondern nur eine andere Verteilung. Eine entscheidende Aussage der linken Seite liegt dort, wo sich zeigt, daß die Betonstauchung und damit auch Spannung mit zunehmendem μ/μ_G parabelförmig zunimmt bis zum Rechenwert, der für $\mu/\mu_G = 1$ erreicht wird. Stahlbetonstäbe können Zwang rissefrei über die Viskosität abbauen, aber nur bei $\mu/\mu_G >> 0$ und großer Kriechzahl φ . Rechts stehen die Bruchmomente, die ungefähr sich über die Waageachse und Lotachse gegen-

über dem Gebrauchszustand spiegeln. Wo links unten ε_e = const, jetzt rechts oben ε_b = const, wo links oben ε_b wächst mit μ/μ_G jetzt rechts unten ε_e wächst mit μ/μ_G. Dieser Anstieg kommt aus der plastischen Verzerrung der Stahleinlagen und bringt grobe Risse. Freudenthal [2] weist zurecht darauf hin, wie gefährlich diese Verformung ist. Sie tritt nur auf für $\mu/\mu_G << 1$. Fig. 1 zeigt: in einem Querschnitt kann man nicht beides haben: große Viskosität und große Plastizität. An der Stelle $\mu/\mu_G \sim 1$ hat ein Stahlbetonstab ohne Kriechen eine Verformmöglichkeit, die der eines Stahlstabes im elastischen Bereich entspricht. Darauf läßt sich keine Traglast aufbauen.

Viskosität des Betons tritt nur auf, wenn die ständigen Lasten oder Kräfte einen wesentlichen Teil der Gesamtlast oder Kraft ausmachen.

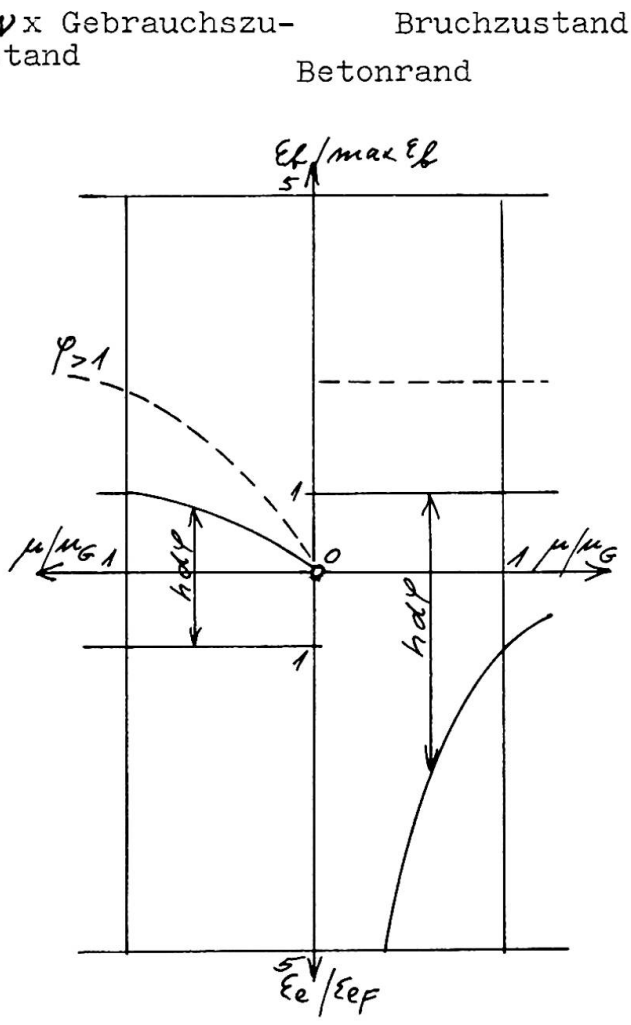

Fig. 1

Damit gilt: eine rissefreie Umverteilung tritt nur für ständige Lasten, Schwinden und einsinniger Stützensenkung auf und das nur für $\mu/\mu_G >> 0$ und $\varphi > 1$. Kurzzeitliche Temperaturschwankungen und Verkehrslasten arbeiten bei $\mu/\mu_G \sim 1$ am spröden Stab und bei $\mu/\mu_G << 1$ am plastischen Stahlstab mit reißendem Beton. Fig. 1 verdeutlicht, wie μ_G der ausschlaggebende Kennwert jeder Stahlbetonbemessung ist. Der Wert μ/μ_G ersetzt die im Einführungsbericht unter 3.1.3 mit a,b,c und d genannten Kriterien. In diesem Wert gehen die nur überschläglich bekannten Schwind- und Kriechzahlen ein. Damit bleibt die Bewehrungsgrenze überschläglich, damit aber auch die als Rechenwert gebrauchte Betonfestigkeit. Der Betonwürfel bedeutet

nicht annähernd so viel für die Bemessung, wie heute oftmals behauptet. Er liefert einen überschläglichen Rechenwert der Bemessung, der überhaupt nur gefragt ist, wenn stark bewehrt wird. Viel stärker als die Würfelfestigkeit an sich beeinflussen die viskosen Eigenschaften des Betons das Tragverhalten der Stahlbetonstäbe. Das Vorstehende gilt genauso für Spannbetonstäbe. Diese zeichnen sich dadurch aus, daß viel mehr Schnitte in die Randgebiete $\mu/\mu_G \geqq 1$ fallen. Sie haben mehr viskose und weniger plastische Eigenschaften. Sie können damit Dauerlasten und Dauerzwänge rissefrei umverteilen, sind dafür aber bei Kurzlasten und Wechselzwängen spröde.

Für Beanspruchungen nahe der Bruchfestigkeit des Betons hat der Beton auch plastische Eigenschaften. Sie kommen aus der beginnenden Gefügezerstörung und dürfen nur dann auftreten, wenn Zwang abgebaut werden muß. Die Plastizität des Betons tritt nur auf für $\mu/\mu_G > \sim 1$.

Fig. 1 verdeutlicht wie eingeschränkt Traglastverfahren bei Stahl- und Spannbetonstäben anwendbar sind. Sie können allenfalls dazu verwandt werden, Dauerzwänge in ihrer Bedeutung herabzusetzen.

---

(1) M. Save und Ch. Massonet im Einführungsbericht, S. 3 unten, S. 15.

(2) A.M. Freudenthal im Vorbericht, S. 31.

ZUSAMMENFASSUNG

Viskosität gehört zum Beton und Plastizität zum Stahl des Stahlbetonstabes. Beide treten je nach Wert μ/μ_G auf und nicht gleichzeitig in einem Schnitt. Die Rechnung kann für Dauerzwang die Viskosität nutzen, die Plastizität nur, wenn man sich mit groben Rissen abfindet.

SUMMARY

Viscosity belongs to concrete and plasticity to steel of the reinforced concrete bar. Both appear in accordance with the value μ/μ_G and not simultaneously in a section. The analysis can profit from the viscosity for continuous constraints, the plasticity only if one puts up with coarse cracks.

RESUME

Dans une poutre en béton armé, la viscosité est en rapport avec le béton et la plasticité avec l'acier. Ces deux phénomènes apparaissent selon la valeur du rapport μ/μ_G , mais pas simultanément dans la même section. Le calcul peut, pour des contraintes permanentes, utiliser la viscosité, la plasticité seulement dans le cas où l'on accepte de grosses fissures.

Remarques de l'auteur du rapport introductif
Bemerkungen des Verfassers des Einführungsberichtes
Comments by the Author of the Introductory Report

M. SAVE CH. MASSONNET
Belgique

0. INTRODUCTION

Synthétiser en 20 pages (maximum imposé par l'A.I.P.C.) un sujet qu'on n'épuiserait pas dans un traité de 600 pages, parce qu'il incorpore en fait toute l'évolution du dernier demi-siècle en théorie des structures, a obligé évidemment les rapporteurs à schématiser bien des problèmes.
Il est dès lors naturel que certains commentateurs, tels que le professeur FREUDENTHAL, soulignent maints développements qui n'ont pu être qu'effleurés dans le Rapport.
Nous voulons considérer son mémoire essentiellement comme un complément utile, sur beaucoup de points, à notre Rapport Introductif. Comme, cependant, nous ne pouvons pas le suivre dans certaines de ses affirmations, nous donnons ci-après notre point de vue à ce sujet en reprenant les titres des paragraphes de son rapport.

1. COMPORTEMENT DU MATERIAU

En physicien averti, M. FREUDENTHAL précise la nature des processus de dissipation d'énergie dans une microstructure métallique: glissements transgranulaires plastiques et écoulements intergranulaires visqueux. Il montre comment l'un ou l'autre de ces phénomènes prédomine selon les conditions de température,

de vitesse de mise en charge, etc... L'auteur fait également une synthèse du comportement physique du béton et précise que son domaine de viscoélasticité linéaire ne s'étend que jusqu'à 25 ou 30 % de sa résistance à la compression et devient progressivement non linéaire au-delà. Nous sommes d'accord avec la description qu'il donne des phénomènes accompagnant la ruine d'une poutre en béton armé.

2. CRITERES DE DIMENSIONNEMENT

Nous avons voulu essentiellement, dans notre Rapport, examiner l'influence de la plasticité et de la viscosité des matériaux sur les méthodes de dimensionnement. Nos commentaires s'appliquent surtout aux structures en acier, et les réserves à faire concernant les structures en béton armé ou précontraint sont clairement indiquées.
Pour nous, le premier critère de dimensionnement est la résistance à la ruine. Il s'y ajoute bien entendu un critère de serviceabilité, c'est-à-dire de contrôle des déformations en service, qui est inclus dans toutes les Normes (Norme Belge NBN1 1959 + Addendum: Calcul élastoplastique, 1961; Norme américaine IASC 1969, etc...) Ceci rappelé, nous ne pouvons souscrire à certaines déclarations de M. FREUDENTHAL, ni accepter de nous voir attribuer des opinions ou des intentions (lues entre les lignes) qui sont en opposition avec ce que nous avons écrit dans le Rapport Final du Septième Congrès de 1'A.I.P.C. {37}

2.1 L'obligation de faire un rapport de synthèse nous a amenés de renoncer à un rappel historique. Un tel rappel existe dans le volume I de notre livre "Calcul Plastique des Constructions" {6} * , et on pourra se rendre compte aisément que ce rappel

* Les nombres entre crochets jusque {69} renvoient à la bibliographie du Rapport Introductif; les suivants, à la bibliographie placée à la fin de la présente Note.

rend aux chercheurs allemands et autrichiens l'hommage qui leur est dû.
Il est cependant vrai aussi que le "Traglastverfahren", après une période de faveur, a été quasi abandonné dans les pays précités, alors que les recherches étaient poussées vigoureusement en Grande-Bretagne, sous l'impulsion de Sir John BAKER, puis aux Etats-Unis, principalement à l'Université LEHIGH. Ces deux pays sont les premiers à avoir adopté des Normes sur le calcul plastique, le troisième étant, à notre connaissance, la Belgique.

2.2 L'expérience dite de Stüssi-Kollbrunner a été répétée à Liège en 1963 {70} par l'un de nous, à grande échelle, sur des poutrelles industrielles en acier A 37 et A 52 et les conclusions obtenues ont été opposées à celles du mémoire original de 1935. Le mémoire ayant été publié en trois langues par la revue très connue Acier-Stahl-Steel, on peut s'étonner que M. FREUDENTHAL n'ait pas connaissance de cette publication et ne connaisse pas le point de vue accepté actuellement par la quasi totalité des chercheurs

2.3 Concernant le phénomène de stabilisation (shakedown), les rapporteurs n'ont certes pas méconnu le problème. Ils croient même que les premiers essais de stabilisation sur poutrelles industrielles ont été exécutés à Liège en 1953 par l'un d'entre eux {71} , mais ils acceptent les arguments probabilistes de HORNE {72} , auxquels ils croyaient que M. FREUDENTHAL aurait également souscrit, vu sa compétence bien connue dans le domaine de la théorie probabiliste de la sécurité.

Par raison d'impartialité, les rapporteurs désirent ajouter qu'ils ont toujours eu l'impression qu'il y avait une tendance, dans les pays anglo-saxons, à sous-estimer ce phénomène à cause de la complexité du calcul des charges de shakedown.

Il existe actuellement des programmes d'ordinateur qui permettent d'obtenir aisément les charges de "shakedown". Néanmoins, ils croient que le phénomène n'est important que dans quelques types très spéciaux de structures.

2.4 En ce qui concerne ce que M. FREUDENTHAL appelle les Règles de décision (p. 34 de son mémoire), la critique que le poids minimum ne coïncide pas avec le prix minimum est connue et d'ailleurs exacte. Cependant, elle concerne surtout les structures "raffinées" où la main-d'oeuvre intervient pour une part importante dans le prix total.
Dans le cas des ossatures composées de barres laminées, auxquelles s'applique le dimensionnement plastique, l'hypothèse que le prix des assemblages est une fraction déterminée du prix des barres est assez correcte, de sorte que l'optimisation basée sur le poids minimum est, à notre avis, une approche acceptable.

2.5 En ce qui concerne les phénomènes viscoélastiques dans les structures en béton armé et précontraint, il n'était pas indiqué de traiter le sujet en profondeur dans notre Rapport Introductif puisque cela venait d'être fait au Colloque de Madrid de l'A.I.P.C. (Septembre 1970) sur l'influence du fluage et du retrait sur les constructions en béton. Pour cette raison, le Rapport Introductif se réfère explicitement dans le texte (page 1) au Colloque. Il aurait pu y ajouter les travaux du CEB et de la RILEM consacrés au fluage du béton. Nous accueillons avec beaucoup d'intérêt les remarques du professeur BAŽANT sur les développements récents dans le domaine de l'inélasticité du béton, phénomène dont la très grande complexité nous apparaît clairement.

Ceci précisé, nous maintenons qu'un grand nombre de constructeurs auraient avantage à se servir du modèle viscoélastique linéaire popularisé par les mémoires connus de DISCHINGER {73}, même s'il est bien admis aujourd'hui que les résultats correspondants ne sont qu'une première approximation. En effet, trop de constructeurs se fient encore au modèle élastique, assorti éventuellement de corrections empiriques, ce qui peut conduire, dans le cas des ponts en béton précontraint bâtis en encorbellement, à de très sérieux mécomptes.

3. PROCEDURES DE DIMENSIONNEMENT

Comme il a déjà été dit plus haut au par. 2, il va de soi qu'au contrôle de la résistance limite, il faut toujours ajouter un critère de déformabilité en service. Dès lors le mode de dimensionnement recommandé par nous coïncide avec le double critère de serviceabilité et de résistance à la ruine prôné par M. FREUDENTHAL.

BIBLIOGRAPHIE

{70} MASSONNET, Ch., ANSLIJN, R., MAS, E.: Essais de flexion plastique sur des poutres continues en Acier A 37 et A 52.
Acier Stahl Steel, Déc. 1963 (éditions en anglais, allemand et français).

{71} MASSONNET, Ch.: Essais d'adaptation et de stabilisation plastiques sur des poutrelles laminées.
A.I.P.C., Vol. 13, pp. 239-282, 1953.

{72} HORNE, M.R.: The effect of variable repeated loads in building structures designed by the plastic theory. Mém. A.I.P.C., Vol. 14, p. 53, 1954.

{73} DISCHINGER, F.: Elastische und plastische Verformung der Eisenbetontragwerke und insbesondere der Bogenbrücken. Der Bauingenieur, Vol. 20, pp. 53-63, 286-294, 426-437, 563-572, 1939.

Leere Seite
Blank page
Page vide

I b
Instabilité dans le domaine post-critique
Instabilität im überkritischen Bereich
Post-critical Buckling

Leere Seite
Blank page
Page vide

DISCUSSION LIBRE • FREIE DISKUSSION • FREE DISCUSSION

Nouvelle théorie et essais sur la résistance ultime des poutres en caisson raidies en acier, soumises à flexion pure

Neue Theorie und Versuche über die Traglast ausgesteifter Stahlkastenträger unter reiner Biegung

New Theory and Test on the Ultimate Strength of Steel Stiffened Box Girders under Pure Bending

R. MAQUOI
Chargé de Recherches du Fonds National de la Recherche Scientifique

CH. MASSONNET
Professeur à l'Université de Liège

Belgique

Une série d'accidents spectaculaires (Vienne, 6 novembre 1969, Milford Haven, 2 juin 1970, Melbourne, 15 octobre 1970, Coblence, 10 novembre 1971) a polarisé l'attention des ingénieurs sur les méthodes de dimensionnement des grands ponts en caisson en acier raidis.

Nous voudrions, dans les quelques minutes dont nous disposons, attirer l'attention des participants au Congrès sur certaines des recherches en cours dans ce domaine.

La plupart des ponts du type considéré ont été dimensionnés, ces dernières années, en se basant sur la théorie linéaire du voilement.
Les coefficients de sécurité généralement adoptés étaient les mêmes que pour les âmes des grandes poutres en double té, à savoir

1,35 pour le cas I de sollicitation
1,25 pour le cas II de sollicitation.

L'estimation de la contrainte critique se faisait souvent en utilisant les abaques contenus dans les deux livres du Professeur KLÖPPEL et de ses collaborateurs, MM. SCHEER et MÖLLER.

Les résultats expérimentaux sur des modèles de poutres en caisson fléchies, présentés par le Professeur P. DUBAS au Colloque de Londres "Design of Plate and Box Girders for Ultimate Strength" (25-26 mars 1971) ont montré que la contrainte moyenne de ruine d'une plaque comprimée uniformément et raidie par des raidisseurs théoriquement strictement rigides ($\gamma = \gamma^*$) était normalement inférieure à sa contrainte critique de voilement linéaire, c'est-à-dire qu'on ne pouvait compter sur aucun effet postcritique, et que les coefficients de sécurité actuels étaient par conséquent absolument insuffisants.

Nous basant sur les travaux théoriques de SKALOUD et NOVOTNY, nous avons montré au même Colloque, mon collaborateur R. MAQUOI et moi-même, que ce résultat imprévu de DUBAS aurait pu être prédit théoriquement.

Ceci nous a conduit à développer une théorie non linéaire de la résistance à la ruine des grandes poutres en caisson raidies, qui a paru dans le volume 31-II des Mémoires de l'A.I.P.C. (pp. 91 à 140) et dont nous voudrions vous présenter brièvement ici les principes essentiels:

Nous admettons pour simplifier que nous pouvons nous borner à étudier la résistance limite de la membrure comprimée du caisson (Fig. 1). A la ruine, la partie ABCD de cette membrure limitée entre les deux lignes nodales successives AB et CD se comporte comme une plaque membrane orthotrope à raidisseurs dissymétriques.

Vu le grand nombre de raidisseurs longitudinaux, nous supposons leurs rigidités réparties continûment c'est-à-dire "tartinées"; nous avons développé la théorie non linéaire de ces plaques membranes en généralisant la théorie linéaire de PFLUGER et nous aboutissons au système de deux équations aux dérivées partielles du 4ème ordre non linéaires et couplées ci-dessous:

$$\frac{\phi''''}{D_x} + 2\frac{\phi''\dot{}\dot{}}{\overline{D}} + \frac{\phi\dot{}\dot{}\dot{}\dot{}}{D_y} = (1-\overline{\nu}^2)\left[(w_o'+w')^2 - (w_o''+w'')(w_o\dot{}+w\dot{})- w_o'^2 + w_o''\, w_o\dot{}\right],$$

$$\overline{B}_x w'''' + 2\overline{C}\,\dot{w}''\dot{} + \overline{B}_y\, w\dot{}\dot{}\dot{}\dot{} = \phi'' (w_o''+w'') + \phi\dot{}\dot{} (w_o\dot{}+w\dot{}) - 2\phi'' (w_o'+w').$$

Ces équations donnent le déplacement transversal w et la fonction de contrainte d'Airy ϕ.
Nous supposons que le panneau a une déformée initiale sinusoïdale

$$w_o = f_o \cos\frac{\pi x}{a}\cos\frac{\pi y}{b}$$

Pour les déplacements additionnels w, nous devons nous contenter d'admettre une expression approchée affine au mode de voilement linéaire (et à w_o) c'est-à-dire

$$w = f \cos\frac{\pi x}{a}\cos\frac{\pi y}{b}.$$

En supposant que les bords latéraux AD et BC du panneau sont libres de contraintes de membrane, à cause de la déformabilité des âmes du caisson perpendiculairement à leur plan et que les bords transversaux AB et CD doivent rester rectilignes, nous pouvons intégrer exactement l'équation donnant la fonction de contrainte ϕ.

La flèche supplémentaire f croît avec l'effort de compression, qui n'est pas réparti uniformément et on obtient la loi de croissance de f en employant la méthode de GALERKIN.

Finalement, nous admettons, pour ne pas devoir nous livrer à une analyse élasto-plastique extrêmement complexe, que la ruine de la plaque se produit quand la contrainte de compression membranaire moyenne $\overline{\sigma}_x$ le long des bords non chargés AD et BC atteint la limite élastique du métal. Cette condition nous permet d'établir la relation non linéaire donnant la flèche additionnelle f de la plaque en fonction de sa flèche initiale f_o et des autres données du problème. f étant connu, il est aisé d'établir l'expression du rendement d'ensemble de la plaque à raidisseurs "tartinés".

$$\rho_t = \frac{\text{Effort réel à la ruine}}{\text{Effort plastique maximum } \Omega R_e}$$

où R_e est la limite élastique.

Nous trouvons pour ρ_t une expression relativement simple.

Il faut cependant tenir compte de ce que la plaque réelle a un nombre fini de raidisseurs et que la tôle se voile dans tous les champs partiels compris entre deux raidisseurs successifs. Cela donne au diagramme des contraintes de compression à la ruine une allure festonnée. Il est possible de tenir compte de la perte de rendement supplémentaire correspondante en introduisant la notion de rendement local de la tôle

$$\rho_l = \frac{\text{Effort réel}}{\text{Effort maximum}} .$$

L'expression de ρ_l découle directement de l'expression de la largeur effective de cette tôle, pour laquelle nous avons adopté une formule déduite de nombreux essais de compression jusqu'à la ruine sur des tôles raidies qui est très voisine de celle de WINTER.

Le rendement global de la tôle raidie à raidisseurs discrets est donné par l'expression

$$\rho_g = \rho_t \cdot \rho_l .$$

Un pont en caisson devrait se dimensionner, selon nous, en exprimant que, sous la charge de ruine, la contrainte moyenne de compression dans le panneau ABCD ne dépasse pas la contrainte moyenne de ruine

$$R_r = \rho_g R_e$$

Notre théorie explique l'accident survenu au Praterbrücke à Vienne et est en assez bon accord avec les résultats expérimentaux du Professeur DUBAS.

Cependant, afin de tester cette théorie, nous entreprenons actuellement dans mon laboratoire à Liège une série d'essais jusqu'à la ruine sur des modèles de poutres en caisson munies de 7 raidisseurs longitudinaux. Les figures 2 et 3 donnent quelques précisions à ce sujet.

En conclusion, nous voudrions insister sur le fait que calculer les raidisseurs de la plaque comme des barres comprimées indépendantes, comme plusieurs chercheurs l'ont proposé tout récemment, reviendrait à ignorer l'effet stabilisant des contraintes de membrane et conduirait, selon nous, à un gaspillage d'acier excessif.

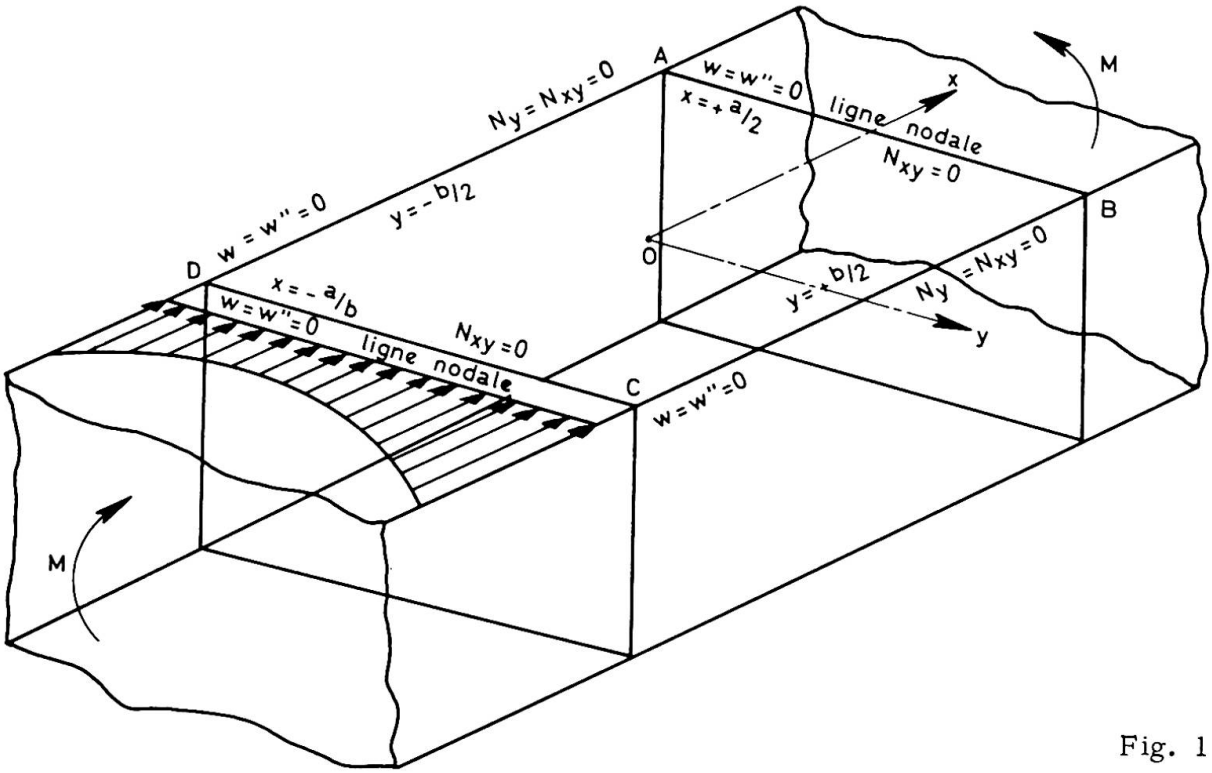

Fig. 1

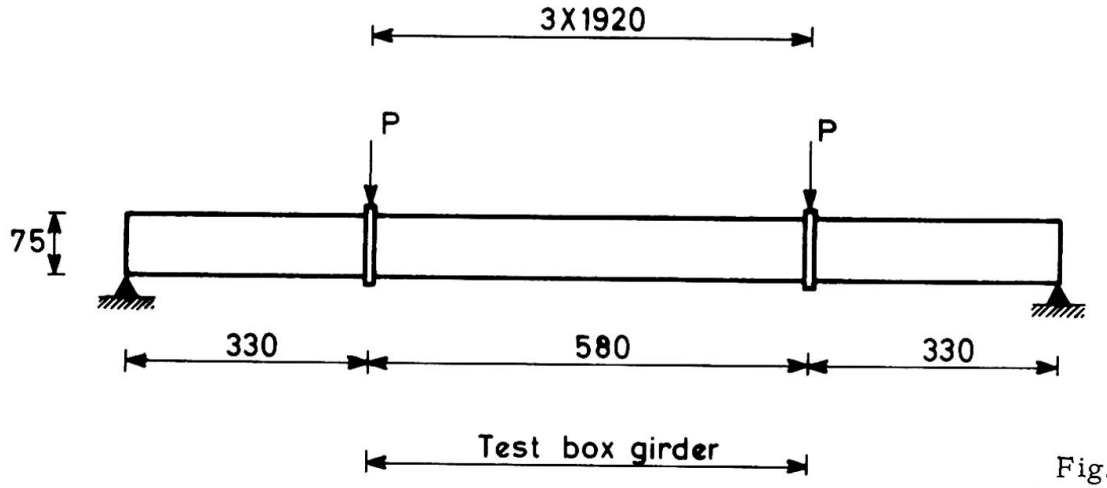

Fig. 2

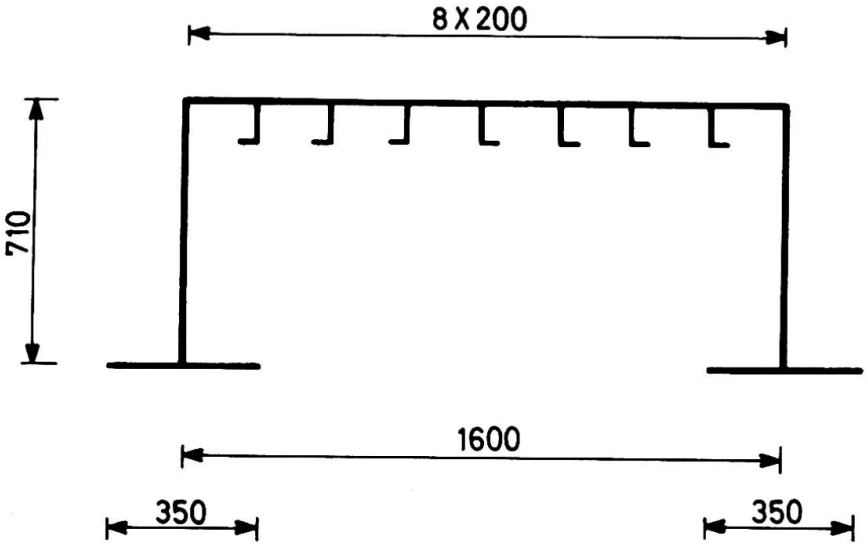

Fig. 3

Stresses in Thin-Cylindrical Webs of Curved Plate Girders

Contraintes dans l'âme mince de poutres courbées cylindriquement

Spannungen in dünnen, zylindrischen Stegen von gekrümmten Vollwandträgern

RYSZARD DABROWSKI
Poland

See Colloquium London 1971, page 337, Volume 11 of the Reports of the Working Commissions
Voir Colloque Londres, 1971, page 337, Volume 11 des Rapports des Commissions de Travail
Siehe Seminar London 1971, Seite 337, Band 11 der Berichte der Arbeitskommissionen

Leere Seite
Blank page
Page vide

Ib

Failure Load and Effective Width of Compressed Steel Plates with Initial Stresses and Initial Deflections

Charges ultimes et largeur réelle de tôles d'acier soumises à la compression avec contraintes internes et déflections initiales

Bruchlast und tatsächliche Breite gedrückter Stahlplatten mit Eigenspannungen und Anfangsdurchbiegung

HENRIK NYLANDER
Sweden

Column buckling is influenced by the local plate buckling. The local plate buckling is dependent on initial stresses due to welding and initial deflections of the plates.

The author has studied the plate buckling in the overcritical range using a model of calqulation, which enables to consider the initial stresses and the initial deflection in a relatively simple manner.

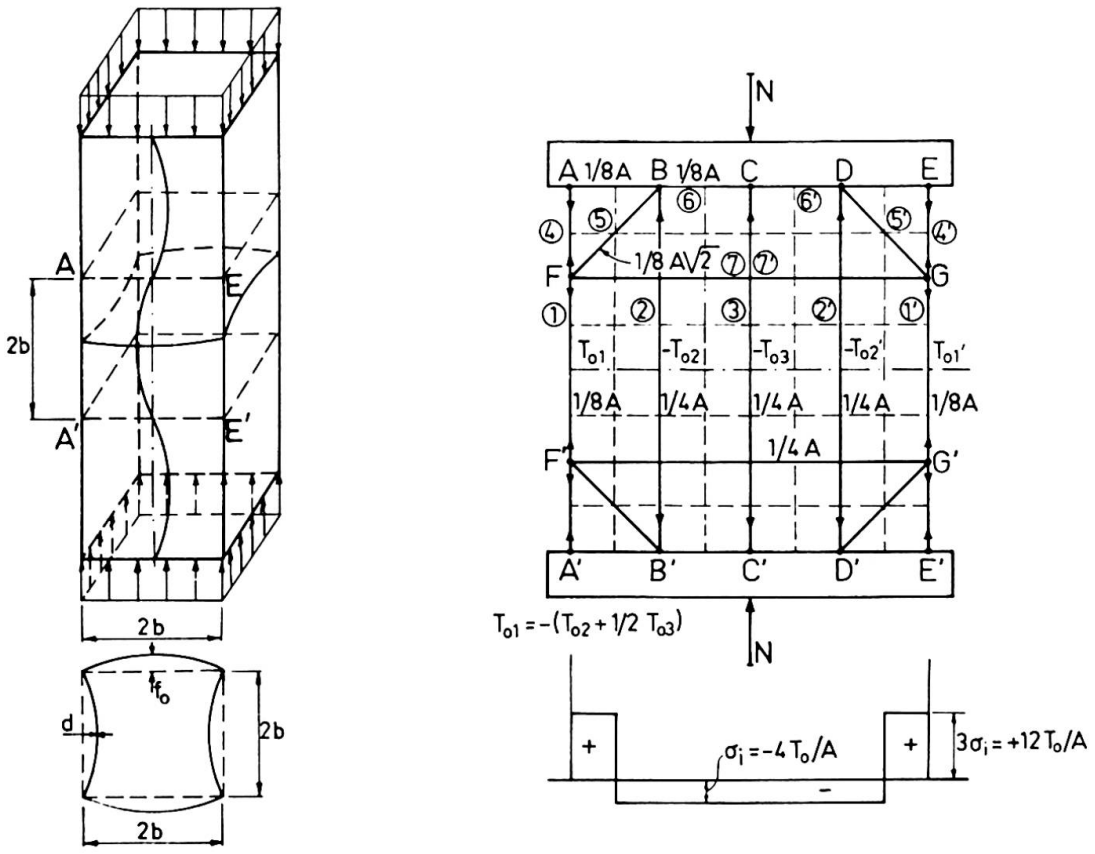

Fig. 1 a and 1 b Model of Calqulation

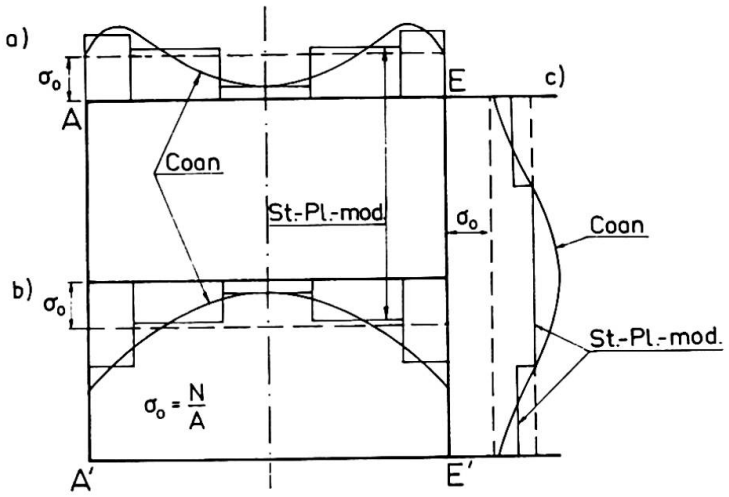

Fig. 1 c
Distribution of compressive stresses in the direction of the load N at the edge A-E (a)) at the line of symmetry (b)) and at the edge E-E′ (c)). Comparison with solution by Coan $\sigma_o/\sigma_{el} = 1{,}74$.

The investigation is part of a research project regarding the carrying capaciy of welded hollow columns, built up by thin plates. The project is carried out at the Department of Building Statics and Structural Engineering at the Royal Institute of Technology, Stockholm and at the Swedish Institute of Steel Construction, Stockholm.

The model of calqulation consists of a plate acting only in plate bending and of the strips 1-7 and 1′- 7′, taking the membrane stresses only. (Fig. 1) The strips are connected to the plate at the points A-G and A′- G′ The areas of the strips are shown in Fig. 1, where A = 2b·d is equal to the area of the cross section of the plate. The normal forces in the strips are caused by 1) the initial stresses, 2) the normal force N in the plane of the plate, which gives forces in the different strips in proportion to their areas and 3) of forces which are caused by the changes of length of the strips as the bending deformation of the strips follows the bending deformation of the plate.

The mathematical treatment is omitted in this connection. It is the author′s intention to publish the theory and the rather comprehensive results in a near future.

A treatment of the problem starting from the fundamental Eq. by von Kármán and Marguerre adjusted to take into account the influence of the initial stresses is in the author′s opinion very difficult. In fig. 1 c a comparison is made with a solution by Coan |1| for a case where $\sigma_i = 0$. The membrane stresses in the direction of the compressive load N at the supports at the middle of the plate and along a free edge are considered. It is seen from the Figure that it is a good agreement between Coan′s results and the results from the calqulations for the model in Fig. 1 b both regarding the maximum values and the distributions of stresses.

It is hardly possible to precise adequate criteria of failure for the highly statically indeterminate system in question where the elastoplastic state of stresses must be considered. The author has instead of trying to give a complex theory started from a relatively detailed study of the stresses in different parts of the elastic plate caused by bending and torsional moments

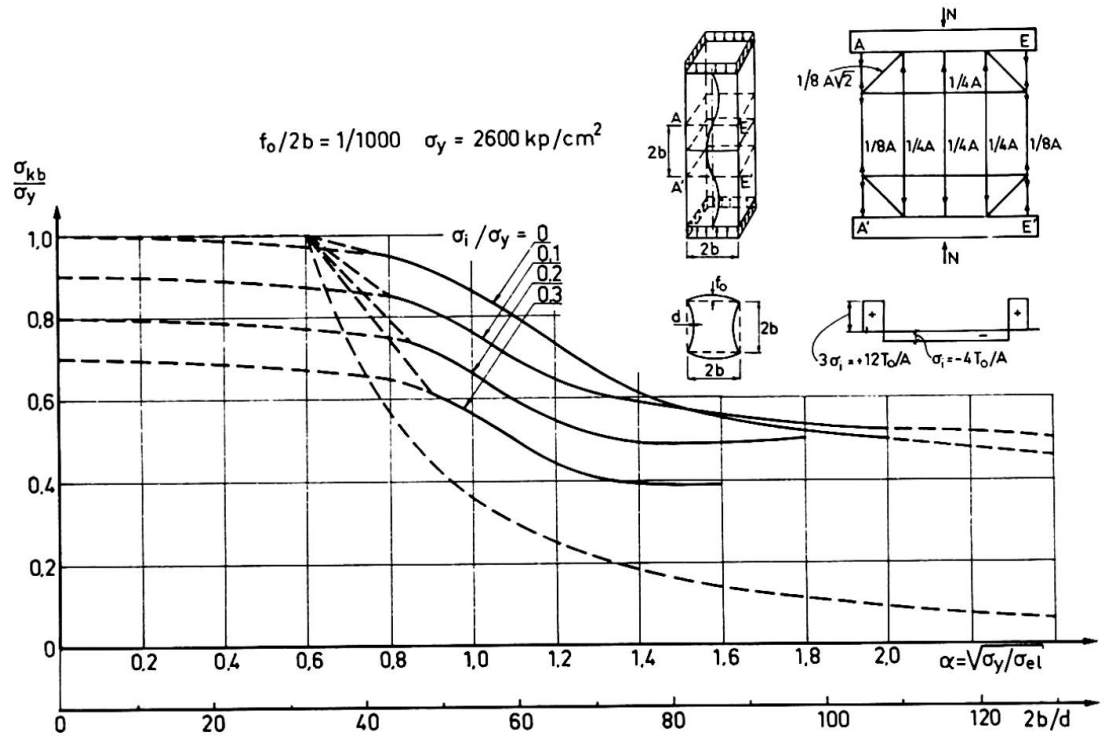

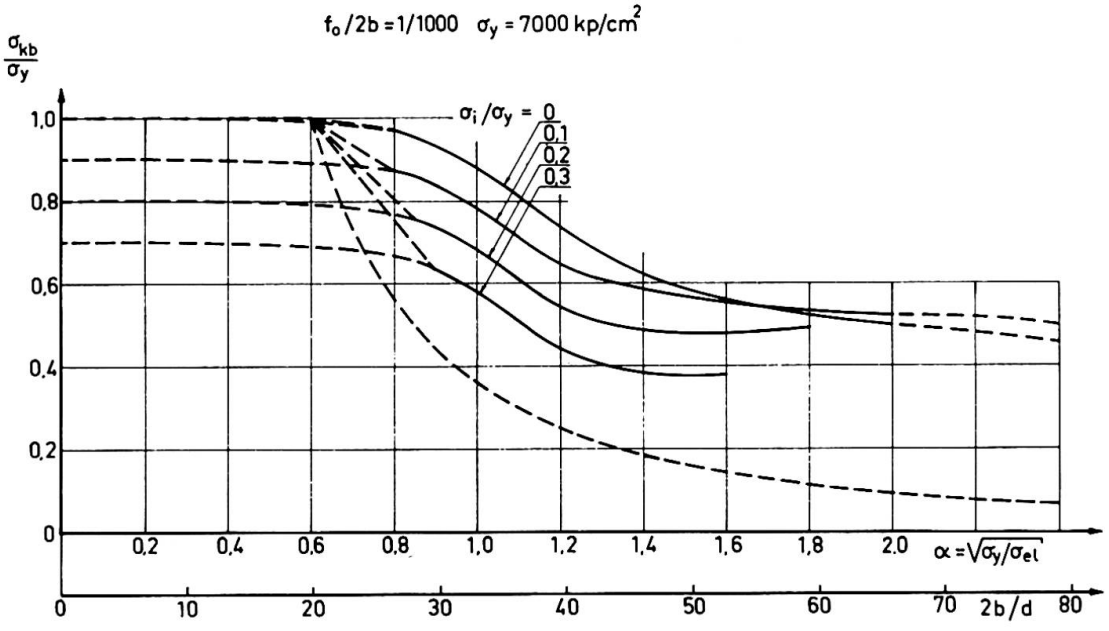

Fig. 2 a and 2 b. Values of $\sigma_{kb} = N/2bd$ at buckling failure divided with σ_y for different σ_i/σ_y as function of $\alpha = \sqrt{\sigma_y/\sigma_{el}}$

a) σ_y = 2 600 kp/cm^2 b) σ_y = 7 000 kp/cm^2

and the normal forces. Then that load has been determined at which total yielding (yield stress over the whole cross section) will occur at the point considered, if the bending and torsional moments as well as the normal forces have the values calqulated from the theory of elasticity. At the judgement of the failure load the following points have been considered:

1. The midpoint of strip (A-A′, Fig. 1 a). Yielding due to normal force (compression) in the direction of the load N.
2. The midpoint of the strip 2 (B-B′, Fig. 1 a). Yielding due to bending moment and normal force in the direction of the compressive load N.
3. The centre of the plate (midpoint of strip 3). Yielding due to bending moment and normal force in the direction of the compressive load N.
4. The corner points. Yielding due to torsional moment and normal force in the direction of the load N.

The results are given in Fig. 2 for two values of the yield stress: 2 600 kp/cm^2 and 7 000 kp/cm^2 and for the ratio initial deflection over plate width $f_o/2b$ = 1/1 000. For most of the calqulated points of the diagrams the alternatives 2) and 3) above were most dangerous and the failure loads were for these points calqulated as the average values of the failure loads for the alternatives 2) and 3).

For $\sigma_i/\sigma_y = 0$ and $\alpha \geq 1{,}2 \leq 2{,}0$ and for $\sigma_i/\sigma_y = 0{,}1$ and $\alpha \geq 1{,}8$ alternative 4) was most dangerous. For $\sigma_i/\sigma_y = 0$ and $\alpha > 2{,}0$ alternative 1) was most dangerous.

The effective width b_e (see Fig. 3) is of importance for the column buckling. Calqulated values at failure load are given in Fig. 3 for different σ_i/σ_y ($f_o/2b$ = 1/1 000; σ_y = 2 600 kp/cm^2). It is seen from the Figure that the initial stresses highly affect the values of b_e/b.

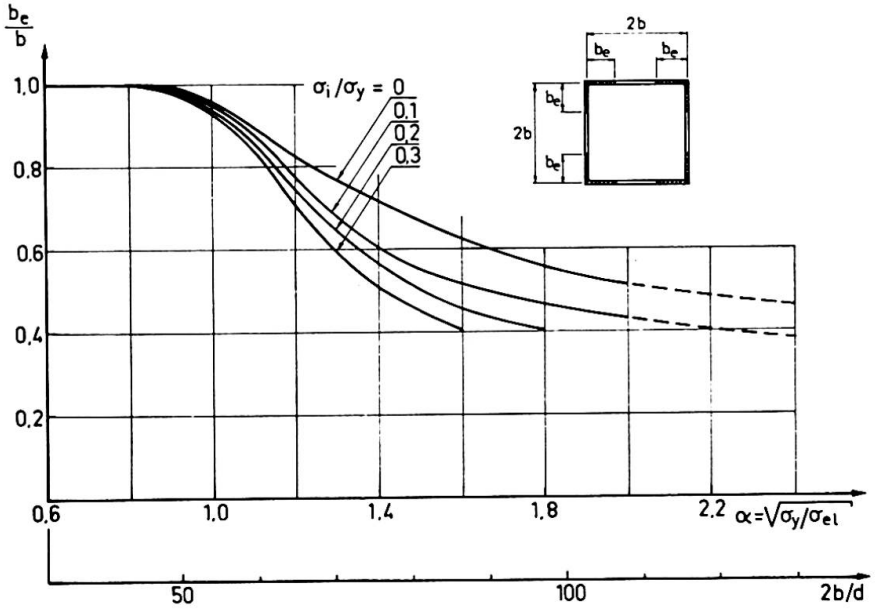

Fig. 3 Ratio b_e/b for the failure load as a function of α (σ_y = 2 600 kp/cm^2)

It is seen from Fig. 2 that the initial stresses have a very important negative influence on the critical buckling stresses especially for $0,8<\alpha<1,6$. The initial stresses have a negative effect on the effective width b_e (see Fig. 3). Both these effects reduce the column buckling load. The applied distribution of the initial stresses is unfavourable. Calqulations of a case where $\sigma_i = 0$ in the strip 3 have given higher failure loads. It is therefore a need of studying the influence of the fabrication methods on the distribution of initial stresses. Finally the author among investigations will remind of those by Nishino, Ueda, Tall |2|; Dwight, Moxham |3| and Dwight, Ractcliffe |4| of buckling of welded columns of hollow sections, where it was pointed out that the initial stresses have a large unfavourable effect on the failure load.

REFERENCES

|1| Coan, J.M.: Large Deflection Theory for Plates With Small Initial Curvature Loaded in Edge Compression. Journ. of Appl. Mech., June 1951.

|2| Nishino, F.; Ueda, Y. and Tall, L.: Experimental Investigations of the Buckling of Plates with Residual Stresses. Am. Soc. Testing Mats., p. 12, 1967.

|3| Dwight, J.B. and Moxham, K.E.: Welded Steel Plates in Compression. The Struct. Eng., No. 2, 1969.

|4| Dwight, J.B. and Ractcliffe, A.I.: The Strength of Thin Plates in Compression. Thin Walled Structures, Crosby Lockwood, 1969.

SUMMARY

The behaviour of compressed steel plates in the overcritical range is studied. A simplified model of calculation, Fig. 1, which enables to consider initial stresses. and deflections is used. The results are intended to serve as a basis for design rules. It is shown that the initial stresses reduce the failure load especially for the dimensions corresponding to $0,8 < a < 1,6$, Fig. 2. Furthermore the effective width is reduced by the initial stresses, Fig. 3. Here omitted results for other distributions of the initial stresses are more favourable.

RESUME

L'auteur étudie ici le comportement de plaques en acier comprimées, dans le domaine post-critique. Il emploie un modèle mathématique simplifié, fig. 1, qui permet de tenir compte des tensions et des déviations initiales, Les résultats sont destinés à servir de base pour déterminer des règles de dimensionnement. On remarque que les tensions initiales réduisent la charge ultime, spécialement pour les dimensions correspondant à $0,8 < a < 1,6$, fig. 2. De plus la largeur effective est réduite par les tensions initiales, fig. 3. Les résultats pour d'autres distributions des tensions initiales, qui ne sont pas mentionnées ici, sont plus favorables.

ZUSAMMENFASSUNG

Es wird das Verhalten gedrückter Stahlplatten im überkritischen Bereich untersucht, dabei wird ein vereinfachtes Berechnungsmodell (Fig. 1) verwendet, das die Berücksichtigung der Eigenspannungen und Anfangsdurchbiegungen erlaubt. Die Ergebnisse sind als Basis für die Bemessung gedacht. Es wird gezeigt, dass die Eigenspannungen die Bruchlast reduzieren, insbesondere für Dimensionen entsprechend $0,8 < a < 1,6$ (Fig. 2). Zudem wird die tatsächliche Breite infolge der Eigenspannungen vermindert (Fig. 3). Die hier ausgelassenen Ergebnisse für andere Eigenspannungsverteilungen sind günstiger als die gezeigten.

Contribution to the Free Discussion Regarding the Paper "Interaction of Postcritical Plate Buckling with Overall Column Buckling of Thin-Walled Members" by J. De Wolf, T. Pekoz and G. Winter

Contribution à la discussion libre de l'article "Interaction of Postcritical Plate Buckling with Overall Column Buckling of Thin-Walled Members" par J. De.Wolf, T. Pekoz et G. Winter

Diskussion bezüglich des Beitrages "Interaction of Postcritical Plate Buckling with Overall Column Buckling of Thin-Walled Members" von J. De Wolf, T. Pekoz und G. Winter

MIROSLAV ŠKALOUD
Assoc. Professor, D.Sc., Ing.
Senior Research Fellow at the Institute
of Theoretical and Applied Mechanics
Czechoslovak Academy of Sciences
Prague, CSSR

To begin with, I would like to congratulate Professor Winter and his co-workers on obtaining very interesting and valuable results regarding the limiting state of thin-walled columns.

I would also like to take this opportunity to mention that our team at the Institute of Theoretical and Applied Mechanics in Prague has been concerned with the interaction of overall column buckling with plate buckling for some 14 years. Several investigations, both theoretical and experimental, have been carried out. For example, a few years ago, twenty eight thin-walled columns were tested, with the slenderness ratio of the column and the width-to-thickness ratio of its plate elements being varied in a way that both the column and plate buckling could be studied.

It is beyond the scope of this contribution to the Free Discussion to describe all our results and observations; therefore, I have to limit myself to a few conclusions, which may be of some interest in connection with Professor Winter's

paper.

To start with, it is, perhaps, worth mentioning that in all our tests a pronounced interaction of column buckling with the buckling of its plate elements was observed. It follows from this observation that it is not possible to separate (as is frequently done when following the currently held design concept) the behaviour of the column as a whole from that of its plate elements. A steel column is always a system of plates, the overall deformation of which and the local one (i.e. buckling of plate elements) are interconnected.

Further, I would like to draw attention to the fact that the performance of thin-walled columns is considerably affected by unavoidable initial irregularities (like an initial curvature, residual stresses, etc.).

For example, in the case of a centrally loaded column, the initial irregularities make the column deflect from the very beginning of loading. As a result of the flexure of the column as a whole, the loads of the plates on the concave side of the deflected column are increased, whereas those acting on the plates on the convex side are reduced. That is why, in the most loaded section of the bar, the load acting on the concave side plate can be substantially (in the case of very slender bars even several times) larger than that which acts on the plate element on the convex side of the deflected column (Fig. 1). Furthermore, it is of importance that this increased load of the plate on the concave side is, at the most stressed section of the column, frequently substantially greater than the avarage value $\sigma = P/A$, which is considered in the design if an "ideal" column without initial deviations is assumed.

The influence of the initial irregularities upon the

loading of the plate elements is reflected in the character of the waving of these elements (Fig. 2). That is why plate buckling is more pronounced on the concave side of the deflected bar than it is on the convex one. Moreover, in view of the fact that in the case of the plate on the concave side the load acting on it is larger in the central section than at the boundaries of the bar, the buckled pattern is more pronounced in the middle of the column than at its ends. On the other hand, the plate on the convex side is less loaded in the central part of the bar than at the boundary sections; therefore, the wave pattern tends to be less pronounced in the middle of the column than in the boundary zones. The aforesaid analysis shows that the currently held model of behaviour, according to which the plate elements of a centrally compressed bar are uniformly loaded and, consequently, uniformly waved, is not compatible with the behaviour of ordinary thin-walled steel columns.

The effect of initial deviations upon the limiting state and the ultimate load is shown in Fig. 3, where the experimental load-carrying capacities of one test series are plotted in comparison with a/ the critical load σ_{cr} of the bar as a whole, evaluated regardless of plate buckling, b/ the critical load σ_{cr}^{p} for the buckling of the weakest plate element, and c/ the critical load σ_{cr}^{e} determined for the stability of the column as a whole with due regard to plate buckling and, therefore, for an effective cross section. In this case, the effective widths of the plate elements were determined by using Winter's formula.

An inspection of the figure indicates that there is no definite relation between the experimental ultimate load on one side and a/ the critical load σ_{cr}^{p} of the weakest plate

element and b/ the critical load σ'_{cr} of the column as a whole, on the other. The curve σ'^{e}_{cr} calculated for the effective cross section is closer to the experimental results than the two aforementioned quantities; however, it does not seem to follow the experimental results either. As it disregards the effect of initial irregularities, it frequently gives values higher than is the actual limiting state of the thin-walled column.

I would like to conclude by making a suggestion to the Working Comission II. I think that the above discussed problems of interaction belong to the most important lines of the present research on the behaviour of steel structures. This problem is being dealt with at several places; for ex. at Cornell, in Cambridge, in Liège, in Darmstadt and in Prague, It may, perhaps, be time to give thought whether it would not be profitable to organize a colloquium with this line of work. This colloquium, which could be organized in a way similar to last year's London colloquium on plate girders, and in which all researchers concerned would take part, could significantly contribute to further progress in the aforementioned field.

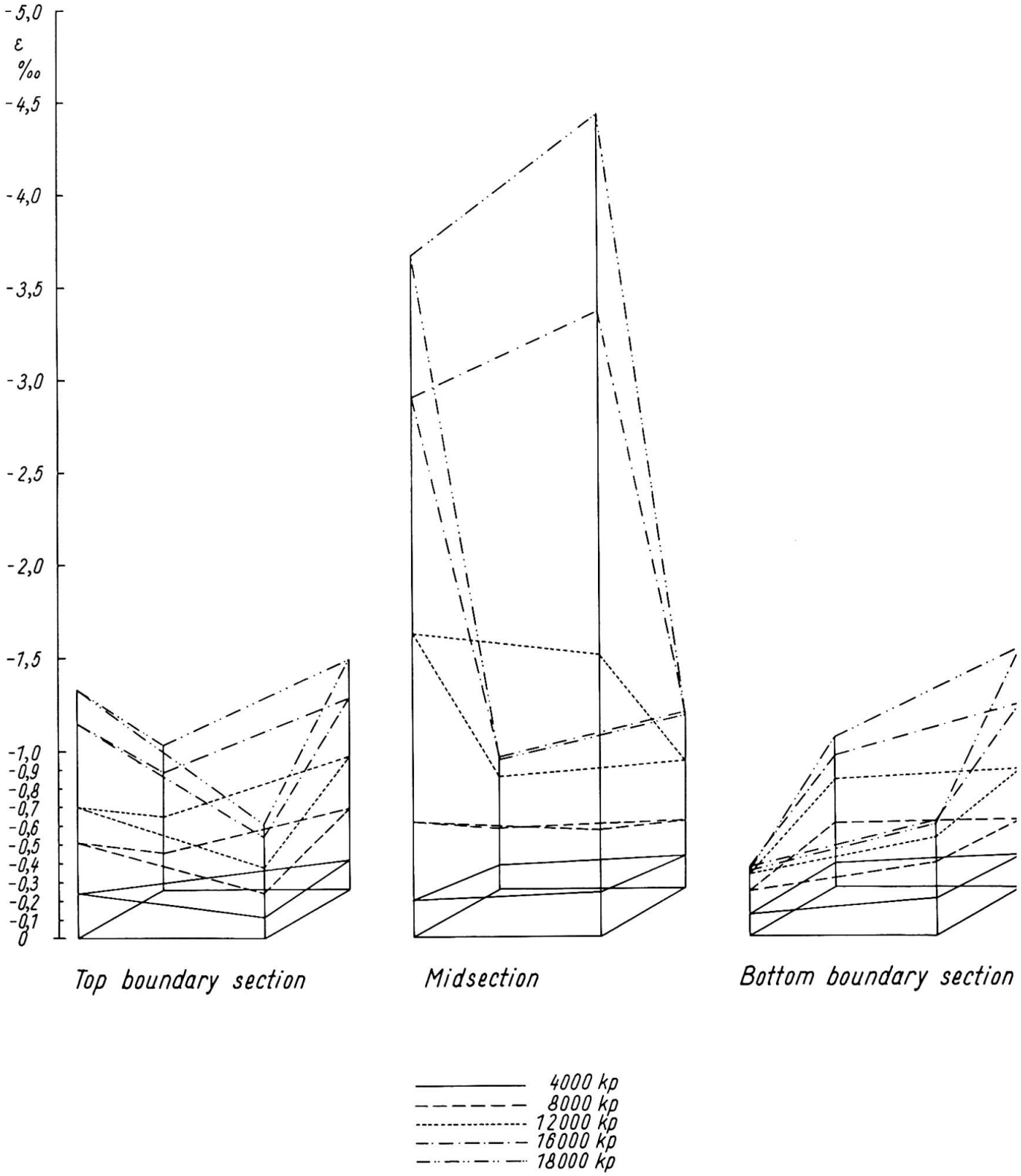
-5,0
ε
‰
-4,5
-4,0
-3,5
-3,0
-2,5
-2,0
-1,5
-1,0
-0,9
-0,8
-0,7
-0,6
-0,5
-0,4
-0,3
-0,2
-0,1
0
Top boundary section
Midsection
Bottom boundary section
4000 kp
8000 kp
12000 kp
16000 kp
18000 kp

Fig. 1

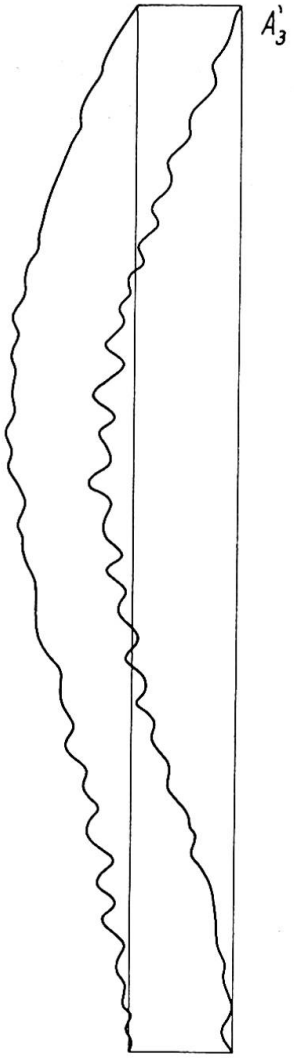

Fig. 2

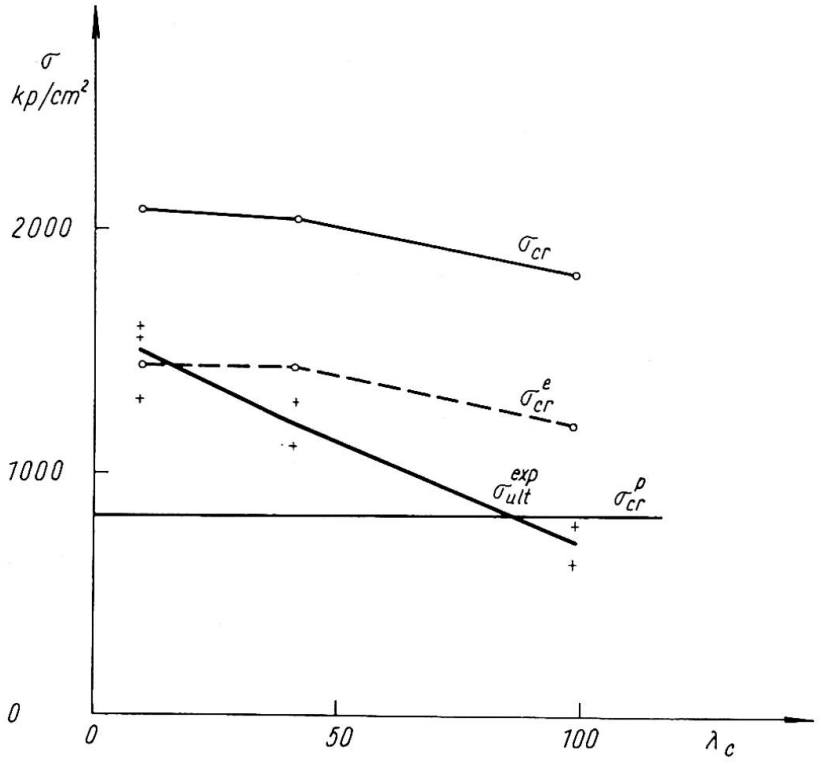

Fig. 3

Application d'une méthode de calcul par éléments finis à l'étude du comportement des plaques minces raidies dans le domaine des grands déplacements

Anwendung einer Berechnungsmethode mittels endlicher Elemente zur Untersuchung des Verhaltens dünner ausgesteifter Platten im Bereich grosser Verschiebungen

Application of a Method of Calculation by Finite Elements for the Study of the Behaviour of Thin-Walled Stiffened Plates in the Range of Large Displacements

H. GACHON
Professeur à l'ENSAM de Paris
et Conseiller Technique au CTICM

A. BARRACO
Ingénieur de Recherches au CTICM

Paris, France

Ce mémoire expose une méthode d'analyse approchée, par éléments finis, du champ de déplacements des plaques minces raidies très déformables et présente une étude comparée du comportement d'une structure par la simulation sur ordinateur et par l'expérimentation sur modèle.

Cette méthode trouve, en particulier, son application dans l'étude du comportement non linéaire, correspondant au domaine dit "post-critique", des panneaux plans ou à faible courbure constituant les parois des structures légères ou des poutres de grande portée.

Le modèle mathématique étudié est défini à partir d'un maillage principal à éléments finis rectangulaires et d'un maillage secondaire à éléments triangulaires (triangles rectangles) utilisable aux frontières du domaine.

Les hypothèses sont exprimées sur le champ des déplacements en introduisant un champ cinématiquement admissible. L'application du principe des travaux virtuels ou du principe de variation des déplacements conduit à satisfaire aux exigences de la compatibilité non seulement aux noeuds du maillage, mais encore le long de l'interface des éléments rectangulaires contigus. La continuité des déformations est assurée dans le plan moyen de la plaque.

Les raidisseurs associés à la plaque mince peuvent être orientés suivant des directions parallèles, orthogonales ou obliques (cas des membrures obliques des poutres de hauteur variable) et disposés symétriquement ou non par rapport au plan moyen de la plaque. Ils sont à parois minces et à section droite ouverte ou fermée. Ils peuvent être traités dans le domaine des déplacements finis.

Nous avons admis pour le matériau une loi de comportement élastique et des déformations infinitésimales.

L'introduction d'une déformée initiale de faible courbure aussi bien en ce qui concerne la plaque que les raidisseurs et d'un état de contraintes propres dans la plaque permet de compléter la prise en compte des données initiales dans le but d'une bonne simulation du comportement réel de la structure.

Le champ de déplacement s'établit sous forme d'une combinaison linéaire de fonctions dont les paramètres correspondent respectivement aux degrés de liberté du modèle mathématique adopté et définissent les coordonnées du vecteur déplacement. La détermination du vecteur déplacement s'effectue par accroissements tangents ou paraboliques à partir des différents états successifs du modèle en donnant aux charges des petits accroissements. Chaque état du modèle est caractérisé par une matrice de raideur tangente.

Les études de simulation du comportement des structures dans le domaine des déplacements finis portent actuellement sur différents modèles expérimentaux traités au préalable en laboratoires :

1. - une série de panneaux rectangulaires simples, raidis sur leur contour, appuyés suivant les raidisseurs d'extrémité et chargés ponctuellement à mi-portée de la membrure supérieure.

2. - une poutre en I, à âme raidie transversalement, de 8 m de portée.

3. - deux poutres en I, à âme mince raidie transversalement et longitudinalement, de 20 m de portée.

Nous présentons, ci-après, une étude comparée du comportement d'un panneau de poutre en I chargé localement dans son plan, par la simulation sur le modèle mathématique ainsi défini et par la mesure sur un modèle expérimental.

1. - SCHEMA DE DISCRETISATION

$$f_1(\xi) = 1 - 3\xi^2 + 2\xi^3 \qquad (f_1^{IV}(\xi) = 0)$$

$$g_1(\xi) = 3\xi^2 - 2\xi^3 \qquad (g_1^{IV}(\xi) = 0)$$

$$f_2(\xi) = \xi - 2\xi^2 + \xi^3 \qquad (f_2^{IV}(\xi) = 0)$$

$$g_2(\xi) = -\xi^2 + \xi^3 \qquad (g_2^{IV}(\xi) = 0)$$

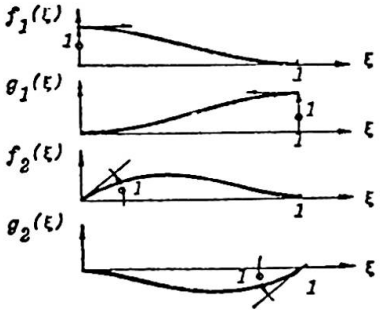

2. - CHAMP DE DEPLACEMENT DANS UN ELEMENT DE PLAQUE

$$u_i^k(x^o, y^o) = \{\widetilde{\phi(x^o, y^o)}\}\{D_i\}^k \qquad (i = 1, 2, 3)$$

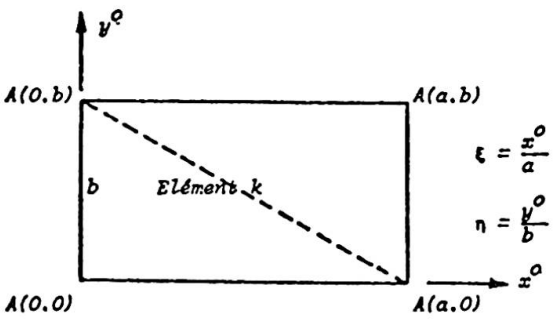

$$u_i^k(x^\circ, y^\circ) = \left\{ \begin{array}{l} f_1(\xi)\,.\,f_1(\eta) \\ a\,.\,f_2(\xi)\,.\,f_1(\eta) \\ b\,.\,f_1(\xi)\,.\,f_2(\eta) \\ a.b.f_2(\xi)\,.\,f_2(\eta) \\ g_1(\xi)\,.\,f_1(\eta) \\ a\,.\,g_2(\xi)\,.\,f_1(\eta) \\ b\,.\,g_1(\xi)\,.\,f_2(\eta) \\ a.b.g_2(\xi)\,.\,f_2(\eta) \\ g_1(\xi)\,.\,g_1(\eta) \\ a\,.\,g_2(\xi)\,.\,g_1(\eta) \\ b\,.\,g_1(\xi)\,.\,g_2(\eta) \\ a.b.g_2(\xi)\,.\,g_2(\eta) \\ f_1(\xi)\,.\,g_1(\eta) \\ a\,.\,f_2(\xi)\,.\,g_1(\eta) \\ b\,.\,f_1(\xi)\,.\,g_2(\eta) \\ a.b.f_2(\xi)\,.\,g_2(\eta) \end{array} \right\} \left\{ \begin{array}{l} u_i \\ u_i\,,\,x^\circ \\ u_i\,,\,y^\circ \\ u_i\,,\,x^\circ_j\,y^\circ_j \quad 0.0 \\ u_i \\ u_i\,,\,x^\circ \\ u_i\,,\,y^\circ \\ u_i\,,\,x^\circ_j\,y^\circ_j \quad a.0 \\ u_i \\ u_i\,,\,x^\circ \\ u_i\,,\,y^\circ \\ u_i\,,\,x^\circ_j\,y^\circ_j \quad a.b \\ u_i \\ u_i\,,\,x^\circ \\ u_i\,,\,y^\circ \\ u_i\,,\,x^\circ_j\,y^\circ_j \quad o.b \end{array} \right\}^k$$

$(i = 1,2,3)$

3. - CHAMP DE DEPLACEMENT DANS UN RAIDISSEUR

$$\{\Delta_1\}_O = \begin{Bmatrix} u_r\,(O) \\ u_r\,,_r(O) \end{Bmatrix} \qquad \{\Delta_1\}_C = \begin{Bmatrix} u_r\,(C) \\ u_r\,,_r(C) \end{Bmatrix}$$

$$\{\Delta_2\}_O = \begin{Bmatrix} u_t\,(O) \\ u_t\,,_r(O) \end{Bmatrix} \qquad \{\Delta_2\}_C = \begin{Bmatrix} u_t\,(C) \\ u_t\,,_r(C) \end{Bmatrix}$$

$$\{\Delta_3\}_O = \begin{Bmatrix} \omega\,(O) \\ \omega\,,_r(O) \end{Bmatrix} \qquad \{\Delta_3\}_C = \begin{Bmatrix} \omega\,(C) \\ \omega\,,_r(C) \end{Bmatrix}$$

$$\{\Delta_4\}_O = \begin{Bmatrix} \theta\,(O) \\ \theta\,,_r(O) \end{Bmatrix} \qquad \{\Delta_4\}_C = \begin{Bmatrix} \theta\,(C) \\ \theta\,,_r(C) \end{Bmatrix}$$

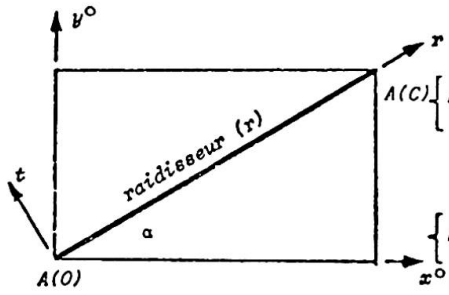

Posons : $\{\Delta_i\}^r = \begin{Bmatrix} \Delta_i\,_O \\ \Delta_i\,_C \end{Bmatrix}$ composantes de déplacement de $A(O)$ et $A(C)$ dans (r, t, z)

- Champ de déplacement dans le système (r, t, z)

$$u_i^r(r) = \widetilde{\{\rho(r)\}} \,.\, \{\Delta_i\}^r \qquad (u_i = u_r\,,\, u_t\,,\, \omega\,,\, \theta)$$

$$\widetilde{\{\rho(r)\}} = \left| f_1(\xi)\,,\, c.f_2(\xi)\,,\, g_1(\xi)\,,\, c.g_2(\xi) \right| \qquad \left(\xi = \frac{r}{c}\right)$$

4· PANNEAU DE POUTRE EN I

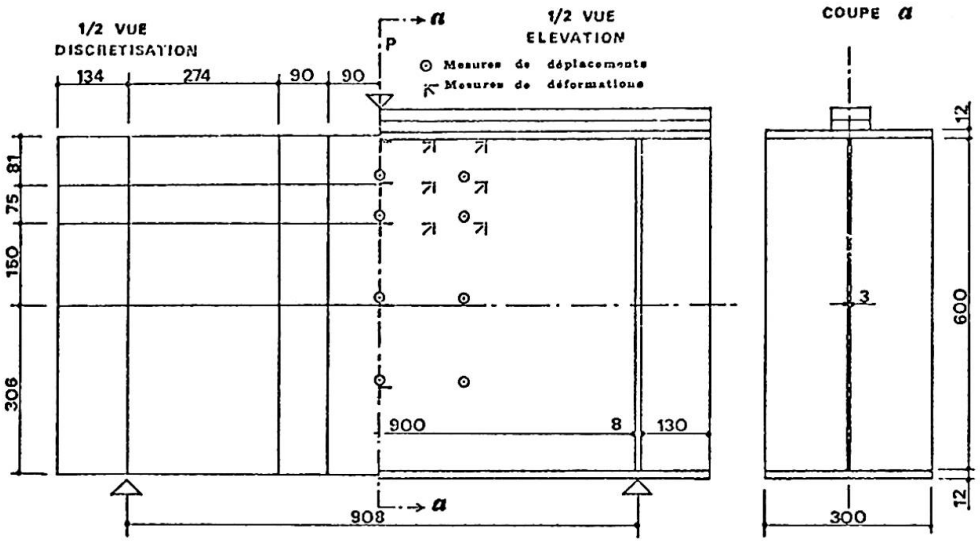

5- DEFORMEE DE LA MEMBRURE SUPERIEURE

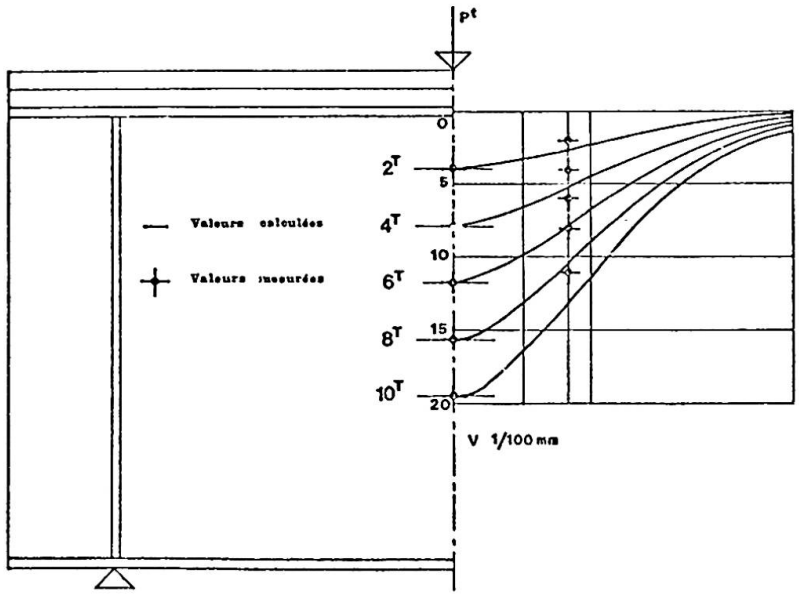

6·DEFORMATION DE L'AME HORS DE SON PLAN

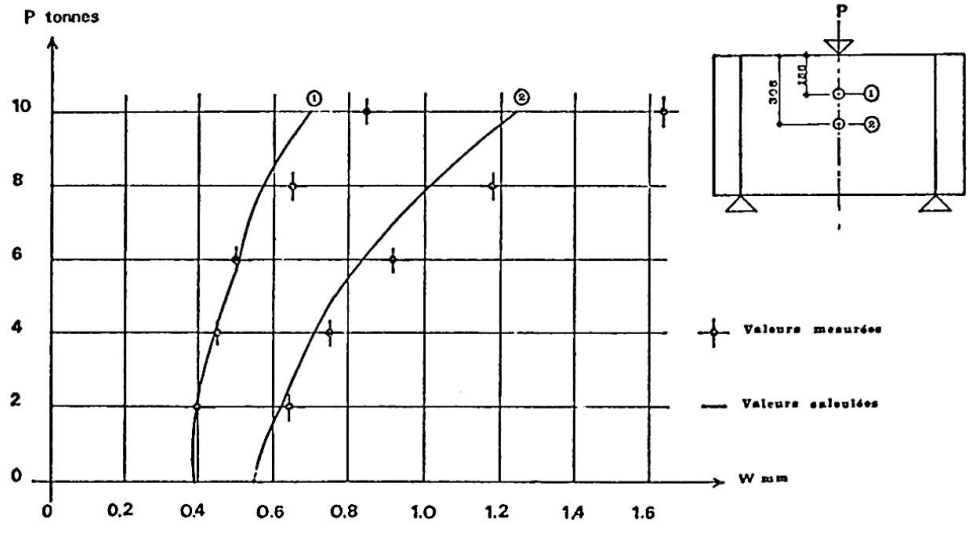

7-DEPLACEMENT $w+w^o$ DANS LA SECTION MEDIANE

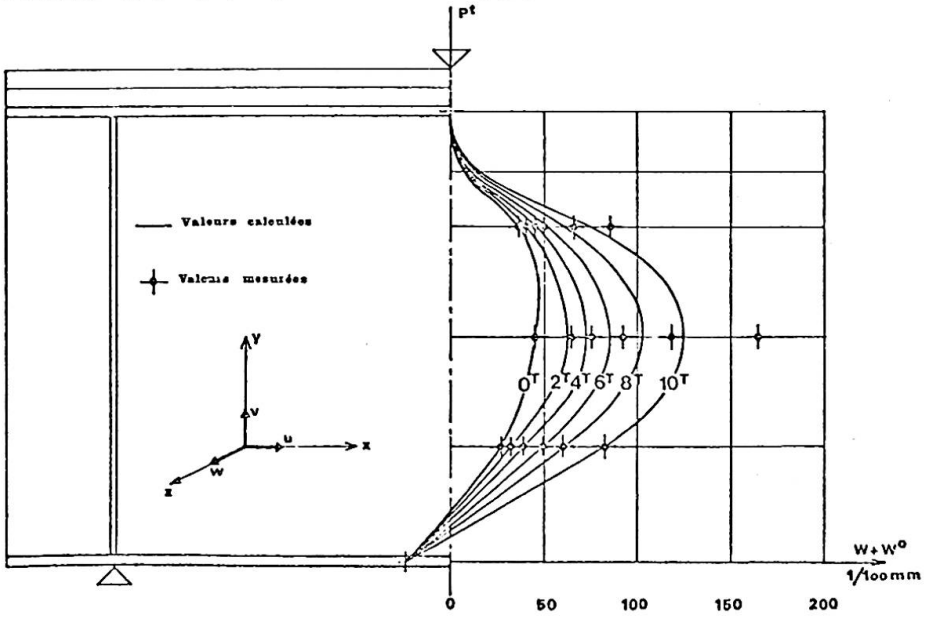

8·DEFORMATION ε_{xx} DANS LA SECTION MEDIANE

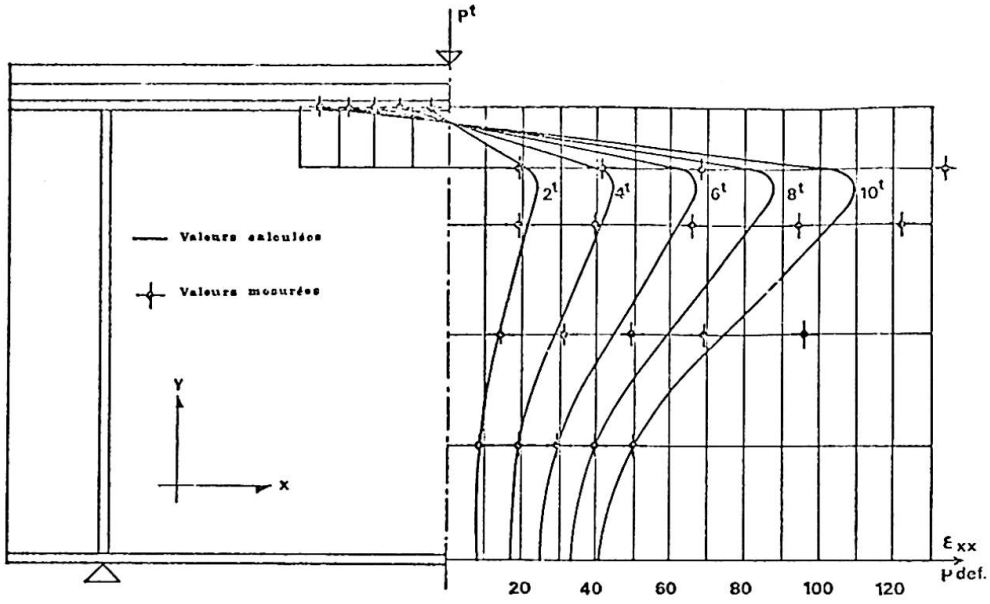

9-DEFORMATION ε_{yy} DANS LA SECTION MEDIANE

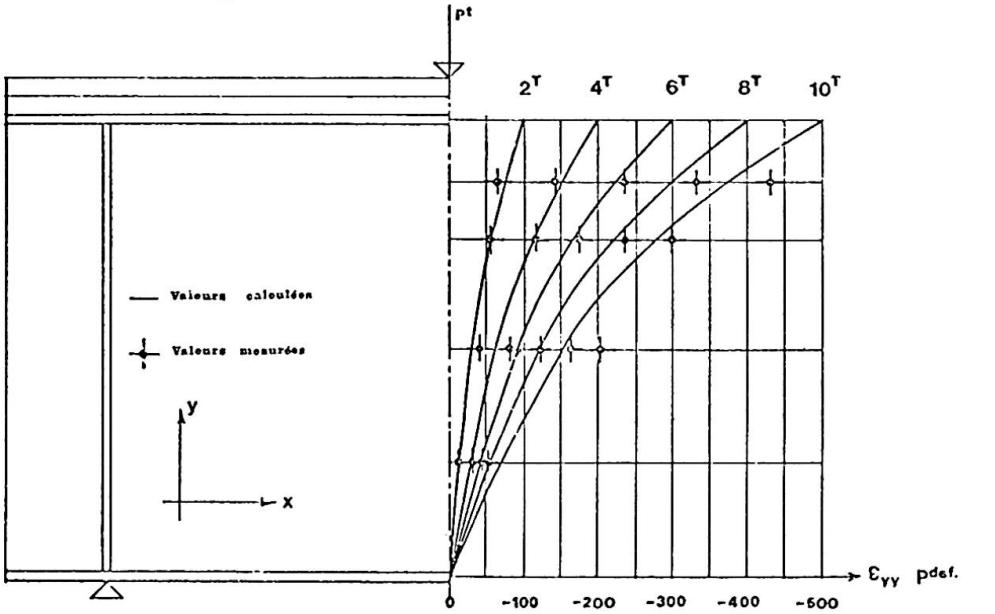

RESUME

Ce mémoire expose une méthode d'analyse, par éléments finis, du champ de déplacement de plaques minces raidies présentant un champ de contraintes propres et une courbure initiale. Il présente une étude comparée, d'un panneau de poutre en I, chargé localement dans son plan, par la simulation sur modèle mathématique et par la mesure sur modèle expérimental.

ZUSAMMENFASSUNG

Diese Arbeit zeigt eine mittels endlicher Elemente durchgeführte Analysenmethode des Verschiebungsfeldes dünner ausgesteifter Platten mit einem Feld von Eigenspannungen und anfänglicher Krümmung. Durch Simulation an einem mathematischen Modell und durch Messung am experimentellen Modell legt sie eine vergleichende Studie über ein in seiner Ebene örtlich begrenztes T-Balkenfeld vor.

SUMMARY

This paper exposes an analysis by the finite element method of the displacement field of thin stiffened plates presenting a field of residual stresses and an initial curvature. It shows a comparing study of a I-girder panel loaded locally in its plain, by simulation on a mathematical model and by measuring on an experimental model.

Post-Buckling Behaviour of Webs under Concentrated Loads

Comportement post-critique de voilement des âmes soumises à des charges concentrées

Überkritisches Beulverhalten von Stegblechen infolge Einzellasten

ALLAN BERGFELT
Professor, Structural Engineering
Steel and Timber Structures
Chalmers University of Technology
Göteborg, Sweden

Some comments are here given on the paper [1] by M. Škaloud and P. Novák : Post-buckled Behaviour and Incremental Collapse of Webs Subjected to Concentrated Loads. This paper gives results from tests performed in order to make it possible to build up a complete theory.

It is of course interesting to compare their results with already existing preliminary formulas. In a paper [2] to the London colloquium 1972 on Design of Plate and Box Girders for Ultimate Strength, I gave a preliminary formula and a diagram illustrating the influence of flange stiffness on the ultimate bearing capacity under a concentrated load (A. Bergfelt : Studies and Tests on Slender Plate Girders without Intermediate Stiffeners. I, Shear strength and II, Local web crippling).

Putting the test results of Škaloud and Novák into my formula, fig. 1 illustrates that their results confirm at least its tendency. The curve in the figure is from fig. 14 of my London paper, completed with the influence (from fig. 11 of the paper) of a somewhat distributed load, as in the tests of Škaloud and Novák. The curve is valid for point load action combined with small bending stresses. As my investigation considered girders without intermediate stiffeners and the girders of their tests had stiffeners with the same distance as the height of the girder it is of course a slight difference in behaviour, especially for extremely thick flanges. In that case the web is not so dominating, but the girder to some extent also acts as a Vierendeel-beam consisting of the flanges and the stiffeners. Owing to this fact their result for flanges with a thickness of about 10

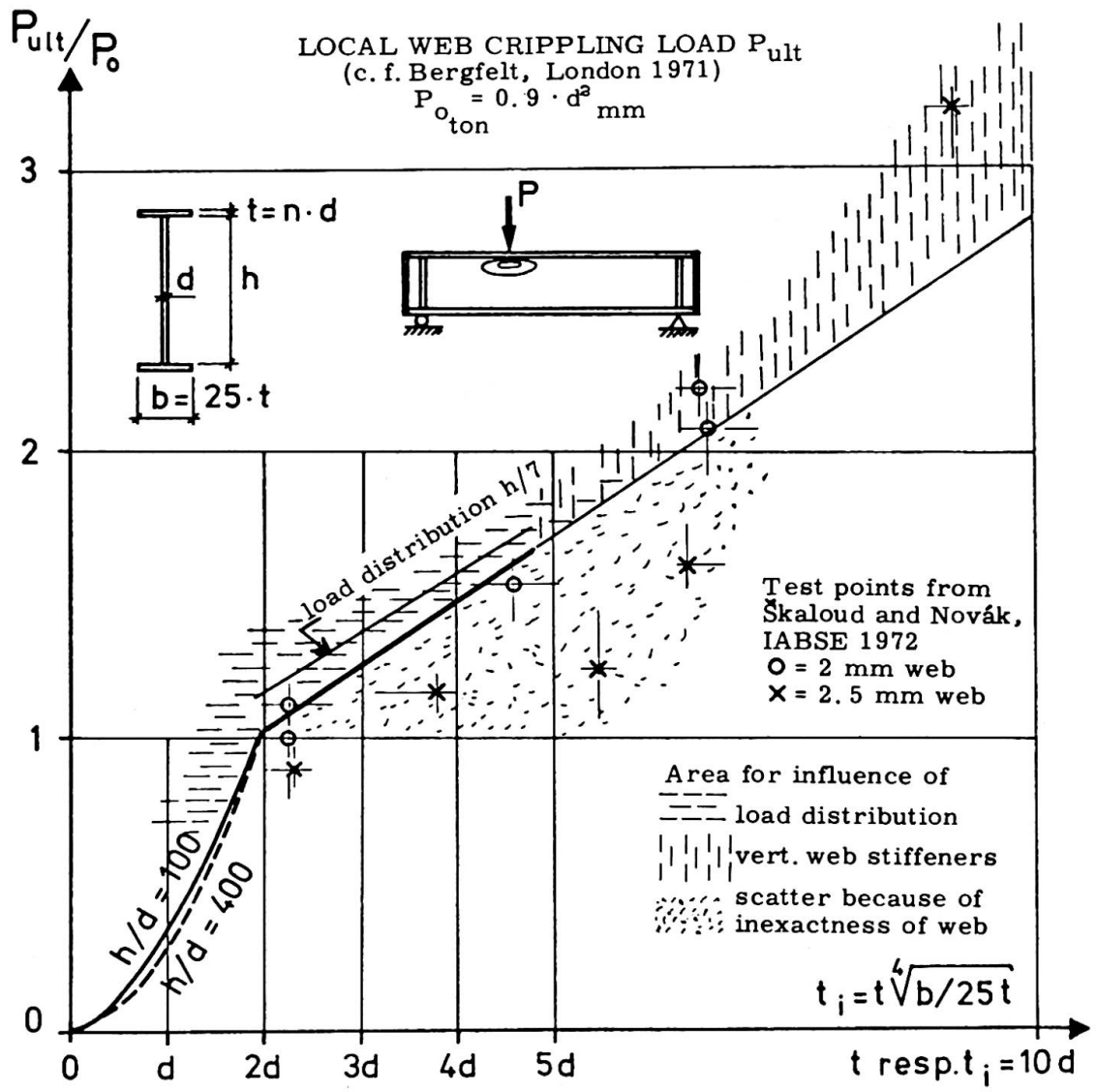

Fig. 1 Test values according to Škaloud and Novák [1] marked in the diagram from [2].

times the thickness of the web is as seen from the only test in that region, a little higher than predicted from my curve. The scatter of the test values due to fabrication and material deficiencies is within the predicted limits.

The curve in the original figure was based on tests on girders with flanges about b = 25 t, which is commonly used. When the ratio of flange dimensions differs very much from that mentioned it is of course necessary to adjust t – as single variable for stiffness – to $t_i = t\sqrt[4]{b/25 \cdot t}$ as in fig. 1.

The test points of Škaloud and Novák are marked in fig. 1 as if the web thickness was really the nominal values 2 and 2.5 mm given in their paper. When their careful measurements are published and used some adjustments can of course be motivated. The steel quality is not reported but seems to have some influence, which is for the moment the scope of tests at my laboratory.

In order to illustrate the influence of stiffeners when the flanges are very thick the bearing capacity of the flange can be computed as if there was no web at all. Considering the flange 250 x 30.88 mm, which corresponds to t_i near 10, its bearing capacity is 12.5 ton (plastic design and σ_Y = 2200 kg/cm^2).

As the test load was 18.0 ton, the influence of the web is only 5.5 ton (which in this case happens to be just about the 5.6 ton taken by the web with a very weak flange only).

As pointed out in the paper much work remains to be done and it is considered favourable that several laboratories are interested in the problem.

*

The second part of the paper by Škaloud and Novák deals with cyclic load tests. They state that the maximum loads in several cases were higher than in the static tests and that the cyclic loads did not cause any reduction in ultimate strength.

The reason for this result is, as I think, the short loading times which result from 3 loading cycles per second. There is no time for yielding.

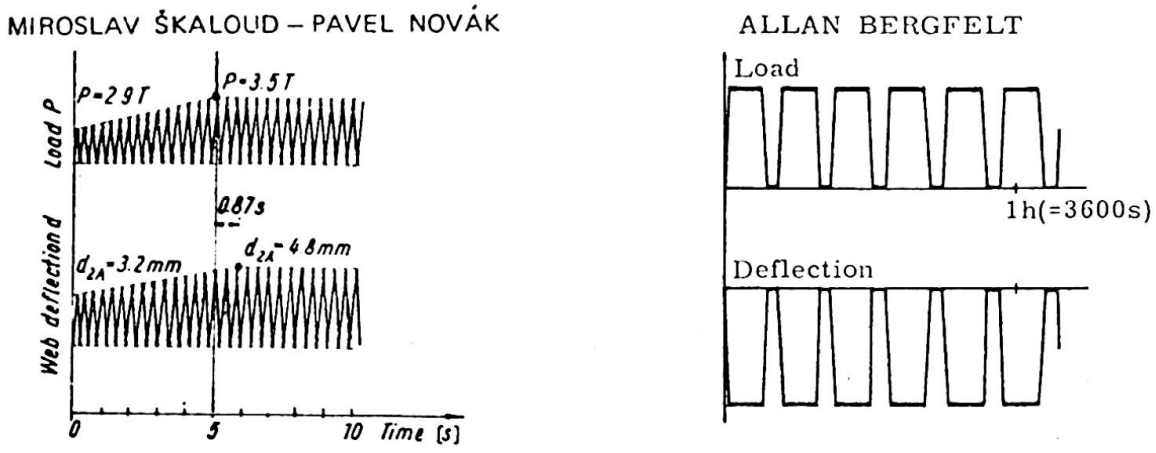

Fig. 2 Load-time dependency as used in the tests of [1] and [2]

As mentioned in my London paper 1971 I have made loadings with longer periods, for instance with so long periods that there are only 5 cycles per hour Now test girders have been loaded up to about 1000 such cycles, which could be called repeated statical loads, and there are of course no increase in ultimate strength. It ought to be a reduction which was, however, in our tests very small. I have performed tests with 1000 cycles to more than 90% of the ultimate statical load without collapse. It is called attention to the fact that ultimate loads are meant, which as also observed in the paper by Škaloud and Novák could be 2-6 times higher than some elastic critical load for the dimensions of our test girders.

The comparison with statical loading tests holds true even in tests with combined action of bending stresses and stresses caused by the point load. Tests have been performed with bending stresses in the girder up to about half the yield stresses.

In order to obtain a well-founded general formula for cyclic loads it is necessary to test both slow and rapid cycles. So extremely slow loadings as corresponding to only 5 cycles per hours as mentioned above is probably not necessary. Perhaps for instance one cycle per minute is satisfactory. The rapid tests of Škaloud and Novák are necessary for machine foundations and bridges, while my slow tests are needed for roof structures. Anyhow it is very positive that testings at different laboratories complete each other.

References

[1] ŠKALOUD, M., and NOVÁK, P.: Post-buckled Behaviour and Incremental Collapse of Webs Subjected to Concentrated Loads. IABSE, Ninth Congress Amsterdam 1972, p. 101.

[2] BERGFELT, A.: Studies and Tests on Slender Plate Girders Without Intermediate Stiffeners. I, Shear strength and II, Local web crippling. IABSE Colloquium on Design of Plate and Box Girders for Ultimate Strength, London 1971.

SUMMARY

The test values according to Škaloud and Novák (1) for local web crippling under a concentrated static load, are compared with a preliminary formula given in (2). Comments are given on the influence of the rates of loading on the collapse under cyclic loadings.

RESUME

Dans ce travail, les valeurs obtenues lors d'essais par Škaloud et Novák (1) pour la ruine locale de l'âme soumise à une force statique concentrée, sont comparées à celles déterminées théoriquement dans (2). Ensuite l'auteur commente l'influence de la fréquence de charge sur l'état de ruine dans le cas de charges périodiques.

ZUSAMMENFASSUNG

Die Versuchsergebnisse nach Škaloud und Novák (1) für lokales Stegblechbeulen unter statischer Einzellast werden mit einer vorläufigen Formel aus (2) verglichen. Ueber den Einfluss der Laständerungsrate auf den Kollaps unter Wechsellasten wird berichtet.

Leere Seite
Blank page
Page vide

Criteria of Column Strength in Paper by De Wolf, Pekoz and Winter — the Significance of Imperfections

Critères de résistance des colonnes dans les travaux de De Wolf, Pekoz et Winter — l'importance des imperfections

Kriterien der Festigkeit von Stützen im Beitrag von De Wolf, Pekoz und Winter — die Bedeutung von Unvollkommenheiten

PAUL GRUNDY
Department of Civil Engineering
Monash University
Clayton, Victoria, Australia

The authors, De Wolf, Pekos and Winter, have considered an important question - design curves for columns with local plate buckling. They are modest about progress to date, but I am compelled to ask whether their basic philosophy will yield the desired results.

The authors report that three column tests were discounted presumably because eccentricities of load could not be eliminated. In structural design we are not so much concerned with the average margin of safety between load and strength as we are concerned with minimising the number of failures. We are not interested in the average, or even maximum attainable, column strength, but in the minimum strength below which the risk of failure is acceptably low.

In this class of structure, so sensitive to imperfections, it is necessary to base our philosophy on probable imperfections. The load-shortening characteristics of plates are very sensitive to initial plate curvature. An initially curved plate is less stiff, axially, than a flat plate when the load is less than the initial buckling load. It is more stiff after buckling.

A thinwalled column has both local plate initial curvature and overall initial curvature. Unsymmetrical initial plate curvature can cause an overall curvature to develop from the start. Overall initial curvature will cause plate buckling to initiate unsymmetrically in the cross-section with subsequent magnification of initial deflection with further load. Dr. Skaloud's report of experiments earlier in this session supports this observation.

I am therefore compelled to ask whether the effective width concept will lead to reliable design curves for thin-walled columns. Without considerable manipulation, the effective width concept does not give the current axial stiffness of plate elements which must be known for a stability analysis at any given load. The effective width changes with load and it is also sensitive to initial imperfections. I believe a more fruitful line of attack lies in assessment of column stiffness at the current load level, using reasonable

imperfections. In this way, the three tests discarded by the authors might turn out to be useful data in the overall estimation of column strength on a statistical basis.

Finally, I would like to observe that there seems to be a pressure on the designer of columns built up from separate plates to seek an apparent optimum proportion in which plate buckling stress, column buckling stress and yield stress are about the same value. It seems that predictions of strength are most subject to error in this region; and test results are most variable, due to the extreme sensitivity of the system to imperfections. This variability is enough to wipe out any benefits of this apparent optimum proportioning of column cross-section.